UNIVERSITÀ
DEGLI STUDI
DI PADOVA

UNIVERSITA' DEGLI STUDI DI PADOVA

DIPARTIMENTO DI BIOLOGIA

SCUOLA DI DOTTORATO DI RICERCA IN : BIOSCIENZE E BIOTECNOLOGIE
INDIRIZZO: NEUROBIOLOGIA
CICLO: XXVIII

REGULATION OF AUTOPHAGY AND THE UBIQUITIN– PROTEASOME SYSTEM BY THE FoxO TRANSCRIPTIONAL NETWORK DURING MUSCLE ATROPHY

Direttore della Scuola: Ch.mo Prof. Paolo Bernardi
Coordinatore d'indirizzo: Ch.ma Prof.ssa Daniela Pietrobon
Supervisore: Prof. Marco Sandri

Dottoranda: Francesca Pescatore

INDEX

SUMMARY

Skeletal muscle can adapt its mass in response to physical activity, metabolism and hormones. The control of muscle size depends on the coordinated balance between protein synthesis and protein degradation. Mechanical overload or anabolic hormonal stimulation shifts the balance towards protein synthesis leading to an increase in fiber size, a process called hypertrophy. Conversely, in catabolic conditions protein degradation exceeds protein synthesis resulting into muscle weakness and muscle atrophy. Muscle loss and weakness occurs in several pathological conditions like disuse, denervation, immobilization, sepsis, burn injury, cancer, AIDS, diabetes, heart and renal failure and in aging. Muscle atrophy is an active process which requires the activation of specific signalling pathways and transcriptional programs. Gene expression studies revealed a set of genes, named atrogenes (atrophy related genes), which are commonly up- and down-regulated in different catabolic conditions (Bodine et al., 2001; Gomes et al., 2001; Lecker et al., 2004; Sacheck et al., 2007; Sandri et al., 2004). These genes encode for enzymes that catalyze important steps in autophagy-lysosome pathway, ubiquitin-proteasome system, unfolded protein response, ROS detoxification, DNA repair, mitochondrial function and energy balance pathways. Skeletal muscle growth is regulated by the IGF1-AKT-mTOR-FoxO signalling pathway (Sandri, 2013). FoxO family of transcription factors activity is suppressed during growth by AKT. On the other hand, in the absence of growth factors, like IGF1 or insulin, AKT is not activated and does not block FoxOs which can translocate into the nucleus and interact with promoters of their target genes (Sandri et al., 2004). Activation of FoxOs promotes the expression of the essential atrophy-related ubiquitin ligases atrogin-1 and MuRF-1 and leads to a dramatic loss of muscle mass (Kamei et al., 2004; Sandri et al., 2004). In addition, autophagy and expression of autophagy-related genes is also under FoxO3 control (Mammucari et al., 2007; Zhao et al., 2007). Thus FoxO coordinates the two major proteolytic

system of the cell, the autophagy-lysosome and the ubiquitin-proteasome. However, the activation of the few atrogenes reported to be regulated by FoxO cannot sustain all the protein breakdown during atrophy. Nevertheless several other genes among the atrogenes are of potential interest but their particular role and regulation in muscle wasting is still unknown. Moreover, other unknown players are certainly important for muscle protein breakdown. For this reason, in this PhD project we propose, by a loss of function approach, to unravel the role of FoxO family in gene regulation and muscle adaptation during catabolic conditions. The FoxO family in skeletal muscle is comprised of four isoforms: FoxO1, FoxO3, FoxO4 and FoxO6. Therefore, to simultaneously delete the three major expressed FoxO genes in skeletal muscle, we generated muscle-specific conditional FoxO1,3,4 knockout mice. These animals resulted to be fully viable, phenotypically normal and indistinguishable in appearance from aged-matched control mice. To characterize the role of FoxO1,3,4 in skeletal muscle, we analyzed the phenotype of knockout mice under conditions of muscle wasting. Initially we used starvation as a model of muscle loss. because it is an established condition that induces nuclear translocation of FoxO members and their binding to target promoters (Mammucari et al., 2007; Sandri et al., 2004). Interestingly, FoxO1,3,4 knock-out mice were completely protected from muscle loss and muscle weakness after fasting. Moreover, deletion of FoxO resulted in suppression of autophagy during fasting. To further determine if the role of FoxO1,3,4 is critical in different catabolic conditions, we then used denervation as another model of muscle atrophy. Quantification of fibre size revealed that FoxO-deficient muscles were partially protected from atrophy. Thus, FoxO family members are necessary for muscle loss but their involvement in the atrophy programme depends on the catabolic condition.

Since muscle atrophy is characterized by a transcriptional-dependent regulation of atrogenes we decided to perform gene expression profiling in fed and fasting conditions in FoxO1,3,4 -/- and controls to identify genes under FoxO regulation. Then, we compared the list of FoxO-dependent genes with the list of atrogenes and we founded that 29 of 63 atrophy related-genes

were not induced in FoxO null muscles during fasting. Interestingly, the lists of FoxO-dependent genes during denervation and fasting do not completely overlap confirming that FoxO trascription factors are more sensitive in conditions of nutrient deprivation. Finally we identified new FoxO-dependent ubiquitin ligases including MUSA1 recently identified in our lab and another one that we name SMART (Specific of Muscle Atrophy and Regulated by Transcription). We confirmed by IP experiments that SMART forms an SCF complex with Skp1, Cullin1 and Roc1 and therefore belongs to the SCF family of E3 ligases. To validate the hypothesis that SMART had a role in promoting atrophy during denervation, we knocked down SMART in tibialis anterior in vivo in innervated and denervated muscles. Importantly, SMART inhibition significantly protected denervated muscles from atrophy. Therefore, SMART is an additional critical gene whose upregulation is required for atrophy. In conclusion, this PhD project identified the FoxO signature in protein breakdown. This information would be valuable in order to block muscle wasting in many systemic disease and to promote pharmacological strategies against muscle loss.

RIASSUNTO

Il muscolo scheletrico è in grado di adattare la sua massa in risposta all' esercizio fisico, al metabolismo e a gli ormoni. Il controllo della massa muscolare dipende quindi da un coordinato equilibrio tra sintesi e degradazione proteica. L'esercizio fisico e gli stimoli anabolici spostano questo equilibrio verso la sintesi proteica, la quale porta ad un aumento delle dimensioni delle fibre muscolari attraverso un processo noto come ipertrofia. Al contrario, in condizioni cataboliche, la degradazione proteica aumenta rispetto alla sintesi portando a debolezza muscolare e atrofia. La perdita di massa e forza sono una conseguenza di diverse condizioni patalogiche come il disuso, la denervazione, l' immobilizzazione, la sepsi, ustioni, cancro, AIDS, diabete ed invecchiamento. L'atrofia muscolare è un processo catabolico che richiede l'attivazione di specifiche vie di segnale e programmi trascrizionali. Studi di espressione genica hanno identificato un set di geni, chiamati *atrogenes* (geni correlati all'atrofia), che sono comunemente up-regolati e down- regolati in differenti condizioni cataboliche. (Bodine et al., 2001; Gomes et al., 2001; Lecker et al., 2004; Sacheck et al., 2007; Sandri et al., 2004).

Questi geni codificano per enzimi che catalizzano importanti *step* nei principali *pathway* cellulari come il sistema autofagico lisosomiale, il sistema ubiquitina-proteasoma, stress del reticolo, sistemi di riparazione del DNA ed enzimi che regolano attività mitocondriali. La crescita muscolare è regolata dalla via di segnale IGF1-AKT-mTOR-FoxO (Sandri, 2013). L' attività dei fattori trascrizionali FoxO è quindi abolita durante la crescita muscolare tramite l' attivazione della chinasi AKT. In assenza però di fattori di crescita come IGF1 o insulina, la chinasi AKT non è attivata e risulta dunque incapace di bloccare FoxO che può traslocare nel nucleo e legare i promotori dei suoi geni target (Sandri et al., 2004). L' attivazione dei fattori FoxO promuove l'espressione di essenziali ubiquitine ligasi legate all' atrofia atrogin-1 e MuRF-1 e porta ad una drammatica perdita della massa muscolare (Kamei et al., 2004; Sandri et al., 2004), inoltre è noto che l'autofagia e l'espressione di

alcuni dei geni correlati all' atrofia sono sotto il controllo del fattore trascrizionale FoxO3 (Mammucari et al., 2007; Zhao et al., 2007). I fattori FoxO coordinano i due principali sistemi proteolitici della cellula: il sistema autofagico lisosomiale e il sistema ubiquitina proteasoma. Tuttavia, l' attivazione degli *atrogenes* controllati trascrizionalmente da FoxO non è sufficiente, da sola, a giustificare la completa perdita della massa muscolare; tra gli *atrogenes* vi sono dunque diversi altri geni che giocano un ruolo di potenziale interesse nella regolazione nell' atrofia muscolare la cui funzione però, è ancora sconosciuta.

Per questo motivo, nel mio progetto di dottorato, abbiamo caratterizzato attraverso la metodica del *loss of function* il ruolo dei fattori trascrizionali FoxO nella regolazione genica e nell' adattamento del muscolo scheletrico in condizioni cataboliche. La famiglia dei fattori trascrizionali FoxO comprende 4 isoforme FoxO1, FoxO3, FoxO4 e FoxO6. Per eliminare simultaneamente i fattori FoxO specificamente nel muscolo abbiamo generato dei topi knock-out muscolo specifici per i fattori FoxO1,3,4 che sono principalmente espressi nel muscolo. Questi animali sono risultati essere vitali, ed apparentemente indistinguibili dai loro topi di controllo. Per caratterizzare il ruolo dei fattori Foxo1,3,4 nel muscolo scheletrico, abbiamo analizzato il fenotipo dei topi knock-out in condizioni in cui vi era perdita di massa. Inizialmente abbiamo utilizzato il digiuno, una delle condizioni in cui FoxO è attivo e trasloca nel nucleo dove trascrive i suoi geni target, come modello di atrofia.

I topi FoxO1,3,4 erano completamente protetti dalla perdita di massa e forza in seguito al digiuno, ed inoltre la delezione dei fattori FoxO portava ad un completo blocco del flusso autofagico durante il digiuno. Per determinare se il ruolo dei fattori FoxO è critico nelle differenti condizioni di atrofia, abbiamo deciso di utilizzare la denervazione come altro modello di perdita di massa muscolare. La quantificazione dell' area delle fibre mostrava in questo caso una parziale protezione dall' atrofia suggerendo che i fattori FoxO sono necessari nel promuovere la perdita di massa ma il loro coinvolgimento nel programma atrofico dipende dal dipo di condizione catabolica. Com'è noto l' atrofia muscolare è caratterizzata dall' attivazione di uno specifico

programma genico, dunque, abbiamo per prima cosa identificato i geni regolati trascrizionalmente da FoxO attraverso un' analisi di *gene expression profiling* condotta su topi FoxO1,3,4 knock-out e controlli , alimentati e a digiuno. Abbiamo quindi paragonato la lista dei geni regolati da FoxO con la lista degli *atrogenes* e abbiamo trovato che 29 di 63 *atrogenes* non erano espressi nei muscoli dei topi FoxO knock-out durante il digiuno. Degno di nota è che la lista dei geni controllati da FoxO nella denervazione e nel digiuno non era completamente sovrapponibile confermando che i fattori FoxO erano maggiormente coinvolti nel processo atrofico in condizioni di carenza di nutrienti. Infine abbiamo identificato nuove ubiquitine ligasi regolate dai fattori FoxO tra cui MUSA1, recentemente identificata nel nostro laboratorio, e una nuova unquitina ligasi a cui abbiamo dato il nome di SMART (Specific of Muscle Atrophy and Regulated by Transcription). Attraverso esperimenti di immunoprecipitazione abbiamo confermato che SMART apparteneva alla famiglia delle E3 ubiquitina ligasi SCF dal momento che formava un complesso con le altre componenti Skp1, Cullin1 e Roc1 . Successivamente per validare l'ipotesi che SMART avesse un ruolo nel promuovere l' atrofia muscolare abbiamo bloccato la sua espressione nei muscoli tibiali di topi innervati e denervati e abbiamo constatato che il blocco di SMART proteggeva i muscoli denervati dall' altrofia. Pertanto, SMART rappresenta un nuovo gene critico per il programma atrofico. In conclusione, questo progetto di dottorato identifica il ruolo di FoxO nella perdita di massa muscolare. Queste informazioni potrebbero risultare utili per combattere l' atrofia muscolare in molte malattie sistemiche suggerendo nuove strategie farmacologiche che blocchino la perdita di massa muscolare.

INTRODUCTION

1.1 SKELETAL MUSCLE

1.1.1 STRUCTURE AND FUNCTION

Skeletal muscle is one of the most dynamic and plastic tissues of the human body. In humans, skeletal muscle comprises approximately 40 % of total body weight and contains 50–75 % of all body proteins. Muscle is composed by multinucleated ,elongated and cylindrical cells called muscle fibres that run parallel to each other within a muscle. These cells are incredibly large, with diameters of up to 100 μm and lengths of up to 30 cm. Muscles fibres are organized in bundles and separated by specific membrane system. Each muscle is surrounded by a connective tissue membrane called epimysium; each bundle of muscle fiber is called a fasciculus and is surrounded by a layer of connective tissue, called perimysium. Within the fasciculus, each individual muscle fiber is surrounded by connective tissue called the endomysium (Figure 1).

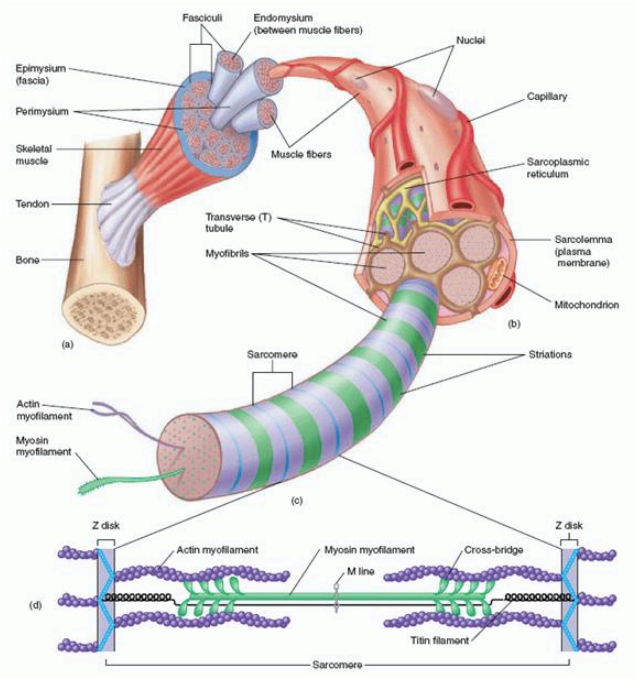

Fig.1: Schematic representation of skeletal muscle structure.

The contractile machinery of skeletal muscles is organized in highly ordered supramolecular structures, the sarcomeres, which are associated in series, to form the myofibrils, and in parallel, thus generating the striated pattern of muscle fibers. The sarcomere was described first thank to microscopy techniques that individuated isotropic (light band) and anisotropic (dark band) zones, forming the specific striated aspect of the skeletal muscle. For this reason, sarcomere is usually defined as the segment between two neighbour Z-lines, that appears as a series of dark lines. Surrounding the Z-line, there is the region of the I-band (the light band). Following the I-band there is the A-band (the dark band). Within the A-band, there is a paler region called the H-band. Finally, inside the H-band there is a thin M-line, the middle of the sarcomere. These bands are not only morphological unit but also functional, because are characterized by the presence of different contractile proteins required for muscle contraction. In fact, actin filaments (thin filaments) are the major component of the I-band and extend into the A band. Myosin filaments (thick filaments) extend throughout the A-band and are thought to overlap in the M band. A huge protein, called titin, extends from the Z-line of the sarcomere, where it binds to the thin filament system, to the M-band, where it is thought to interact with the thick filaments. Several proteins important for the stability of the sarcomeric structure are found in the Z-line as well as in the M band of the sarcomere (Figure2). Actin filaments and titin molecules are cross-linked in the Z-disc via the Z-line protein alpha-actinin. The M-band myosin as well as the M proteins bridge the thick filament system to the M-band part of titin (the elastic filaments). Moreover several regulatory proteins, such as tropomyosin and troponin bind myosin molecules,modulating its capacity of contraction.

Muscle contraction is due to the excitation-contraction coupling, by which an electrical stimulus is converted into mechanical contraction. The general scheme is that an action potential arrives to depolarize the cell membrane. By mechanisms specific to the muscle type, this depolarization results in an increase in cytosolic calcium that is called a calcium transient. This increase in calcium activates calcium sensitive contractile proteins that then use ATP

to cause cell shortening. Concerning skeletal muscle, upon contraction, the A-bands do not change their length, whereas the I bands and the H-zone shorten. This is called the sliding filament hypothesis which is now widely accepted. There are projections from the thick filaments, called cross-bridges which contain the part (head) of myosin linked to actin. Myosin head is able to hydrolyze ATP and converting chemical energy into mechanical energy.

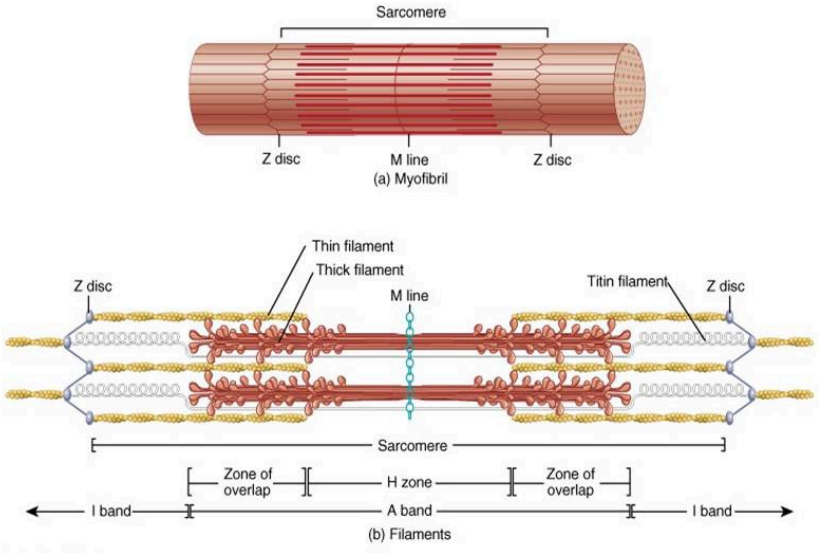

Fig.2: Schematic representation of skeletal muscle sarcomere.

To allow the simultaneous contraction of all sarcomeres, the sarcolemma penetrates into the cytoplasm of the muscle cell between myofibrils, forming membranous tubules called transverse tubules (T-tubules) (Figure 3). The T-tubules are electrically coupled with the terminal cisternae which continue into the sarcoplasmic reticulum. Thus the Sarcoplasmic Reticulum, which is the enlargement of smooth Endoplasmic Reticulum (ER) and which contains the majority of calcium ions required for contraction, extends from both sides of T-tubules into the myofibrils. Anatomically, the structure formed by T-tubules surrounded by two smooth ER cisternae is called the triad and it allows the transmission of membrane depolarization from the sarcolemma to the ER. The contraction starts when an action potential diffuses from the motor neuron to the sarcolemma and then it travels along T-tubules until it

reaches the sarcoplasmic reticulum. Here the action potential changes the permeability of the sarcoplasmic reticulum, allowing the flow of calcium ions into the cytosol between the myofibrils. The release of calcium ions induces the myosin heads to interact with the actin, allowing the muscle contraction. The contraction process is ATP dependent, the energy is provided by mitochondria which are located closed to Z line and also is determine by fibre type composition.

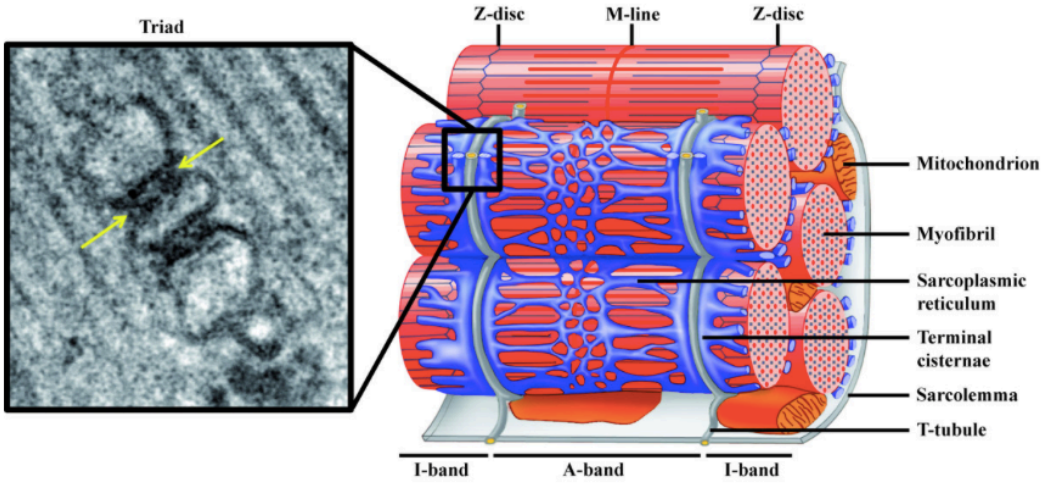

Fig.3: Schematic representation of organization of T-tubuls and triad in skeletal muscle.

Mammalian muscle fibres are divided into distinct classes : type I, also called slow fibres, and type II fast fibres. This classification is specific only for the mechanical properties. However, the diversity between muscle fibers is due also a peculiar features such as for example myosin ATPase enzymes, predominance of glycolytic or mitochondrial activities and is exents to any subcellular system . The different fibre types are also characterized by different Myosin Heavy Chain (MHC) proteins expression. The fibre type I expresses the slow isoform of MHC (MHCβ or MHC1), and shows a great content of mitochondria, high levels of myoglobin, high capillary densities and high oxidative capacity. Muscles containing many type I fibres display red colour for the great vascularization and for the high myoglobin content. The type II, fast, myofibers are divided in three groups depending on which myosin is expressed. In fact distinct genes encode for MHC IIa,IIx (also called IId) and IIb. Type IIa myofibers are faster than type I, but they are still

relatively fatigue-resistant. IIa fibers are relatively slower than IIx and IIb and have an oxidative metabolism due to the rich content of mitochondria (Schiaffino and Reggiani, 2011)(Schiaffino and Reggiani, 1996). Given all these characteristics, IIa fibres are also defined fast oxidative fibres. They exhibit fast contraction, high oxidative capacity and a relative fatigue resistance. The IIx and IIb fibre types are called fast-glycolitic fibres and show a prominent glycolitic metabolism containing few mitochondria of small size, high myosin ATPase activity, expression of MHC IIb and MHC IIx proteins, the fastest rate of contraction and the highest level of fatigability.

The fibre-type profile of different muscles is initially established during development independently of neural influence, but nerve activity has a major role in the maintenance and modulation of its properties in adult muscle. Indeed during postnatal development and regeneration, a default nerve activity-independent pathway of muscle fibre differentiation, which is controlled by thyroid hormone, leads to the activation of a fast gene program. On the contrary, the post natal induction and maintenance of the slow gene program is dependent on slow motoneuron activity. The muscle fibre-type then undergoes further changes during postnatal life, for example fibre-type switching could be induced in adult skeletal muscles by changes in nerve activity (Murgia et al., 2000).

The transcription of different fiber type-specific genes must be precisely coordinated in skeletal muscle fibers to maintain muscle function during the transition phase. Different signaling pathways control muscle fiber type–specific gene programs, moreover fiber type transformation involves changes in all muscle cell compartments, including components of the excitation-contraction coupling, cell metabolism, and contractile machinery. Muscle fiber type switching involves the coordinated antithetic regulation of different fast and slow gene programs. The first mechanism involves the role of transcription factors, such as the calcineurin-dependent nuclear factor of activated T-cells (NFAT) transcription factors that may act as activators or repressors of distinct MyHC genes. A second mechanism, operating in cis , involves the role of bidirectional promoters located between closely

associated MyHC genes and a third mechanism for coordinated regulation of fast and slow gene programs involves some muscle-specific microRNAs (miRNAs) that are located within MYH genes .These include miR-208b and miR-499 , indeed experiments of deletion have shown that miR-208b and miR-499 play redundant roles in the specification of muscle fiber identity by activating slow and repressing fast myofiber gene programs: deletion of either miR-208b or miR-499 did not alter the fiber type profile, whereas double knockout mice showed a marked slow-to-fast switch in fiber type profile and MyHC expression .(Schiaffino and Reggiani, 2011). (Figure 4)

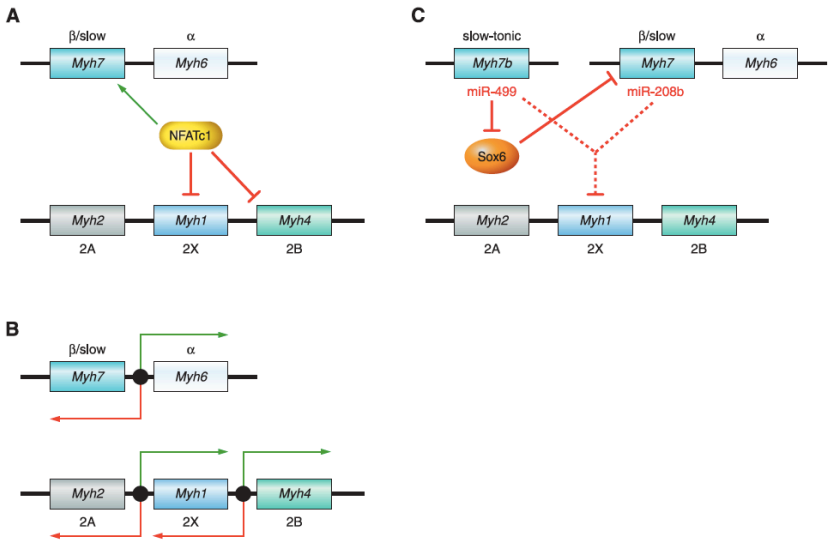

Fig.4: The mechanisms for the coordinated regulation of different Myh genes during fiber type switching.
A)transcription factors acting as both activators (green) and repressors (red) of Myh genes, such as NFATc1; B) bidirectional promoters generating both sense (green) and antisense (red) transcripts of tandem genes C) microRNAs hosted in Myh genes, like miR-499 embedded in Myh7b and mir-208b embedded in Myh7, which inhibit transcriptional repressors.Dotted lines indicate that the mechanism of repression of fast Myh genes by miR-499 and miR-208b is indirect and as yet undefined.

1.2 MUSCLE HYPERTROPHY AND ATROPHY

Maintenance of skeletal muscle mass is essential for health and survival. Skeletal muscle mass and muscle fiber size vary according to physiological and pathological conditions and this is due to several mechanisms that regulate the rate of muscle growth and muscle loss. This event is the result of a balance between protein synthesis and degradation. In particular, muscle

growth is mainly due to protein synthesis, that, when exceeds, leads to muscle hypertrophy. On the contrary, excessive protein degradation, loss of organelles and cytoplasm are major causes of muscle atrophy.

1.2.1 MUSCLE HYPERTROPHY

Skeletal muscle is a highly plastic tissue that modifies its size through the regulation of signaling pathways that control protein synthesis and protein degradation. The adaptive changes of muscle fibers can occur in response to different stimuli like for example neural stimulation, loading conditions, exercise, and hormonal signals. Muscle hypertrophy happen when the overall rates of protein synthesis exceed the rates of protein degradation and it is characterized by an increase in size of skeletal muscle through a growth in size of its component cells. Actually, two major signaling pathways control protein synthesis, the IGF1–Akt–mTOR pathway, acting as a positive regulator, and the Myostatin–Smad2/3 pathway, acting as a negative regulator, but also additional pathways have recently been identified (figure 5).

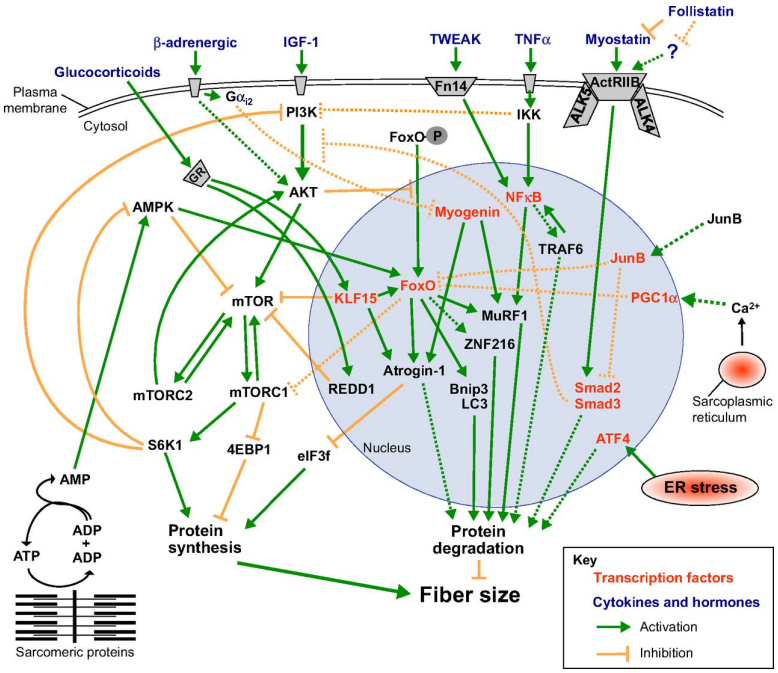

Fig.5: Major pathways that control muscle fiber size. (Bonaldo and Sandri, 2013).

It has been well demonstrated that the Akt/mTOR signaling pathway is a major regulator of muscle growth, indeed muscle-specific IGF-1 over-expression in transgenic mice results in muscle hypertrophy and, importantly, the growth of muscle mass matches with a physiological increase of muscle strength. Furthermore, the over-expression of a constitutively active form of AKT, a downstream target of IGF-1, in adult skeletal muscle induced muscle hypertrophy and also AKT transgenic mice display muscle hypertrophy and protection from denervation-induced atrophy, showing that AKT pathway promotes muscle growth and simultaneously blocks protein degradation (Schiaffino et al., 2013).

Moreover, Akt kinase promotes hypertrophy by activating downstream signalling pathways throught the phosphorilation of different substrates that can act in different ways on protein synthesis. The pathways downstream of mammalian target of rapamycin (mTOR) and the pathway activated by phosphorylating and thereby inhibiting glycogen synthase kinase 3 (GSK3) (Rommel et al., 2001). In the first case, AKT activates mTOR, that is a key regulator of cell growth, promoting the activation of S6 kinase (S6K) and blocking the inhibition of eif4e binding protein 1 (4EBP1) on eukaryotic translation initiation factor 4E (eif4e), thus leading to protein synthesis. In the other case, the inhibition of GSK3β from AKT stimulates proteins synthesis, since GSK3β normally blocks protein translation initiated by eIF2B protein (Glass, 2005). However, Akt is able to suppress catabolic pathways blocking protein degradation. IGF-1 treatment or AKT overexpression inhibits FoxO expression in myotubes and also prevents induction of atrophy mediators, Atrogin-1 and MuRF1 (Sandri et al., 2004; Stitt et al., 2004). Recently, it has been reported that also TGF-β pathway contributes to regulation of muscle mass in adulthood (Sartori et al., 2009). Activation of TGF-β signaling for example by myostatin treatment or overexpression was linked with decreased phosphorylation of Akt and other mTOR downstream target such as ribosomal protein S6, p70S6K and 4E-BP1 (Amirouche et al., 2009).

Bone morphogenetic protein (BMP) signalling, acting through Smad1, Smad5 and Smad8 (Smad1/5/8), is one of the fundamental hypertrophic signals in mice. In support of this, Sartori et al. showed that when the BMP pathway is blocked or myostatin expression is increased, more Smad4 is phosphorylated by Smad2/3, leading to an activation of atrophic pathway. Importantly, they identify a new E3 ubiquitin-ligase, named MUSA1, that is negatively regulated by BMP SMAD1-5-8 signal and is required for muscle mass loss. This work provided evidences that also BMP signalling is involved in the regulation of adult muscle mass in normal and pathological conditions (Sartori et al., 2013).

1.2.2 MUSCLE ATROPHY

The loss of muscle mass also known as muscle atrophy, is a complex process that occurs as a consequence of a variety of stressors, including neural inactivity, mechanical unloading, inflammation, metabolic stress, and elevated glucocorticoids. In 1969, Goldberg demonstrated that an increase in protein degradation contributed to the loss of muscle mass and myofibrillar proteins following denervation and glucocorticoid treatment (Goldberg, 1969). In all of these catabolic states, the loss of muscle mass involves a common pattern of transcriptional changes, including induction of genes for protein degradation and decreased expression of various genes involved in different cellular processes like energy production and various genes for growth-related processes. This group of coordinately regulated genes are called "atrogenes"(Lecker et al., 2006). Among the upregulated atrophy-related genes there is a subset of transcripts related to protein degradation pathways. In particular, there is a dramatic (8- to 40-fold) induction of two muscle-specific ubiquitin ligases, atrogin-1/MAFbx and MuRF-1, whose induction occurs before the onset of muscle weight loss and which is necessary for rapid atrophy (Gomes et al., 2001). Atrogin-1, also known as MAFbx, contains an F-box domain, a protein motif of approximately 50 amino acids that functions as a site of protein-protein interaction and belong to SCF

complex (Skp1, Cullin, F-box)(Gomes et al., 2001). The F-box protein interacts with the substrates, while Cul1-Roc1 components are associate with the E2 Ub-conjugating enzymes, finally Skp1 is an adaptor that brings F-box protein to the Cul1-Roc1-E2 complex. Most substrates require the phosphorylation to interact with the F-box protein in an SCF complex (Jackson and Eldridge, 2002). MuRF1 belongs to the RING finger E3 ligase subfamily, characterized by three RING-finger domains (Borden and Freemont, 1996) which are required for ubiquitin-ligase activity (Kamura et al., 1999). These domains include a B-box, whose function is still unknown, and a coiled-coil domain, which may be required for the formation of heterodimers between MuRF1 and a related protein, MuRF2. Knockout animals lacking either MuRF1 or atrogin-1 show a reduced rate of muscle atrophy after denervation (Bodine et al., 2001), confirming that these ligases are necessary for the atrophy program. The molecules and cellular pathways regulating skeletal muscle atrophy are still being discovered; however, tremendous progress has been made in the last decade to identify other key transcription factors, signaling pathways, and cellular processes involved in the initiation and sustained breakdown of muscle mass under a variety of conditions (Bodine and Baehr, 2014). Moreover, muscle loss is mediated by two highly conserved pathways: ubiquitin-proteasomal system (UPS) and autophagy-lisosomal pathway (ALP) and several evidences strongly support a major role of UPS during muscle loss.

1.3 PROTEIN DEGRADATION SYSTEMS

Eukaryotes have two major intracellular protein degradation pathways, namely the ubiquitin-proteasome system (UPS) and autophagy. Proteasomal degradation has high selectivity; the proteasome generally recognizes only ubiquitinated substrates, which are primarily short-lived proteins. By contrast, degradation by lysosome is specific for long-lived protein and in this case cytosolic components and organelles can be delivered to the lysosome by autophagy (Mizushima and Komatsu, 2011).

1.3.1 UBIQUITIN PROTEASOME SYSTEM

The Ubiquitin Proteasome System (UPS) is one of the mayor mechanism that control proteolysis and, ubiquitination of protein substrates. It is required to clear the cell from dysfunctional and altered proteins and is reported to increase during catabolic conditions. Through the concerted actions of a series of enzymes, proteins are marked for proteasomal degradation by being linked to the polypeptide co-factor, ubiquitin. The ubiquitination of protein substrates, occurs through the sequential action of distinct enzymes: E1(ubiquitin-activating enzyme), E2(ubiquitin-conjugating enzyme) and E3(ubiquitin-protein-ligase). The rate limiting enzyme of UPS is the E3 which catalyzes the transfer of ubiquitin from the E2 to the lysine in the substrate. This reaction is highly specific. Thus, the amount and the type of proteins degraded by the proteasome is largely determined by which E3 ligases are activated. This tagging process leads to their recognition by the 26S proteasome, a very large multicatalytic protease complex that degrades ubiquitinated proteins to small peptides (figure 6).

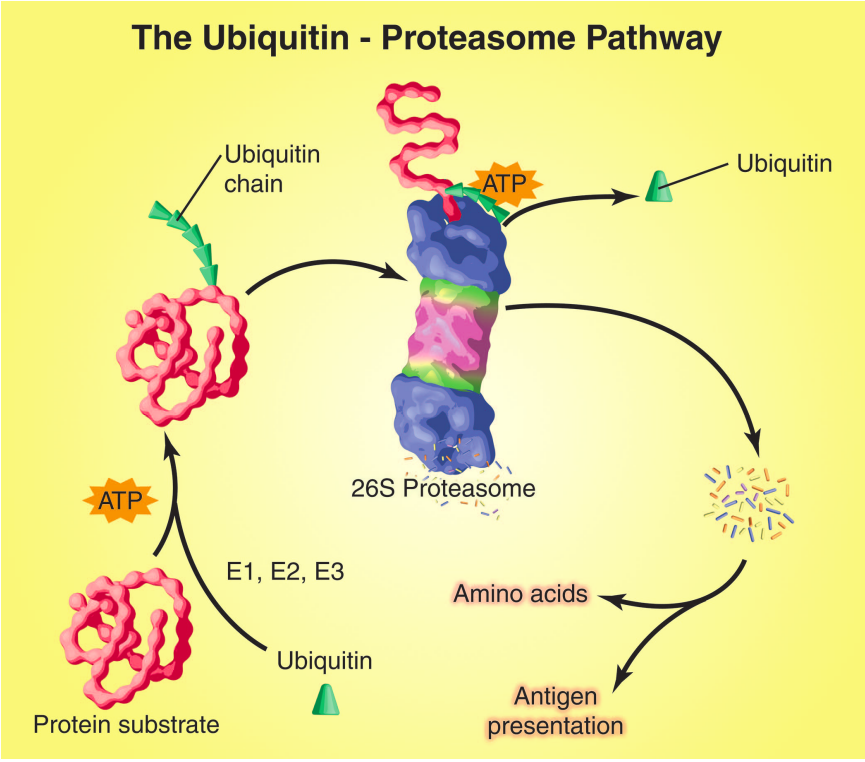

Fig.6: The ubiquitin (Ub)-proteasome pathway (UPP) of protein degradation.(Lecker et al., 2006)

The ubiquitin-proteasomal pathway is constitutively operative in normal skeletal muscle and is responsible for the turnover of most soluble and myofibrillar muscle proteins upon changes in muscle activity (Lecker et al., 2006). A decrease in muscle mass is associated with: (1) increased conjugation of ubiquitin to muscle proteins; (2) increased proteasomal ATPdependent activity; (3) increased protein breakdown that can be efficiently blocked by proteasome inhibitors; and (4) upregulation of transcripts encoding ubiquitin, some ubiquitin-conjugating enzymes (E2), a few ubiquitin-protein ligases (E3) and several proteasome subunits.

Moreover, among the different E3s, only a few have been found to regulate atrophy process and to be transcriptionally induced in atrophying muscle**.** The first to be identified were Atrogin-1/MAFbx and MuRF1. These two E3s are specifically expressed in striated and smooth muscles. Atrogin-1/MAFbx and MuRF1 knockout mice are resistant to muscle atrophy induced by denervation (Bodine et al., 2001), while knockdown of Atrogin-1 spare muscle mass in fasted animals (Cong et al., 2011).

Since two ubiqutin ligases cannot effort for the degradation of all the sarcomeric and soluble proteins, additional E3s are involved in muscle loss in fact the characterization of these E3s and their respective substrates in skeletal muscle atrophy might be an important step to understand the mechanisms that control muscle mass loss and, moreover, to develop targets for pharmacological intervention in muscle disease.

1.3.2 AUTOPHAGY-LYSOSOMAL SYSTEM

Autophagy is an evolutionarily conserved process that is induced under nutrient poor conditions to allow cells to degrade and recycle the breakdown products that are released into the cytoplasm, where they presumably provide a source of metabolites to support biosynthesis and other processes. Autophagy is also responsible for the degradation of protein aggregates, which would otherwise accumulate and cause cytotoxicity. Three main types of autophagy exist: chaperone-mediated autophagy, microautophagy, and

macroautophagy, all of which function to deliver intracellular contents to the lysosome (figure 7). In chaperone-mediated autophagy, cytosolic proteins are selectively and individually transported into the lysosome for degradation. In microautophagy, a portion of the cytoplasm is directly engulfed by the lysosome. In macroautophagy (hereafter referred to as autophagy), cytoplasmic components including proteins and organelles, are engulfed by double-membrane structures known as autophagosomes, which fuse to lysosomal vesicles where the contents are degraded into their components (for example, from proteins to aminoacids).

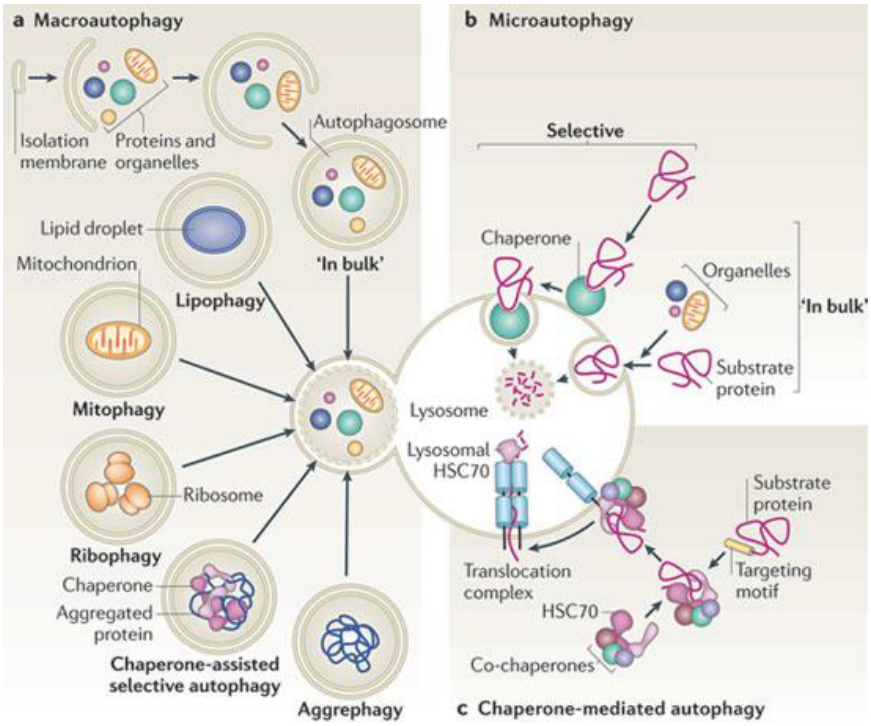

Fig.7: Scheme of the different type of autophagy: macroautophagy (a), microautophagy (b), chaperone-mediated autophagy (c) (Cuervo, 2011).

In addition, autophagy can be upregulated during metabolic, genotoxic, or hypoxic stress conditions and acts as an adaptive mechanism essential for cell survival. The generation of transgenic mice for LC3, the mammalian homolog of the essential autophagy gene Atg8, fused with GFP defined the amount of autophagy in different tissues and the capacity of different organs to respond fasting by activating autophagosome formation. Indeed, skeletal

muscle has been found to be one of the tissues with the highest induction of autophagy. In fast skeletal muscle of transgenic mice, food deprivation induced the rapid appearance of cytoplasmic fluorescent dots, corresponding to autophagosomes (Mizushima et al., 2004). Skeletal muscle is a major site of metabolic activity and serves as a source of aminoacids because during catabolic periods amino acids generated from muscle protein breakdown are utilized by the liver to produce glucose and to support acutephase protein synthesis (Lecker et al., 2006). This role in recycling is complementary to that of the ubiquitin-proteasome system, which degrades proteins to generate oligopeptides that are subsequently degraded into amino acids (Lecker et al., 2006). Restoration of cellular (or local) levels of amino acids reactivates the serine/threonine protein kinase mTORC1 (mammalian target of rapamycin complex 1) and terminates autophagy (Yu et al., 2010). Autophagy is suppressed by mTOR, which is in turn controlled directly by the level of intracellular amino acids and indirectly by growth factors via Akt/PKB and cell energy status via AMPK. Accordingly, rapamycin, a specific inhibitor of mTOR, activates autophagy. However, autophagy can also be induced by mTOR-independent mechanisms: leucine starvation has been reported to induce mTOR-independent autophagy in cultured myotubes (Mordier et al., 2000). Autophagy is induced in skeletal muscle in the immediate post-natal period when glycogen-filled autophagosomes are abundant (Schiaffino and Hanzlikova, 1972). The crucial role of autophagy in the newborn is demonstrated by the finding that mice deficient in autophagy genes Atg5 or Atg7 die soon after birth during the critical starvation period when transplacental nutrient supply is suddenly interrupted (Komatsu et al., 2005; Kuma et al., 2004). Autophagy is also implicated in wide range of diverse human diseases, plays a role also in muscular disorders, such as Pompe and Danon disease and X-linked myopathy, liver diseases and pathogen infection (Levine and Kroemer, 2008). In particolar in skeletal muscle, both excessive and defective autophagy are highly correlated with the loss of muscle mass (Petrovski and Das, 2010), instead muscle atrophy can be a consequence of lack of autophagy, shown through muscle-specific ablation of the *Atg7* gene

(encoding autophagy-related protein-7) (Masiero et al., 2009) or the *Atg5* gene (Raben et al., 2008), two key autophagy genes; although in Atg5-deficient muscle, pathology was less severe. Moreover, Grumati *et al*. showed that muscle atrophy in *Col6a1*-deficient mice (models of Bethlem myopathy and Ullrich congenital muscular dystrophy (UCMD) was ameliorated by a low-protein diet and by genetic and pharmacologic approaches that can activate autophagy. Indeed, loss of collagen-6 leads to an activation of Akt, which decreases autophagy through inactivation of the transcription factor FoxO3 and activation of mTOR (Grumati et al., 2010).

1.4 THE FoxO FAMILY OF TRASCRIPTION FACTORS

The FoxO family is a subclass of Forkhead transcription factors. In humans, Forkhead proteins (Fox) have been divided on the basis of sequence similarity, into 19 subgroups which are classified by alphabetic letters form A to S. Fox proteins contain a sequence of 80–100 amino acids forming a motif that binds to DNA: the forkhead motif. This motif is also known as the winged helix due to the butterfly like appearance of the loops in the protein structure of the domain (Kaestner et al., 2000). FoxO subfamily is conserved from *Caenorhabditis elegans* to mammalians. In addition to the forkhead DNA-binding-domain motif, FoxO factors contain a nuclear localization sequence (NLS), a nuclear export sequence (NES), and a transactivation domain in their C terminal region in which a helical motif (LXXLL, where L is a leucine and X any amino acid) is quite important for FoxO transcriptional activity (Nakae et al., 2006). Importantly, FoxO1, 3 and 6 proteins have similar length of approximately 650 amino-acid residues, whereas FoxO4 sequence is shorter and contains about 500 amino-acid residues (Figure 8). Analysis of multiple sequence alignment shows that several regions of FoxO proteins are highly conserved. The regions which display the highest sequence homology include N-terminal region surrounding the AKT phosphorylation site (Thr32), the DBD (Dna binding domain), the region containing (NLS) and the COOH-terminal trans activation domain (Obsil and Obsilova, 2008). Because the

DNA binding domain is shared, FoxOs should bind similar or identical DNA sequences within the genome. The core of consensus sequence has been determined by using gel shift experiments and it has the following sequence: 5'-TTGTTTAC-3'. The members of the forkhead box class O (FoxO) subfamily are involved in several physiological and pathological processes, including aging, cancer, and neurological diseases and regulate metabolism, cellular proliferation, apoptosis, stress tolerance and possibly lifespan, thus they are highly conserved through evolution.

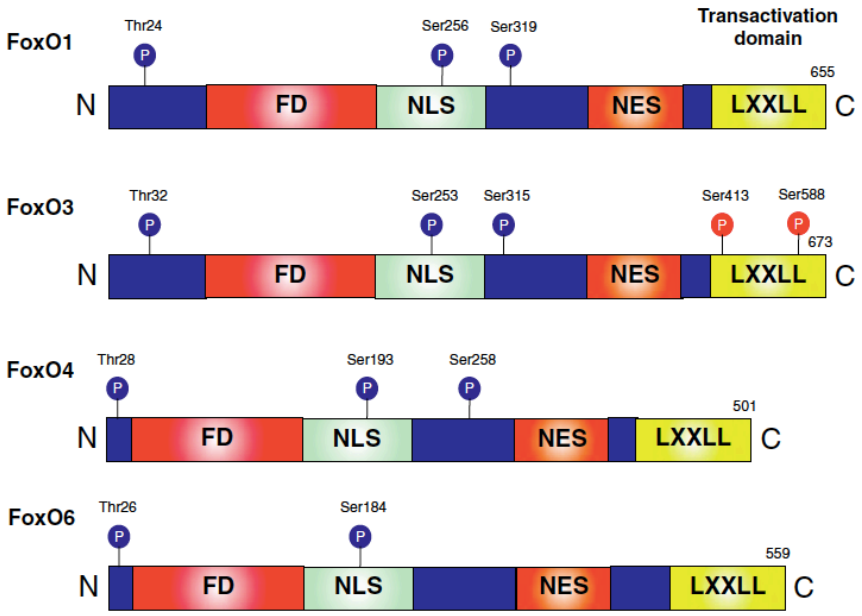

Fig.8; Description of mammalian FoxO proteins expressed in skeletal muscle. The following are indicated: locations of the forkhead domain (FD), nuclear localization sequence (NLS) nuclear export sequence (NES)and helical motif (LXXLL),Akt phosphorylation sites (blue circles) and AMPK phosphorylation sites (red circles) (Sanchez et al., 2014).

Caenorhabditis elegans and Drosophila each possess one FoxO factor, whereas the mammalian FoxO family comprises four members (FoxO1, FoxO3, FoxO4, and FoxO6) that mainly differ in their tissue-specific expression. Nonetheless, it is notable that, contrary to FoxO1,3 and 4, which are expressed relatively ubiquitously, FoxO6 is expressed predominantly in the central nervous system (Salih et al., 2012), although it is also present in oxidative muscles (Chung et al., 2013). All these trascription factors are

inhibited by growth factor signaling. In the presence of insulin and insulin like growth factor (IGF) the phosphoinositide 3 kinase (PI3K)-AKT signaling pathway is activated and protein Kinase AKT directly phosphorilates FoxO factors at three conserved residues, resulting in FoxO exclusion from the nucleus and repression of transcriptional activity (Brunet et al., 1999). An exception is FoxO6, which is phosphorylated at only 2 of three phosphorylation sites and it is not regulated by nucleus cytoplasmic shuttling (Jacobs et al., 2003). In the absence of insulin or growth factor signaling, or during starvation, FoxOs translocate to the nucleus where they activate programs of gene expression. On the other hand, also the adenosine monophosphate-activated-protein kinase (AMPK), positively regulated by stimuli that decrease cellular energy levels, phosphorylates FoxO3 at six regulatory sites (Thr-179, Ser-399, Ser-413, Ser-355, Ser-588, and Ser-626) in vitro and promotes its activation (Greer et al., 2007) (figure 9).

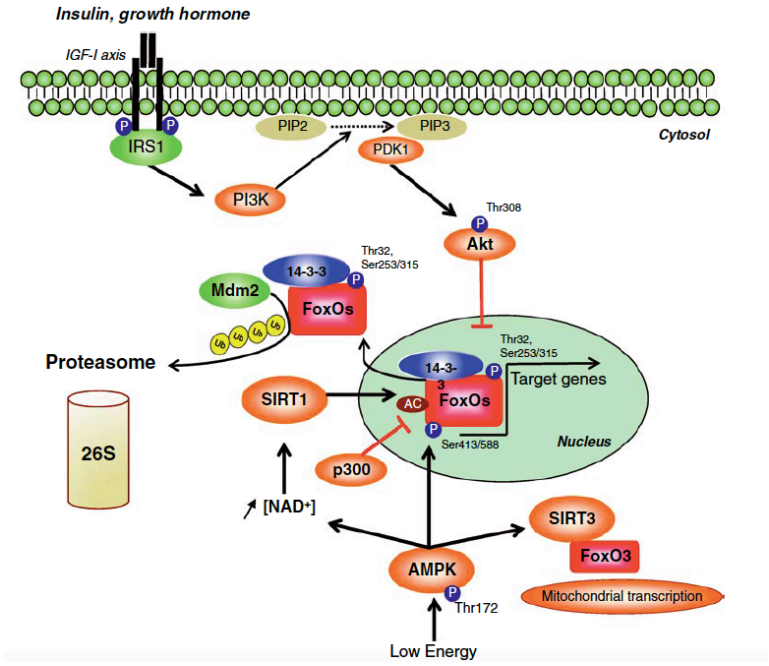

Fig.9; Antagonist regulation of FoxO proteins by the IGF-1/ PI3K/Akt axis and AMPK (Sanchez et al., 2014).

Moreover, AMPK activation is associated with increasing levels of FoxO1 and FoxO3 mRNAs and protein content. FoxOs are targeted for phosphorylation by a plethora of protein kinases in different residues. Each kinase modifies

different sites on FoxOs and results in different changes in FoxO functions. These include JNK (Essers et al., 2004), MST1 (Lehtinen et al., 2006), ERK and p38 MAPK (Asada et al., 2007). This results in different type of post-translational modifications (PTMs) such as acetylation/deacetylation, mono or polyubiquitination, glycosylation and arginine and lysine methylation (Eijkelenboom and Burgering, 2013). These post-translational modifications (PTMs) modify their transcriptional activities and also regulate the subcellular localization of FoxO family proteins, as well as their half-life, DNA binding, transcriptional activity and ability to interact with other cellular proteins. Like phosphorylation, acetylation also regulates different FoxO protein functions. Multiple deacetylases and acetylases have been identified to modify FoxOs to change their DNA-binding activity, stability and interaction with other proteins. FoxOs can be deacetylated by sirtuins and HDACs; however, the exact effect of FoxO deacetylation is still not clear. Sirt1, an NAD-dependent class III HDAC, deacetylates FoxO3 and forms a complex with FoxO3 in response to oxidative stress (Brunet et al., 2004). However, the acetylation of FoxOs attenuates FoxO-mediated transcriptional activity. For example, peroxide stress induces the binding of CBP to FoxO4 and acetylates FoxO4, leading to the inhibition of FoxO4 transcriptional activity (van der Horst et al., 2004). Recently, Bertaggia and colleagues have demonstrated in skeletal muscle that FoxO3 interacts with the histone acetyl-transferase p300, and its acetylation causes cytosolic relocalization and degradation. In particular they founded lysine 262 critical for FoxO3 activity (Bertaggia et al., 2012). Moreover, others have confirmed the negative action of p300 and CBP on FoxOs in skeletal muscle. In fact overexpression of HAT in soleus muscle inhibits FoxO3 and FoxO4 action while has no effect on FoxO1 (Senf et al., 2011) (figure 10).

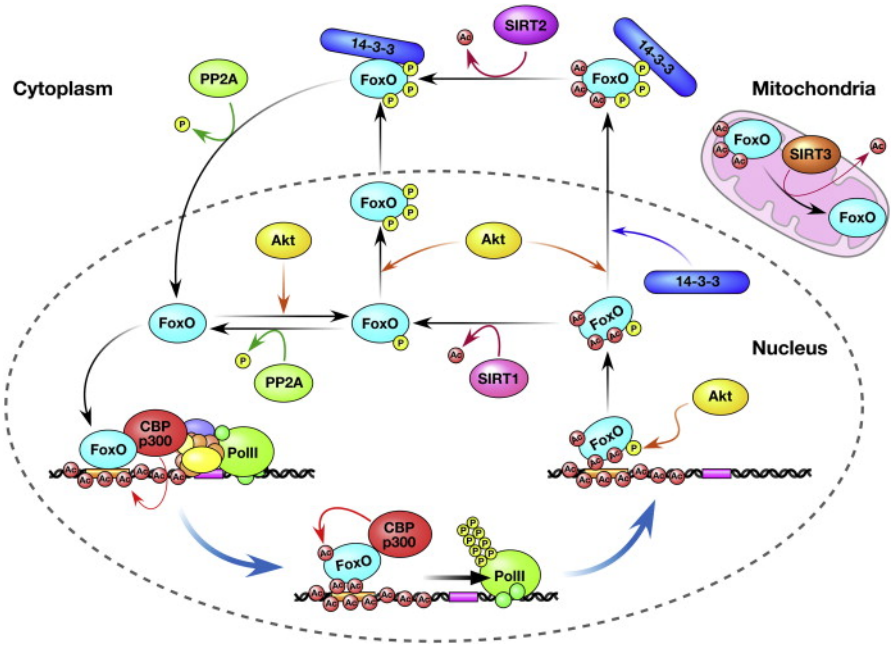

Fig.10; Schematic model for the regulation of FoxO transcription factors by reversible phosphorylation and acetylation (Daitoku et al., 2011).

The degradation of FoxOs is mediated by the ubiquitin- proteasome pathway. It has been shown that FoxO proteins are also subject to poly- and mono-ubiquitination. The most important regulators of FoxOs trascription factor degradation are several E3 ubiquitin ligases: Skp2, a subunit of the skp1/cul1/F-box protein that ubiquitinates and promotes the degradation of FoxO1 when it is phosphorylated by Akt (Huang et al., 2005), MDM2 an ubiquitin ligase specific for p53 which is able to bind FoxO1 and 3 to promote their poly-ubiquitination and degradation (Fu et al., 2009). As I mentioned, MDM2 is considered to be an E3 that promotes FoxO1-3 poly-ubiquitination, recent findings have shown that MDM2 also promotes FoxO4 nuclear localization and increases transcriptional activity under oxidative stress (Brenkman et al., 2008). The diversity of this upstream regulation and the downstream effects of FoxOs suggest that they function as homeostasis regulators to maintain tissue homeostasis over time and coordinate a response to environmental changes, including growth factor deprivation, metabolic stress (starvation) and oxidative stress. Nevertheless, depending of their activation level, FoxO proteins can exhibit ambivalent functions. For

example, a basal level of FoxO factors are necessary for cellular homeostasis and also to maintain quality control. However, exacerbated activation may occur in the course of several diseases, resulting in metabolic disorders and atrophy.

1.5 REGULATION OF SKELETAL MUSCLE HOMEOSTASIS BY FoxO PROTEINS.

Skeletal muscle shows singular adaptive capabilities in response to such stimuli as nutritional interventions, environmental factors (hypoxia), loading conditions, and contractile activity. All of these stimuli induce changes in energy metabolism and muscle mass, especially by altering the balance between protein synthesis and protein degradation or fiber composition.
For this reason, FoxO trascription factors are increasingly taken into consideration. Four FoxO family members are expressed in mammals, FoxO1 (also known as FoxO1a), FoxO3 (also known as FoxO3a), FoxO4, and FoxO6, and all of them are expressed in skeletal muscles. Emerging evidence from multiple systems indicate that FoxOs orchestrate the expression of genes involved in cellular quality control, and in particular the protein homeostasis (proteostasis) network. The regulation of these proteins, especially their dynamic control by two major actors in skeletal muscle homeostasis, AKT and AMPK, are specific, as is the implication of each FoxO member in the regulation of cellular processes in response to physiological and pathophysiological conditions. In particular, FoxO1 and FoxO3 play a crucial role in the regulation of skeletal muscle mass and homeostasis.

1.5.1 FoxO1 AND FoxO3 REGULATE ENERGY METABOLISM IN SKELETAL MUSCLE.

The skeletal muscle is one of the major peripheral tissues that are responsible for insulin-mediated fuel metabolism and energy expenditure. Skeletal muscle accounts for >30% of resting metabolic rate and 80% of

whole-body glucose uptake. FoxO1 is particularly involved in the regulation of energy metabolism in muscle, indeed it maintains energy homeostasis during fasting and provides energy supply through breakdown of carbohydrates, a process that leads to atrophy and underlies glycemic control in insulin resistance.

Expression of FoxO1 is increased in skeletal muscle by energy deprivation (such as fasting, calorie restriction, and severe diabetes), suggesting that FoxO1 may mediate the response of skeletal muscle to changes in energy metabolism. Skeletal muscle metabolism switches from oxidation of carbohydrates to fatty acids as the major energy source during fasting when the plasma glucose concentration is low. FoxO1 controls this switch by upregulating 3 enzymes: pyruvate dehydrogenase kinase-4 (PDK4) that shuts down glucose oxidation by targeting pyruvate dehydrogenase (PDH) (Furuyama et al., 2003), lipoprotein lipase that hydrolyzes plasma triglycerides into fatty acids, and fatty acid translocase CD36 that facilitates fatty acid uptake into skeletal muscle (Bastie et al., 2005). Last, FoxO1 regulates the expression of adipon.ectin receptors (AdipR), which transmit a signal for increased fatty acid oxidation in muscle and adiponectin sensitivity (Tsuchida et al., 2004) (figure 11).

Concerning FoxO3, its role in mitochondrial energy metabolism under nutrient restriction has recently been assessed (Peserico et al., 2013). Specifically, Peserico et all showed that in myoutubes a low glucose condition leads FoxO3 accumulation into mitochondria in an AMPK dependent manner. In this way, FoxO3 is able to form a multicomplex with SIRT3 (a specific mitochondria sirtuin), mitochondrial RNA polymerase at mitochondrial DNA-regulatory regions (mtDNA-RR) and regulates mitochondrial transcription . In summary, in the FoxO family, FoxO1 appears to be the major regulator of muscle energy homeostasis through the regulation of glycolytic and lipolytic flux. Importantly, the function of FoxO3 in mitochondrial metabolism is emerging. The involvement of FoxO4 and 6 in skeletal muscle energy metabolism still remains to be characterized (Sanchez et al., 2014).

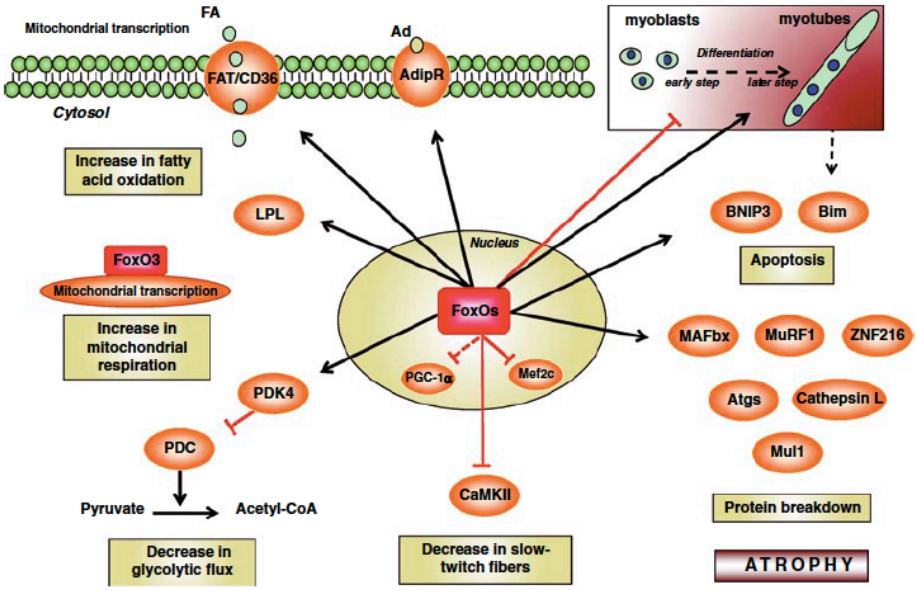

Fig 11: Metabolic regulation by FoxO1 and FoxO3 in skeletal muscle (Sanchez et al., 2014).

1.5.2 FoxO1 AND FoxO3 GOVERN PROTEIN BREAKDOWN

Cross-talk between protein breakdown and protein synthesis is necessary to maintain muscle mass. The role of FoxO transcription factors in the regulation of skeletal muscle protein degradation it has well studied. Activation of FoxO1 or FoxO3 in the skeletal muscle, in catabolic conditions, can increase protein breakdown through ubiquitin-proteasome and autophagy-lysosome pathways, the 2 major mechanisms causing muscle atrophy. The ubiquitin–proteasome system is assumed to play a major role in muscle protein degradation since the discovery of two E3 ubiquitin ligases, MAFbx/atrogin-1 and MuRF1, which are overexpressed in various atrophy models. The function of E3 ubiquitin ligases is to target specific protein substrates for degradation by the 26S proteasome and FoxO1 and 3 are required for the transcription of MAFbx/atrogin-1 and MuRF1.

In vivo studies of FoxO1 inactivation or overexpression have showed that it affects to a great extend skeletal muscle mass. Mice overexpressing FoxO1 lose their glycemic control due to a decrease in skeletal muscle mass (Kamei et al., 2004). These effects of FoxO1 are mediated by its actions in three genes, *atrogin-1* and *myostatin* and *4E-binding protein-1*. FoxO1 promotes the expression of *atrogin-1*, a muscle-specific ubiquitin ligase which along with MuRF1 controls muscle atrophy (Sandri et al., 2004). Indeed, inactivation of FoxO1 in myotubes or rodent muscle decreases both muscle atrophy and *atrogin-1* expression. In addition, constitutive activation of FoxO1 in the same cells enhances the transcriptional activity of myostatin, another muscle-specific protein causing muscle loss, through direct binding of FoxO1 to the myostatin promoter (Allen and Unterman, 2007). Finally, FoxO1 induces the translational inhibitor 4E-binding protein-1 by binding to its promoter, thereby suppressing protein synthesis (Southgate et al., 2007). FoxO3 is the master regulator of autophagy in adult muscles (Mammucari et al., 2007). Expression of FoxO3 is sufficient and required to activate lysosomal-dependent protein breakdown in cell culture and in vivo. However, the role of FoxOs trascription factors in the control of autophagy induction, today is not completely defined. Moreover several autophagy genes including LC3, Gabarap, Bnip3, VPS34, Atg12 are under FoxO3 regulation. Gain and loss of function experiments identified BNIP3, a BH3-only protein, as a central player downstream of FoxO in muscle atrophy (Mammucari et al., 2007; Tracy et al., 2007). These studies allowed to identify the most potent autophagy inhibitor in skeletal muscles: AKT kinase. Acute activation of AKT in adult mice or in muscle cell cultures completely inhibits autophagosome formation and lysosomal-dependent protein degradation during fasting (Mammucari et al., 2007; Zhao et al., 2007; Zhao et al., 2008). A clear pathway has been identified in muscle, as we know in presence of nutrients IGF1/Insulin signalling pathway is activated, this leads to the activation of AKT. When AKT is phosphorylated (P-AKT), it activates mTOR, thus increasing protein synthesis rate, and blocking autophagy; on the contrary, P-AKT phosphorylates FoxO, that in this way is sequestered in the

cytosol, and its transcriptional action is blocked, leading to autophagy inhibition. When FoxO is in the nucleus can promote transcription of several genes, in particular some autophagy genes such as *Bnip3*, *LC3* and *p62*, leading to autophagy activation. These evidences suggest that FoxOs factor control the skeletal muscle ubiquitin-proteasome and autophagy–lysosomal pathways independently. Moreover, Zhao et colleagues demostrate that decreased IGF-1-PI3K-Akt signaling activates autophagy not only through mTOR but also more slowly by a transcription-dependent mechanism involving FoxO3. Whereby, expression of a constitutively active form of FoxO3 promotes LC3 lipidation, mimic induction of autophagy (Zhao et al., 2007). Furthermore, overexpression of FoxO3 in cultured mammalian cells leads to a fourfold increase in glutamine synthetase activity and subsequent increase in glutamine levels. Thus, high glutamine levels induce autophagy at least in part by blocking the mTOR pathway (van der Vos et al., 2012) (figure 12).

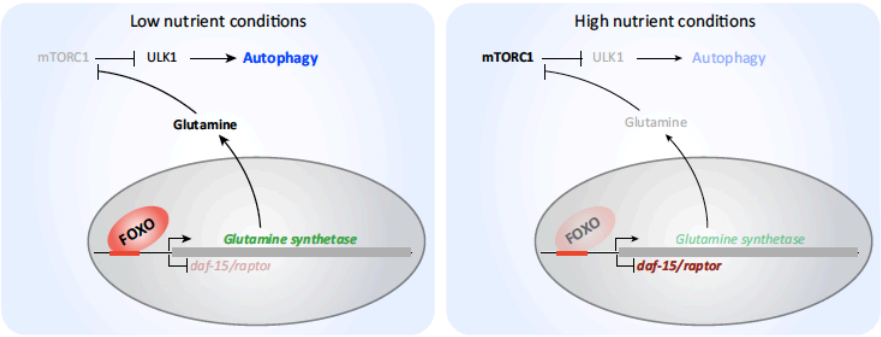

Fig 12; Antagonistic interaction between FOXOs and the mTORC1 pathway in autophagy. (Webb and Brunet, 2014).

Moreover, FoxO1 directly targets cathepsin L, a lysosomal protease in muscle, and induces its expression during fasting connoting a role of FoxO factors in lysosomal degradation (Yamazaki et al., 2010). Although the implication of FoxO proteins in the transcription lysosomal hydrolases has been partially described, their potential role in the genesis of lysosomes has not been investigated. Similarly, the potential role of FoxO1 in skeletal muscle autophagy remains to be characterized.

1.5.3 REGULATION OF MUSCLE MASS BY FoxO TRASCRIPTION FACTORS

The maintenance of muscle mass is achieved by a dynamic balance between atrophy and hypertrophy. Skeletal muscle atrophy occurs under a variety of conditions and can result from alterations in both protein synthesis and protein degradation. Activation of the cell's proteolytic systems is transcriptionally regulated by specific signalling pathways but the identification of the precise signalling cascades that direct muscle wasting is only at the initial phase. Gene expression studies revealed a set of genes which are commonly up- and down-regulated in different atrophying conditions. These genes are called atrophy-related-genes or *atrogenes* (Sacheck et al., 2007). Among these atrophy-related genes were several belonging to the major cellular degradation systems, the ubiquitin proteasome and autophagy-lysosome. FoxO transcription factors are key regulators of muscle atrophy indeed, the up-regulation of several ubiquitin–proteasome and autophagy-related genes is normally blocked by Akt through negative regulation of FoxO. The first ubiquitin ligases that were identified to play a role in muscle loss were Atrogin-1/MAFbx and MuRF1 as I said before. Mice lacking these two enzymes are partially resistant to muscle atrophy induced by denervation (Bodine et al., 2001). However, the action of these two ubiquitin ligases can not account for the degradation of all muscle proteins. A number of additional unknown ubiquitin ligases (E3s) are presumably activated during atrophy to promote the clearance of myofibrillar and soluble proteins and/or to limit anabolic processes. Sandri et al, were the first to discover that FoxO3 was sufficient to induce muscle loss through its induction of Atrogin-1/MAFbx and MURF1 expression. Importantly, in subsequent work, was found that inactivation of autophagic flux by LC3 silencing partially prevents FoxO3 mediated muscle loss, suggesting the major role of the autophagic pathway in FoxO3 mediated atrophy (Mammucari et al., 2007).

Thus, FoxO1 and FoxO3 act through an exacerbation of the ubiquitin-proteasomal and autophagy–lysosomal degradation pathways in muscle

atrophy. Moreover, FoxO factors, especially FoxO3, are involved in mitochondrial dysfunction and elimination by regulating the mitophagic pathway under atrophy. Although all these findings support the concept that FoxO family plays an important role in muscle wasting, the specific function of FoxOs in skeletal muscle maintenance/loss and in atrogenes expression has not been determined by loss-of-function approaches.

1.6 AIM OF THE WORK

Skeletal muscle is a plastic tissue and adapts its mass as a consequence of physical activity, metabolism and hormones. Maintenance of skeletal muscle mass is essential for health and survival. A decrease in protein synthesis and an increase in protein degradation have been shown to contribute to muscle protein loss. In my lab we focus our attention on the study of the signaling pathways that control muscle mass and cause muscle atrophy. In this condition proteolitic pathways, such as Ubiquitin proteasome system (UPS) and Autophagy lysosome system (ALS), are activated and the transcription factors FoxO1 and FoxO3 has been demonstrated to be involved in the regulation of their components.

The aim of my PhD project is focused on the characterization of the role of FoxOs transcription factors in skeletal muscle. In order to clarify this issue, we used muscle-specific FoxO1-3-4 deficient mice and also inducibile muscle specific FoxOs knock-out mice to minimize the chance of any adaptation and compensations that occur with constitutive deletion of genes. Throught loss of function approaches we want to understand which are the FoxO target genes necessary for maintaining an atrophy program and the function of these genes in skeletal muscle during catabolic conditions.

2. MATERIALS AND METHODS

2.1 GENERATION OF MUSCLE-SPECIFIC FoxO1-3-4 KNOCKOUT MICE

Muscle-specific FOXO1,3,4 knockout mice were obtained in my lab. Mice bearing FoxO1,3,4-floxed alleles (FoxO1,3,4f/f) were crossed with transgenic mice expressing Cre either under the control of a Myosin Light Chain 1 fast promoter (MLC1f-Cre) that is expressed only in skeletal muscle during the embryonic development, (Bothe et al., 2000). To obtain inducible muscle-specific FOXO1,3,4 knockout mice, flox/flox mice were crossed with transgenic mice expressing a Cre-recombinase fused with a modified estrogen receptor domain (Cre-ERTM) driven by Human Skeletal Actin promoter (HSA) (Schuler et al., 2005). Tamoxifen-inducible Cre was activated by special tamoxifen diet (Tam400/Cre-ER Harlan) or by i.p. Tamoxifen injection.

2.1.1 Genotyping of muscle specific FoxO1-3-4 knockout mice

Mice were identified by analyzing the presence of Cre recombinase on genomic Dna. To extract Dna we used a lysis buffer containing TRIS-HCL 1M pH 7.5 and Proteinase K 10mg/mL (Life Technologies). The samples were denaturated by incubation for 1 hour at 57°C and then the proteinase K was inactivated at 99°C for 5 minutes. Genomic DNA isolated from FoxO1,3,4f/f mice was subjected to PCR analysis. Cre-mediated recombination was confirmed by PCR with genomic DNA from gastrocnemius muscles using the primers :

Cre forward: NSP-780: CACCAGCCAGCTATCAACTCG
Cre reverse: NSP-979: TTACATTGGTCCAGCCACCAG

We prepared a 20 µl total volume mix for each sample with:

Template DNA: 2 µl

Primer NSP-780 (10 µM): 0.2 µl

Primer NSP-979 (10 µM): 0.2 µl

GoTaq Green master mix 2X (Promega): 10 µl

Water

Program:

step 1: 94° C for 3 minutes

step 2: 94° C for 45 seconds

step 3 61° C for 30 seconds

step 4 72°C 1 minute

step 5: go to step 2 for 40 times

We detected Cre-recombinase DNA (200 bp) with a 2% agarose gel.

The genotyping analysis for each specific FoxO member was performed with the combination of the following primers:

FoxO1 forward: GCT TAG AGC AGA GAT GTT CTC ACA TT,

FoxO1 reverse1: CCA GAG TCT TTG TAT CAG GCA AAT AA

FoxO1 reverse2: CAA GTC CAT TAA TTC AGC ACA TTG A

FoxO3 forward1: AGA TTT ATG TTC CCA CTT GCT TCC T-

FoxO3 forward2: TGC TTT GAT ACT ATT CCA CAA ACC C

FoxO3 reverse: ATT CCT TTG GAA ATC AAC AAA ACT

FoxO4 forward1: TGA GAA GCC ATT GAA GAT CAG A

FoxO4 forward2: CTA CTT CAA GGA CAA GGG TGA CAG

FoxO4 reverse: CTT CTC TGT GGG AAT AAA TGT TTG G

2.2 ANIMALS and *In vivo* TRASFECTION EXPERIMENTS.

Animals were handled by specialized personnel under the control of inspectors of the Veterinary Service of the Local Sanitary Service (ASL 16—Padova), the local officers of the Ministry of Health. Mice were housed in individual cages in an environmentally controlled room (23 °C, 12-h light–dark cycle) with ad libitum access to food and water. All procedures are specified in the projects approved by the Italian Ministero Salute, Ufficio VI (authorization numbers C65) and by the Ethics Committee of the University of Padova. All experiments were performed on 2- to 4-month-old male (28–32g) and female mice (25–28g); mice of the same sex and age were used for

each individual experiment. In vivo transfection experiments were performed by i.m. injection of expression plasmids in TA muscle followed by electroporation. The animals were anesthetized by an intraperitoneal injection of xylazine (Xilor) (20 mg/Kg) and Zoletil (10 mg/Kg). Tibialis anterior (TA) muscle was isolated through a small hindlimb incision, and DNA was injected along the muscle length. Electric pulses were then applied by two stainless steel spatula electrodes placed on each side of the isolated muscle belly (50 Volts/cm, 5 pulses, 200 ms intervals). For fasting experiments, control animals were fed ad libitum; food pellets were removed from the cages of the fasted animals. Denervation was performed by cutting the sciatic nerve of the left limb, while the right limb was used as control. Muscles were removed at various time periods after transfection and frozen in liquid nitrogen for subsequent analyses.

2.3 CUT OF THE SCIATIC NERVE

The right hindlimbs of 3 months old mice were denervated cutting the sciatic nerve unilaterally. The animals were anesthetized by an intraperitoneal injection of ketamine (75 mg/Kg) and xylazine (20 mg/Kg). The sciatic nerve was unilaterally cut at the level of trochanter. About 0.5-1 cm of the peripheral nerve stump was removed and the proximal stump was sutured into a superficial muscle to avoid reinnervation and obtain a permanent denervation of the lower hindlimb. Mice were sacrificed 3 days after operation, for gene expression analyses, or after 14 days for biochemestry analyses.

2.4 MEASUREMENTS OF MUSCLE FORCE *IN VIVO*

Muscle force was measured in a living animal as previously described (Blaauw et al., 2008). We performed this experiment in collaboration with Bert Blaauw (VIMM, Padua). Briefly gastrocnemius (GCN) muscle contractile performance was measured *in vivo* using a 305B muscle lever system

(Aurora Scientific Inc.) in anaesthetized mice. Contraction was elicited by electrical stimulation of the sciatic nerve. Force generation capacity was evaluated by measuring the absolute maximal force that was generated during isometric contractions in response to electrical stimulation (frequency of 75–150 Hz, train of stimulation of 500 ms). Maximal isometric force was determined at L0 (length at which maximal tension was obtained during the tetanus). Force was normalized to the muscle mass as an estimate of specific force. Following force measurements, animals were killed by cervical dislocation and muscles were dissected, weighed and frozen in liquid nitrogen or in isopentane precooled in liquid nitrogen. Ex vivo force measurements on soleus muscles were performed by dissecting it from tendon to tendon under a stereomicroscope and subsequently mounting between a force transducer (KG Scientific Instruments, Heidelberg, Germany) and a micromanipulator-controlled shaft in a small chamber, in which oxygenated Krebs solution was continuously circulated and temperature was maintained at 25 °C. The stimulation conditions were optimized, and the length of the muscle was increased until force development during tetanus was maximal.

2.5 MEASUREMENT *IN VIVO* OF PROTEIN SYNTHESIS

In vivo protein synthesis was measured by using the SUnSET technique (Goodman et al., 2011; Schmidt et al., 2009). Mice were anesthetized and then an i.p. injection of 0.040 mmol/g puromycin was dissolved in 100 ml of PBS was given. At exactly 30 min after injection, tissues were collected and frozen in liquid N2 for immunoblot analysis with a mouse IgG2a monoclonal anti-puromycin antibody (clone 12D10, 1:5,000).

2.6 HISTOLOGY ANALYSES AND FIBRE SIZE MEASUREMENTS

Muscles were collected and directly frozen by immersion in liquid nitrogen. Then we cut muscle cryosections by using Cryostat (Leica CM 1950), 10µm thick for histology and for immunostaining analyses. TA Cryosections, 10µm

thick, were used to analyze tissue morphology with different methods, listed below. Images were collected with an epifluorescence Leica DM5000B microscope, equipped with a Leica DFC300-FX digital charge-coupled device camera, by using Leica DC Viewer software. For electron microscopy, we used conventional fixation-embedding procedures based on glutaraldehyde-osmium fixation and Epon embedding.

2.6.1 Haematoxylin and Eosin staining (H&E)

Haematoxylin colors basophilic structures that are usually the ones containing nucleic acids, such as ribosomes, chromatin-rich cell nuclei, and the cytoplasmc regions rich in RNA. Eosin colors eosinophilic structures bright pink. The method consist of:

Materials	Times
PFA 4%	**10 minutes**
3 washs in PBS	**5 mintes each**
Harris Hematoxylin (SIGMA)	**6 minutes**
Wash in running tap water	**3 minutes**
Alcoholic acid	**10 seconds**
Wash in running tap water	**3 minutes**
Eosin Y Solution Alcoholic (SIGMA)	**1 minute**
Dehydratation	
Ethanol 70%	**5 minutes**
Ethanol 95%	**2 minutes**
Ethanol 100%	**3 minutes**
Xilen 1	**5 minutes**
Xilen 2	**5 minutes**
Mount with Entellan	

2.6.2 Succinate dehydrogenase (SDH)

The succinate dehydrogenase is an enzyme complex, bound to the inner mitochondrial membrane. With this staining it is possible to evaluate approximately the quantity of mitochondria present in the muscle fibres, through colorimetric evaluation. The reaction gives a purple coloration in the oxidative fibres. The sections were incubated for 30 minutes at 37°C with SDH solution (0.2M sodium succinate) (Sigma-Aldrich), 0.2M phosphate buffer (Sigma) ph 7.4 and 50mg of nitro blue tetrazolium (NBT)(Sigma-Aldrich). After the incubation, the sections were washed 3 minutes with PBS and then mounted with Mounting medium (Dako).

2.5.3 Periodic acid-Schiff (PAS)

This method is used to identify glycogen in tissues. The reaction of periodic acid selectively oxidizes the glucose residues, creates aldehydes that react with the Schiff reagent and creates a purple-magenta color. A suitable basic stain is often used as a counter stain. The sections were treated with:

Materials	**Times**
Fix in Carnoy's fixative	**5 minutes**
Wash in water	**3 times**
0.5% periodic acid	**5 minutes**
Wash in water	**3 times**
Schiff's solution (Sigma)	**10 minutes**
Wash in running tap water	**10 minutes**
Mount with Elvanol	

2.6 IMMUNOHISTOCHEMISTRY ANALYSES

TA muscle cryosections, 10 μm thick, were processed for immunostaining. All data are expressed as the mean SEM (error bars). Comparisons were made by using t test, with *P<0.05 being considered statistically significant. The list of the antibody used for immunofluorescence is showed in the same table of antibody used for western blot/IP/CHIP.

2.6.1 Fibre Type Determination

Fibre typing was determined by immunofluorescence using combinations of the following monoclonal antibodies: BA-D5 that recognizes type 1 MyHC isoform and SC-71 for type 2A MyHC isoform an BF-F3 for type 2B , type 2X remain black. Images were captured using a Leica DFC300-FX digital charge-coupled device camera by using Leica DC Viewer software, and morphometric analyses were made using the software ImageJ 1.47 version.

2.6.2 Fibre Cross-Sectional Area (CSA)

Fibre Cross-Sectional Area was measured, by using ImageJ software (National Institutes of Health). All data are expressed as the mean SEM (error bars). Comparisons were made by using t test, with *P<0.05 being considered statistically significant.

2.7 IMMUNOBLOTTING

Cryosections of 20 μm of TA muscles were lysed with 100 μl of a buffer containing 50 mM Tris pH 7.5, 150 mM NaCl, 10 mM MgCl2, 0.5 mM DTT, 1 mM EDTA, 10% glycerol, 2% SDS, 1% Triton X-100, Roche Complete Protease Inhibitor Cocktail and Sigma Protease Inhibitor Cocktail. After incubation at 70°C for 10 minutes and centrifugation at 11000 g for 10 minutes at 4°C, the surnatant protein concentration was measured using BCA protein assay kit (Thermo Scientific) following the manufacturer's instructions.

2.7.1 SDS-PAGE

For Myosin analysis, gastrocnemius muscles were homogenized in myosin extraction buffer containing 1M Tris pH 6.8, 10% SDS and 80% glycerol. SDS–PAGE was performed using polyacrylamide gel with a high glycerol concentration, which allows the separation of MYH isoforms. Myosins were identified with Coomassie blu staining

2.7.2 Protein gel Electrophoresis

The extracted proteins from TA muscle were solubilized in Loading buffer composed by 5µl of 4X NuPAGE® LDS Sample Buffer (Life Technologies) and 1µl of 20X DTT (Life Technologies). The volume of each sample was brought to 20µl with SDS 1X. The samples were denaturated at 70°C for 10 minutes.
Samples were loaded on SDS 4-12% precast polyacrylamide gels (NuPAGE Novex-Bis-tris-gels) or in SDS 3-8% depending on the protein to be analyzed (Life Technologies). The electrophoresis was run in 1X MES/MOPS Running buffer or 1X Tris-Acetate Running buffer respectively (Life Technologies) for 1 hour and 30 minutes at 150V constant.

2.7.3 Transfer of the protein to the PVDF/nitrocellulose membrane

After the electrophoretic run, proteins were transferred from gels to PVDF membranes, previously activated with methanol or nitrollulose membrane. The gel and the membrane were equilibrated in Transfer Buffer. TheTransfer Buffer was prepared as following:
20X NuPAGE® Transfer buffer(Invitogen) 50 ml
10X NuPAGE® Antioxidant (Invitogen) 1ml
20% Methanol (Sigma-Aldrich) 200ml
The volume was brought to 1l with distilled water. The transfer was obtained by applying a current of 400mA for 1 hour and 30 minutes at 4°C. To evaluate the efficiency of transfer, proteins were stained with Red Ponceau 1x

(Sigma). The staining was easily reversed by washing with distilled water.

2.7.4 Incubation of the membrane with antibodies

Once the proteins were transferred on PVDF membranes, the membranes were saturated with Blocking Buffer (5% no fat milk powder solubilized in TBS 1X with 0.1% TWEEN) for 1 hour at room temperature and were incubated overnight with various antibody at 4°C . Membranes were then washed 3 times with TBS 1X with 0.1% TWEEN at RT and incubated with secondary antibody-HRP Conjugate (Bio-Rad), for 1 hour at room temperature. Immunoreaction was revealed by SuperSignal West Pico Chemiluminescent substrate (Pierce) and followed by exposure to Xray film (KODAK Sigma-Aldrich). Antibodies used in this study are shown in TABLE1 and TABLE2.

Antibody	**Customer**	**Dilution**	**Analysis**
mouse IgG2A anti-puromycin	12D10	1:30000	WB
Rabbit anti-FoxO1	Cell signalling #9946	1:1000	WB
Rabbit anti-FoxO3	Cell signalling #9946	1:1000	WB
Goat anti Fbxo30	Santa Cruz Biotechnology	1:100	WB
Goat anti mouse IgG	Biorad 1706516	1:2000	WB
Goat anti rabbit IgG	Biorad 1706515	1:2000	WB
Goat anti mouse IgG-2b DyLight405	Jackson Immunoresearch 115-475-207	1:200	IF
Goat anti mouse IgG-1 DyLight405	Jackson Immunoresearch 115-485-205	1:200	IF
Goat anti mouse IgG (H+L) Cy3	Jackson Immunoresearch 115-026-003	1:200	IF
Goat anti Rabbit IgG-(H+L) Cy3	Jackson Immunoresearch 111-166-003	1:200	IF

Tab. 1: Antibodies used for western blot analyses, IP, immunofluorescence.

Antibody	Customer	Dilution	Analysis
rabbit anti-dystrophin	Abcam ab 15277	1:100	IF
Mouse anti SC-71-s	DSHB	1:100	IF
Mouse anti BF-F3	DSHB	1:100	IF
Mouse anti BA-D5	DSHB	1:100	IF
rabbit anti- actin	Abcam A4700	1:10000	WB
rabbit anti-total Akt	Cell Signaling #9272	1:1000	WB
rabbit anti-phospho-Akt (Ser473)	Cell Signaling #3787	1:1000	WB
rabbit anti-phospho-S6K (Thr 389)	Cell Signaling #9205	1:1000	WB
rabbit anti-total S6K	Cell Signaling #9202	1:1000	WB
rabbit anti-phospho-S6	Cell Signaling #2215	1:1000	WB
rabbit anti-total S6	Cell Signaling #2217	1:1000	WB
rabbit anti-LC3	Sigma L7543	1:1000	WB
rabbit anti-P62	Sigma P0067	1:1000	WB
rabbit anti-phospho-AMPK(Thr 172)	Cell Signaling #2535	1:1000	WB
rabbit anti-total AMPK	Cell Signaling #2532	1:1000	WB
rabbit anti-phospho-4EBP1 (Ser 65)	Cell Signaling #9455	1:1000	WB
rabbit anti-phospho-4EBP1 (Thr 37/46)	Cell Signaling #9459	1:1000	WB
rabbit anti-total 4EBP1	Cell Signaling #9452	1:1000	WB
rabbit anti-Gabarap	Santa Cruz Biotechnology sc-28938	1:1000	WB
rabbit anti-Gadd45α	Santa Cruz Biotechnology sc-797	1:1000	WB
rabbit anti-GFP	Santa Cruz Biotechnology sc- 8334	1:1000	WB
rabbit anti-PACC	Cell Signaling #3661	1:1000	WB
rabbit anti-mTOR	Cell Signaling #2983	1:1000	WB
mouse anti-V5	Life Technologies	1:1000	WB
mouse anti-Fbxo21	Abcam 119762	1:1000	WB
mouse anti-GAPDH	Abcam ab 8245	1:5000	WB
mouse anti-HA	Sigma H3663	1:1000	WB
mouse anti-Flag	Sigma A222	1:1000	IP/WB
mouse IgG2A anti-puromycin	12D10	1:30000	WB
mouse anti-puromycin	Hybridoma Bank PMY-2A4	1:30000	WB
mouse- anti ubiquitinylated proteins (Fk2)	Millipore #04-263	1:1000	WB
mouse- anti ubiquitin antibody, Lysin 63 specific	Millipore #05-1308	1:1000	WB
mouse anti-β-tubulin	Sigma T8328	1:1000	WB

Tab. 2: Antibodies used for western blot analyses, IP, immunofluorescence.

All the peroxidase-conjugated secondary antibodies were from Bio-Rad. Blots were stripped using Stripping Solution, containing 25mM glycine and 1% SDS, pH 2.

2.8 CO-IMMUNOPRECIPITATION (CO-IP)

Co-immunoprecipitation (Co-IP) is a popular technique to identify physiologically relevant protein-protein interactions by using target protein-specific antibodies to indirectly capture proteins that are bound to a specific target protein. For co-IP experiment C2C12 muscle cell lines were transfected with V5- SMART, HA-Skp1, FLAG-Cul1 and FLAG-Roc1 expression plasmids (Sartori et al., 2013). After 24 hours, cells were lysed in a buffer containing 50mM Tris pH 7.5, 100mM NaCl, 5mM ,MgCl2, 1mM DTT, 0.5% Triton X-100, protease and phosphatase inhibitors. About 1mg of total protein was incubated at a ratio of 1:100 with the mouse monoclonal anti-FLAG antibody or non specific mouse IgG along with 30 ml of Protein A/G PLUS-Agarose sc-2003 (Santa Cruz Biotechnology) overnight at 4 °C. The beads were then washed three times with PBS plus Roche Complete Protease Inhibitor Cocktail 1X and were finally resuspended in 30 ml LDS Sample Buffer 1X(NuPAGE Life Technolohy) and 50mM DTT, then boiling at 95°C for 5 min to be analysed by Western blotting.

2.9 GENE EXPRESSION ANALYSIS

2.9.1 Extraction of total RNA

Total RNA was isolated from TA using Trizol (Life Technologies) following the manufacturer's instructions.

2.9.2 Synthesis of the first strand of cDNA

400ng of total RNA was reversly transcribed with SuperScriptTM III (Life Technologies) in the following reaction mix:

Random primer hexamers (50 ng/ μ l random) 1 ml

dNTPs 10 mM 1 ml

H2O Rnase-free 8.5 ml

The samples were mixed by vortexing and briefly centrifuged and denaturated by incubation for 5 min at 70° C to prevent secondary structures of RNA. Samples were incubated on ice for 2 minutes to allow the primers to align to the RNA; and the following components were added sequentially:

First strand buffer 5X(Invitrogen) 5 μ l

DTT 100mM: 2 μ l

RNase Out (Life Technologies): 1 μ l

SuperScriptTM III (Life Technologies): 0.5 μ l

The volume was adjusted to 20 μ l with RNase free water.

The used reaction program was:

step1: 25°C for 10 minutes

step2: 42°C for 50 minutes

step3: 70°C for 15 minutes

At the end of the reaction, the volume of each sample was adjusted to 50ul with RNase free water.

2.9.3 Real-Time PCR reaction

Quantitative Real-time PCR was performed with SYBR Green chemistry (Applied Biosystems). SYBR green is a fluorescent dye that intercalates into double-stranded DNA and produces a fluorescent signal. The Real-Time PCR Instrument allows real time detection of PCR products as they accumulate during PCR cycles and create an amplification plot, which is the plot of fluorescence signal versus cycle number. In the initial cycles of PCR, there is little change in fluorescence signal. This defines the baseline for the

amplification plot. An increase in fluorescence above the baseline indicates the detection of accumulated PCR products. A fixed fluorescence threshold can be set above the baseline. The parameter Ct (threshold cycle) is defined as the fractional cycle number at which the fluorescence passes the fixed threshold. So the higher the initial amount of the sample, the sooner the accumulated product is detected in the PCR process as a significant increase in fluorescence, and the lower is the Ct value.

2.9.4 Quantification of the PCR products and determination of the level of expression

A relative quantification method was used to evaluate the differences in gene expression, as described by Pfaffl (Pfaffl, 2001). In this method, the expression of a gene is determined by the ratio between a test sample and a housekeeping gene. The relative expression ratio of a target gene is calculated based on the PCR efficiency (E) and the threshold cycle deviation (ΔCt) of unknown samples versus a control, and expressed in comparison to a reference gene. The mathematical model used for relative expression is represented in this equation :

$$\text{Ratio} = \frac{(E_{\text{target}})^{\Delta Ct}}{(E_{\text{reference}})^{\Delta Ct}}$$

The internal gene reference used in our real time PCR was pan-actin, whose abundance did not change under the experimental conditions.

2.9.5 Primer pairs design

Gene-specific primer pairs were selected with Primer Blast software (http://www.ncbi.nlm.nih.gov/tools/primer-blast/). Primer pairs were selected in a region close to the 3'-end of the transcript, and amplified fragments of 150-250bp in length. To avoid the amplification of contaminant genomic DNA, the target sequences were chosen on distinct exons, separated

by a long (more than 1000 bp) intron. The temperature of melting chosen was of about 58-60° C. The sequences of the primer pairs are listed in Table 3 and 4.

	Forward primer (5'-3')	Reverse Primer (5'-3')
Nucleolin	**TTTATCAAAGTGCCCCAGAA**	**GTTCTGCCCTCAATTTCCAT**
p62	**CCCAGTGTCTTGGCATTCTT**	**AGGGAAAGCAGAGGAAGCTC**
Pfkfb3	**GCCTCTTGACCCTGATAAATGT**	**TCTTGCCTCTGCTGGACA**
Psma1	**CATTGGAATCGTTGGTAAAGAC**	**GTTCATCGGCTTTTTCTGC**
Psmc4	**AGGACGAGCAGAAGAACCTG**	**AATAGTTAGAGCCTGTGGTGGAG**
Psmd11	**GAGTTCCAGAGAGCCCAGTC**	**AACCCAGTTCAAGGATGCTC**
Psme4	**TTGTAGATGCATGCCGACTC**	**ACCTGGGTGAGTTTTGGTTC**
Tgif	**TTTCCTCATCAGCAGCCTCT**	**CTTTGCCATCCTTTCTCAGC**
Txnl	**GGTGGGAGTGAAGCCGGTCG**	**CGGGGCAATCCGAAGACACG**
UBC	**CGTCGAGCCCAGTGTTACCACC**	**ACCTCCCCCATCACACCCAAGA**
Ube4b	**TGTCATCTTCCTTTCTTCTCTCTC**	**TGGATTTTCATCTCGTGTCTG**
Usp14	**CACGAGTTGCTTCGTATTCC**	**TTCAGGGTTCCTCCTTTCAC**

Tab. 3: Primers used for Quantitative PCR Analyses.

	Forward primer (5'-3')	**Reverse Primer (5'-3')**
4EBP1	**CCTCCTTGTGCCTCTGTCTA**	**GCCTAAGGAAAGATGGGTGT**
Actin	**CTGGCTCCTAGCACCATGAAGAT**	**GGTGGACAGTGAGGCCAGGAT**
Ampd3	**GCGGAGAAGGTGTTTGCTA**	**CAGTCTTGTTGTGTTGGCATC**
ATF4	**TCCTGAACAGCGAAGTGTTG**	**ACCCATGAGGTTTCAAGTGC**
ATP5A1	**GAGAGAGCAGCCAAGATGAAC**	**GACACGGGACACAGACAAAC**
Atrogin-1	**GCAAACACTGCCACATTCTCTC**	**CTTGAGGGGAAAGTGAGACG**
Bnip3	**TTCCACTAGCACCTTCTGATGA**	**GAACACCGCATTTACAGAACAA**
CathepsinL	**GTGGACTGTTCTCACGCTCAAG**	**TCCGTCCTTCGCTTCATAGG**
Eif4g3P3	**GAAACGGAGAAGAGGCTGAG**	**GATACAGGCGGGCATAAACT**
Ezh1	**GTGTTTTCTTTTCTTCTTCTGTGC**	**GTGTTTTCTTTTCTTCTTCTGTGC**

FbxO21	**TCAATAACCTCAAGGCGTTC**	**GTTTTGCACACAAGCTCCA**
FbxO31	**GTATGGCGTTTGTGAGAACC**	**AGCCCCAAAATGTGTCTGTA**
FoxO1	**GCTGGGTGTCAGGCTAAGAG**	**GAGGGGTGAAGGGCATCT**
FoxO3	**CGCTGTGTGCCCTACTTCA**	**CCCGTGCCTTCATTCTGA**
FoxO4	**CGGAGTGAAAGGGACAGTTTAG**	**CCCTGTGGCTGACTTCTTATTC**
GabarapL	**CATCGTGGAGAAGGCTCCTA**	**ATACAGCTGGCCCATGGTAG**
Gadd34	**AGAGAAGACCAAGGGACGTG**	**CAGCAAGGAATGGACTGTG**
Gadd45 a	**GAAAGTCGCTACATGGATCAGT**	**AAACTTCAGTGCAATTTGGTTC**
GAPDH	**CACCATCTTCCAGGAGCGAG**	**CCTTCTCCATGGTGGTGAAGAC**
Itch	**CCACCCACCCCACGAAGACC**	**CTAGGGCCCGAGCCTCCAGA**
JunB	**GATCCCTATCGGGGTCTCAA**	**GAGGCTAGCTTCAGAGATGC**
LC3b	**CACTGCTCTGTCTTGTGTAGGTTG**	**TCGTTGTGCCTTTATTAGTGCATC**
Maf	**GCATCATCAGCCAGTGCGGC**	**AGGTGCGCCTTCTGTTCGCT**
Max	**CGAAAACGTAGGGACCACAT**	**GATCTTGCCTTCTCCAGTGC**
Mt1	**GCCTGCAAGAACTGCAAGTG**	**CCTTTGCAGACACAGCCCT**
MUSA1	**TCGTGGAATGGTAATCTTGC**	**CCTCCCGTTTCTCTATCACG**
MuRF-1	**ACCTGCTGGTGGAAAACATC**	**ACCTGCTGGTGGAAAACATC**
Nrf2	**CTCTGACTCTGGCATTTCACTG**	**ACACTTCAGGGGCACTATCTA**

Tab. 4: Primers used for Quantitative PCR Analyses.

2.9.6 Real-Time PCR reaction

1µl of diluted cDNAs was amplified in 10µl PCR reactions in a ABI Prism 7000 (Applied Biosystem) thermocycler, coupled with a ABI Prism 7000 Sequence Detection System (Applied Biosystems) in 96-wells plates (Micro Amp Optical, Applied Biosystems). In each well 5ul Sample mix and 5ul reaction mix were mixed.

Sample mix was prepared as follows for 5 µl total volume:

Template cDNA: 1 µl

H2O Rnase-free: 4 µl

The SYBR Green qPCR (Applied Biosystem) was used for the Real-Time PCR reaction as follows:

SYBR Green qPCR (Applied Biosystem): 4.8µl

Mix Primer forward /reverse 50mM: 0.2µl

The PCR cycle used for the Real-Time PCR was:

step 1: 95° C for 15 minutes

step2: 95° C for 25 seconds

step3: 58° C for 1 minute

step4: go to step 2 for 40 times.

2.10 PLASMID CLONING

The cloning strategy required insertion of the DNA of interest in a specific plasmid. Then competent bacteria (Top 10) (Life Technologies) were transformed and the plasmid was purified first with Mini-prep kit (Machery-Nagel) and then, to increase the quantity of DNA, in particular for *in vivo* transfection, we prepared Maxi-prep (Qiagen) following the manufacturer's instructions. Final DNA concentration was quantified by Nanovue Plus (GE Haelthcare).

2.10.1 FbxO21 cloning

In vivo transfection experiments used the yellow fluorescent protein (YFP)–LC3 (Mammucari et al., 2007) and Fbxo21SMART-V5 plasmid . For the cloning, FbxO21/SMART gene was amplified from mouse cDNA by PCR using the following primers primers forward: 3'-ACCATGGCGTCGGTAGCGGGGGACA-5' and reverse: 3'-CTCGGCTGTGTCCTCCTTTGCACTG-5' .

The amplified sequence was cloned into pcDNA3.1/V5-His TOPO (Invitrogen) expression vector and sequenced.

2.10.2 *In Vivo* RNAi

In vivo RNAi experiments were performed using at least four different sequences for each gene(Invitrogen BLOCK-iTTM Pol II miR RNAi Selected). The sequences are shown in Table 5. For the validation of shRNA constructs, MEF cells were maintained in DMEM/10% FBS and transfected with shRNA constructs using Lipofectamine 2000 (Invitrogen). Cells were lysed 24 h later and immunoblotting was performed.

mSMART(1)	top (5'-3')	TGCTGTGGAGAAGGAAGCTACAATCTGTTTTGGCCACTGACTGACAGATTGTATTCCTTCTCCA
	botton (5'-3')	CCTGTGGAGAAGGAATACAATCTGTCAGTCAGTGGCCAAAACAGATTGTAGCTTCCTTCTCCAC
mSMART(2)	top (5'-3')	TGCTGAAGACAAGACAGAAAGACTTCGTTTTGGCCACTGACTGACGAAGTCTTTGTCTTGTCTT
	botton (5'-3')	CCTGAAGACAAGACAAAGACTTCGTCAGTCAGTGGCCAAAACGAAGTCTTTCTGTCTTGTCTTC
mSMART(3)	top (5'-3')	TGCTGTTAGGATACACACCAGCTCATGTTTTGGCCACTGACTGACATGAGCTGGTGTATCCTAA
	botton (5'-3')	CCTGTTAGGATACACCAGCTCATGTCAGTCAGTGGCCAAAACATGAGCTGGTGTGTATCCTAAC
mSMART(4)	top (5'-3')	TGCTGTTTGCACACAAGCTCCACAATGTTTTGGCCACTGACTGACATTGTGGATTGTGTGCAAA
	botton (5'-3')	CCTGTTTGCACACAATCCACAATGTCAGTCAGTGGCCAAAACATTGTGGAGCTTGTGTGCAAAC

Tab. 5: Oligos used for siRNA production and used for in vivo trasfection.

2.11 GENE EXPRESSION PROFILING

For each of the 4 conditions (FoxO1,3,4 f/f fed or starved and FoxO1,3,4 -/- fed or starved), we collected the gastrocnemius muscles of three mice thus yielding six muscles per condition. RNA was prepared from these muscles using the TRIzol method (Life Technologies) followed by cleanup with the RNeasy kit (Qiagen). RNA concentration was determined by spectrophotometry and quality of the RNA was monitored using the Agilent 2100 Bioanalyzer (Agilent Technologies). Then, RNA was pooled equimolarly and used for microarray analysis. RNA was prepared, labelled and hybridized to Affymetrix Mouse Genome 430 2.0 Arrays using Affymetrix-supplied kits and according to standard Affymetrix protocols. Expression values were

summarized using the Mas 5.0 algorithm. Genes that were up or downregulated in starvation compared with the fed condition were determined using Excel software. A threshold of 1.5 was used for the fold up or downregulation consistent with the fold change that can be reliably detected with these type of arrays.

2.12 COLCHICINE TREATMENT

We monitored autophagic flux in 30 hours of starvation using colchicine (Ju et al., 2010). Briefly, MLC FoxO1,3,4-/-and FoxO1,3,4 f/f mice were treated with 0,4mg/kg of colchicine or vehicle by i.p. injection and starved. The treatment was repeated 15 hours prior to muscle harvesting.

2.13 STATISTICAL ANALYSIS AND EXPERIMENTAL DESIGN

The sample size was calculated using size power analysis methods for a priori determination based on the s.d., and the effect size was previously obtained using the experimental methods employed in the study. For animal studies, we estimated sample size from expected number of knock-out mice and littermate controls, which was based on mendelian ratios. We calculated the minimal sample size for each group by at least four organisms. Considering a likely drop-off effect of 10%, we set sample size of each group at five mice. To reduce the s.d., we minimized physiological variation by using homogenous animals with same sex and same age. The exclusion criteria for animals were pre-established. In case of death, cannibalism or sickness, the animal was excluded from analysis. Tissue samples were excluded in cases such as cryoartefacts, histological artefacts or failed RNA extraction. We included animals from different breeding cages by random allocation to the different experimental groups. Animal experiments were not blinded, however, when applicable, the experimenters were blinded to the nature of samples by using number codes until final data analysis was performed.

Statistical tests were used as described in the figure legends and were applied on verification of the test assumptions (for example, normality). Generally, data were analysed by two-tailed Student's t-test. For all graphs, data are represented as means±s.e.m. For the measurement variables used to compare KO animals versus controls, or innervated animals versus denervated ones, the variance was similar between the groups.

3. RESULTS

3.1 GENERATION OF MUSCLE-SPECIFIC FoxO1,3,4 KNOCK-OUT MICE

FoxO trascription factors are required for muscle wasting. However, the trascriptional program that regulate skeletal muscle atrophy is poorly understood. To delineate the role of FoxO in gene regulation and muscle adaptation during catabolic condition, we generated FoxO1,3,4 muscle specific knock-out mice.

FoxO1,3,4 floxed mice were crossed with a transgenic line expressing Cre recombinase under the control of MLC1f promoter to generate muscle-specific FoxO1,3,4 triple knock-out mice, which are hereafter referred to as FoxO1,3,4$^{-/-}$. We confirmed the successful deletion of all three FoxOs isoform with PCR analysis from genomic DNA extracted from skeletal muscle (Fig. 1a). Quantitative RT-PCR shows an important downregulation of FoxO1 and FOXO3 transcripts while FoxO4 is almost undetectable (Fig. 1b). Since FoxO4 is mainly expressed in muscles while FoxO1 and 3 are expressed in almost all tissues, the traces of FoxO1 and 3 mRNAs come from endothelial, fibroblasts, macrophages and blood cells. Western Blot analyses confirmed the decrease of FoxO1 and FoxO3 proteins in muscles of FoxO1,3,4$^{-/-}$ mice (Fig. 1c) .Thus, we confirm our genetic model of muscle-specific inhibition of FoxO1,3,4 family.

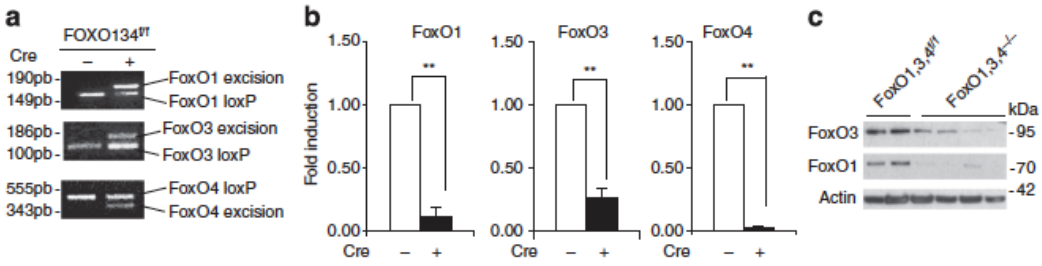

Fig.1: Validation of FoxO1,3,4 knock-out model. (a) Genotyping of the FoxO1,3,4 f/f PCR analysis with genomic DNA from gastrocnemius muscles. **(b)** FoxO1, FoxO3 and FoxO4 mRNA expression levels by RT–PCR in Tibialis Anterior (TA) muscle of FoxO1,3,4-/- and control mice. N=4 each group. **(c)** Western blot analysis shows a reduction of FoxO1 and FoxO3 proteins in gastrocnemius muscles of FoxO1,3,4-/- and not in control mice. Data are representative of three independent experiments.

3.2 FoxO1, FoxO3 and FoxO4 SIMULTANEOUS DELETION IN MUSCLE DOES NOT AFFECT FIBRE TYPE

The resulting FoxO1,3,4-/- mice were indistinguishable in appearance from age-matched control FoxO1,3,4 f/f mice. Histological analysis of adult muscles revealed a normal muscle architecture and absence of myopathic features such as centrally nucleated fibers (Fig. 2a). SDH staining showed no major alteration in distribution of small β-oxidative mitochondrial rich versus large glycolytic mitochondrial poor fibers (Fig. 2b). Since FoxOs are important regulator of energy metabolism in muscle and are important for glucose homeostasis in liver, we decide to monitor glycogen levels. PAS staining revealed an almost identical distribution of glycogen stores (Fig. 2c) in muscle of controls and in FoxOs knock-out mice. Analyses of Myosin Heavy Chain expression and distribution did not reveal any significant difference between wild type and FoxO1,3,4 knockout mice (Fig 2d, e). This first set of experiments suggests that FoxOs are not required for fiber type determination.

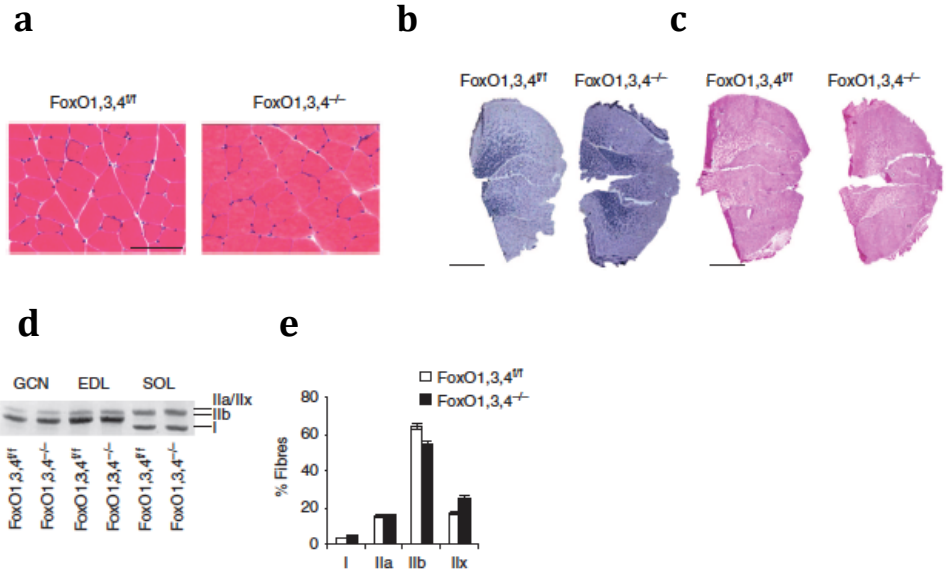

Fig.2: Deletion of FoxOs is permissive for normal muscle function. (a) Haematoxylin and eosin (Scale bar, 100 mm), **(b)** SDH (Scale bar, 1mm) and **(c)** PAS staining (Scale bar, 1mm) showing normal morphology, fibre type and glycogen of FoxO1,3,4-/-gastrocnemius muscle. **(d)** SDS–PAGE and **(e)** immunohistochemistry analysis of myosin heavy chain type I, IIA, IIB and IIX proteins in gastrocnemius muscles showing no differences between FoxO1,3,4-/- and FoxO1,3,4f/f mice. Data are representative of three independent experiments.

3.3 FoxOs INHIBITION PREVENTS MUSCLE LOSS AND WEAKNESS

To further characterize the role of FoxO1,3,4 in skeletal muscles, we then analysed the phenotype of FoxO1,3,4-/- mice under conditions of muscle wasting. Initially, we used fasting as a model of muscle loss since it is an established condition that induces nuclear translocation of FoxO members to the nucleus and we compared FoxO1,3,4 null muscles with controls. Importantly, FoxO1,3,4 knockout mice were completely spared from muscle loss after fasting (Fig. 3a). To understand whether sparing of muscle mass is also functionally relevant, we measured muscle force in living animals. While control fasted animals became significantly weaker than fed ones, FoxO1,3,4 -/- gastrocnemius muscles did not loose strength after fasting (Fig. 3b). Importantly the comparison of force/frequency curve of fasted wild-type versus fasted FoxO1,3,4 null muscle underlined the important protection achieved by the absence of FoxO family when nutrients are low or absent (Fig. 3c). These findings confirm that the absence of FoxO members prevents atrophy and profound weakening.

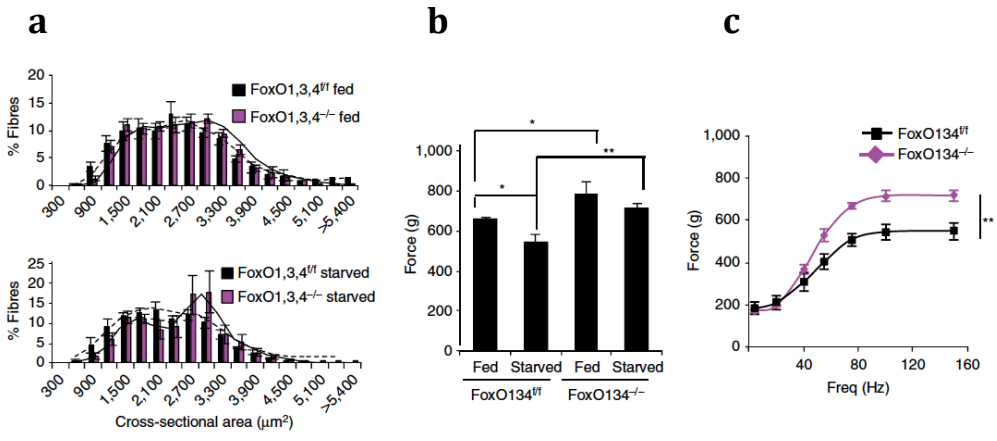

Fig.3: Deletion of FoxOs prevents muscle loss and weakness during fasting. (a) Frequency histograms of cross-sectional areas (mm2) of FoxO1,3,4f/f (black bars) and FoxO1,3,4_/_ (magenta bars) fibres in fed (upper panel) and fasted (lower panel) conditions, n.4, each group. **(b)** Force measurements performed in vivo on gastrocnemius showed that FoxO1,3,4_/_ muscles preserve maximal tetanic force after fasting; n.6 muscles in each group. **(c)** Force/frequency curve of starved gastrocnemius muscle underlines the important protection achieved by the absence of FoxOs; n=6 muscles in each group.

To explain this profound effect on sparing force and muscle mass, we monitored the level of the contractile protein, myosin, when nutrients are removed. As expected, fasting induced an important reduction of myosin content in controls, while FoxO1,3,4 knock-out were completely protected (Fig. 4a). The maintenance of myosins in knock-out muscles is consequent to inhibition of protein ubiquitination. Indeed, fasting resulted in an increase in both lysine-48 and lysine-63 polyubiquitinated proteins (Fig. 4b-c) confirming an activation of the ubiquitination process in controls. Importantly, this increase was totally abolished in FoxO1,3,4 knockout mice.

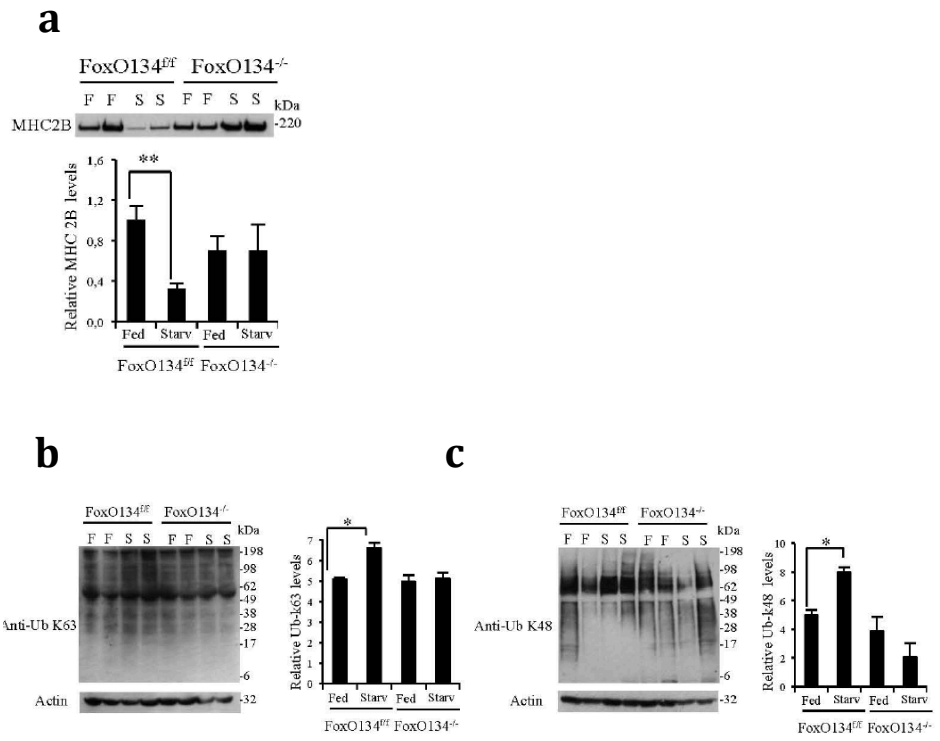

Fig.4: FoxO inhibition prevents protein ubiquitination during starvation. (a) Representative Immunoblot of MCH IIB in fed and in starved muscles of controls and FoxOs knock-out mice. Quantification of MHC IIB content is shown in the graph. n=4 muscles in each group. **(b, c)** Protein extracts from control and starved muscles of FoxO1,3,4-/- and FoxO1,3,4f/f mice were immunoblotted against (b) K63-polyUbiquitin and (c) K48-polyUbiquitin chains. The graphs show densitometry quantification of two different experiments of n=4 for each group. Data are mean ± s.e.m. Error bars indicate s.e.m. *p<0.05 **p<0.01 (Student's t-test).F: fed, S: starved, Starv: starved.

3.4 FoxOs ARE REQUIRED FOR AKT ACTIVITY AND ARE CRITICAL FOR AUTOPHAGY

To explore the basis for sparing of muscle mass in absence of nutrients, we investigate the signalling pathways linked to Insulin/ IGF1 and energy. Interestingly, Akt, S6K and S6 phosphorylation, both in fed and fasted muscles, were reduced in knockout mice, while phosphorylation of 4EBP1, the other mTORC1 downstream target, was increased in FoxO-deficient TA muscles (Fig. 5a). The energy–stress sensor AMPK and its downstream target ACC did not significantly differ from controls in fed and fasting conditions (Fig. 5a). Therefore, the changes in the pathway downstream insulin/nutrients do not match with the important sparing of muscle mass in knockout mice when nutrients are absent. Since the absence of nutrients is a potent stimulus for autophagy-dependent degradation and since FoxO is an inducer, while mTOR is a suppressor of autophagy–lysosome system, we checked the status of this system in FoxO1,3,4-/-mice. We monitored LC3 lipidation, LC3-positive vesicles and autophagy flux in FoxO1,3,4f/f and FoxO1,3,4 -/-mice. Fasting induced LC3 lipidation (Fig. 5b) and vesicles formation (Fig. 5c) in controls but not in FoxO-deficient muscles. Autophagy flux was monitored by treating animals with colchicine, an established inhibitor of microtubule-mediated delivery of autophagosome to lysosome. The inhibition of autophagosome delivery led to accumulation of lipidated LC3 in controls but not in FoxO1,3,4 deficient muscles (Fig. 5d).

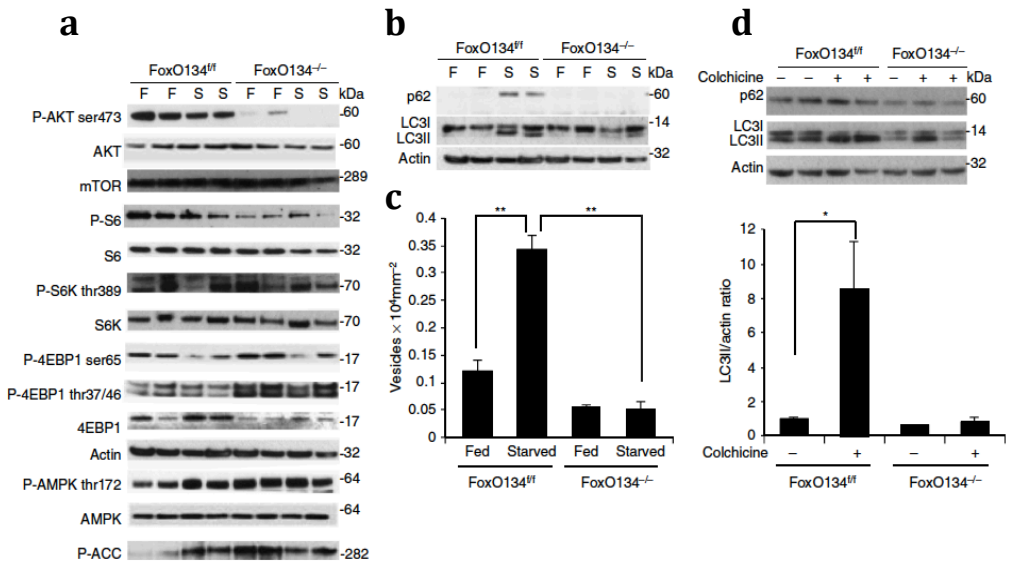

Fig.5: FoxOs are required for Akt activity and are critical for autophagy. (a) Immunoblot of protein extracts from gastrocnemius muscles. Phosphorylation of AKT and S6 is reduced in fed and starved FoxO1,3,4-/- muscles when compared with controls. Data are representative of three independent experiments **(b)** Immunoblot analysis of p62 and LC3 in homogenates of gastrocnemius muscles from fed and starved FoxO1,3,4-/- or controls. Fasting did not induce LC3 lipidation and p62 upregulation in FoxO-deficient muscles. Data are representative of three independent experiments. **(c)** Quantification of GFP–LC3-positive vesicles in FoxO1,3,4f/f and FoxO1,3,4-/-TA muscles; n.4 muscles in each group **(d)** Autophagy flux is not increased in FoxO-deficient TA muscles. Inhibition of autophagy–lysosome fusion by colchicine treatment induces accumulation of LC3II band in starved control but not in starved FoxO1,3,4-/- muscles. Upper panel: immunoblot analysis of gastrocnemius homogenates. Lower panel: quantification of LC3 lipidation. n.4 muscles in each group.

In conclusion, during fasting, despite mTOR signaling being partially inhibited, autophagy enhancement is completely blocked in FoxO1,3,4-/- muscle, suggesting that FoxO is upstream mTOR for autophagy regulation during nutrients deprivation.

3.5 HALF OF THE ATROPHY-RELATED GENES ARE UNDER FOXO REGULATION.

Since muscle atrophy is characterized by transcription-dependent regulation of atrogenes (atrophy-related genes) and FoxO deficiency protects from muscle loss, we aimed to identify genes under FoxO regulation. Gene expression profiles of fed and fasted control and FoxO1,3,4-/- muscles were compared with identify genes with blunted induction in the fasted FoxO1,3,4-/- mice relative to controls. Cross-referencing with the list of known atrogenes (Lecker et al., 2006), these analyses revealed that 29 of the 63 atrophy-related genes require FoxO for their normal induction during fasting (Fig 6).

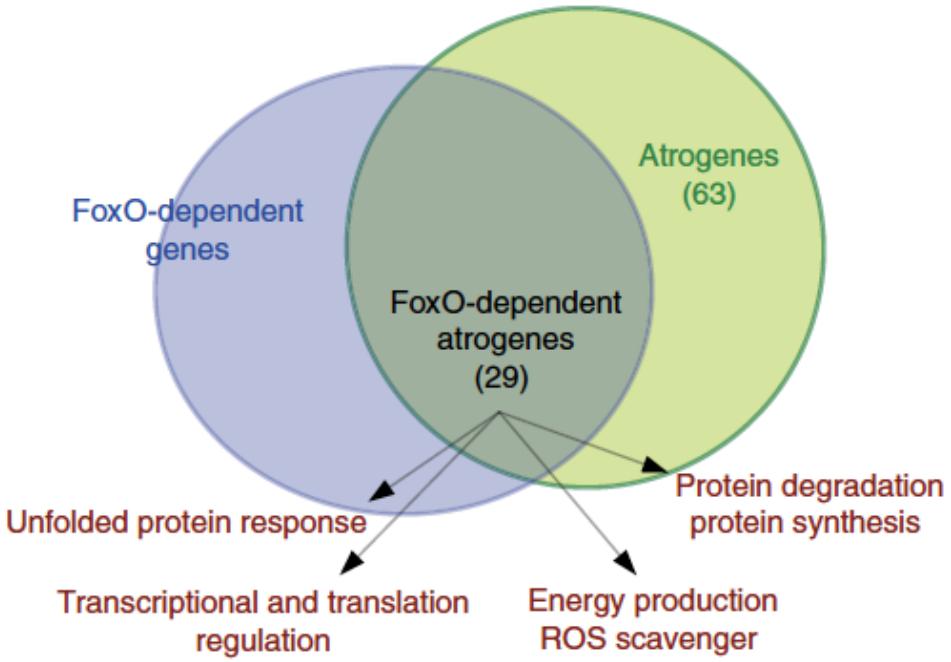

Fig.6: Half of the atrophy-related genes are under FoxO regulation. The scheme shows the overlap between FoxO-dependent genes, identified by gene expression profiling of fed (n=4) and fasted (n=4) muscles from FoxO1,3,4f/f and FoxO1,3,4_/_ and atrophy-related genes or atrogenes. The data in the graphs are shown as mean±s.e.m. Error bars indicate s.e.m. *P<0.05, **P<0.01 (Student's t-test).

Quantitative RT–PCR confirmed that 26 of the atrophy-related genes were not induced in FoxO null muscles during fasting (Fig. 7).

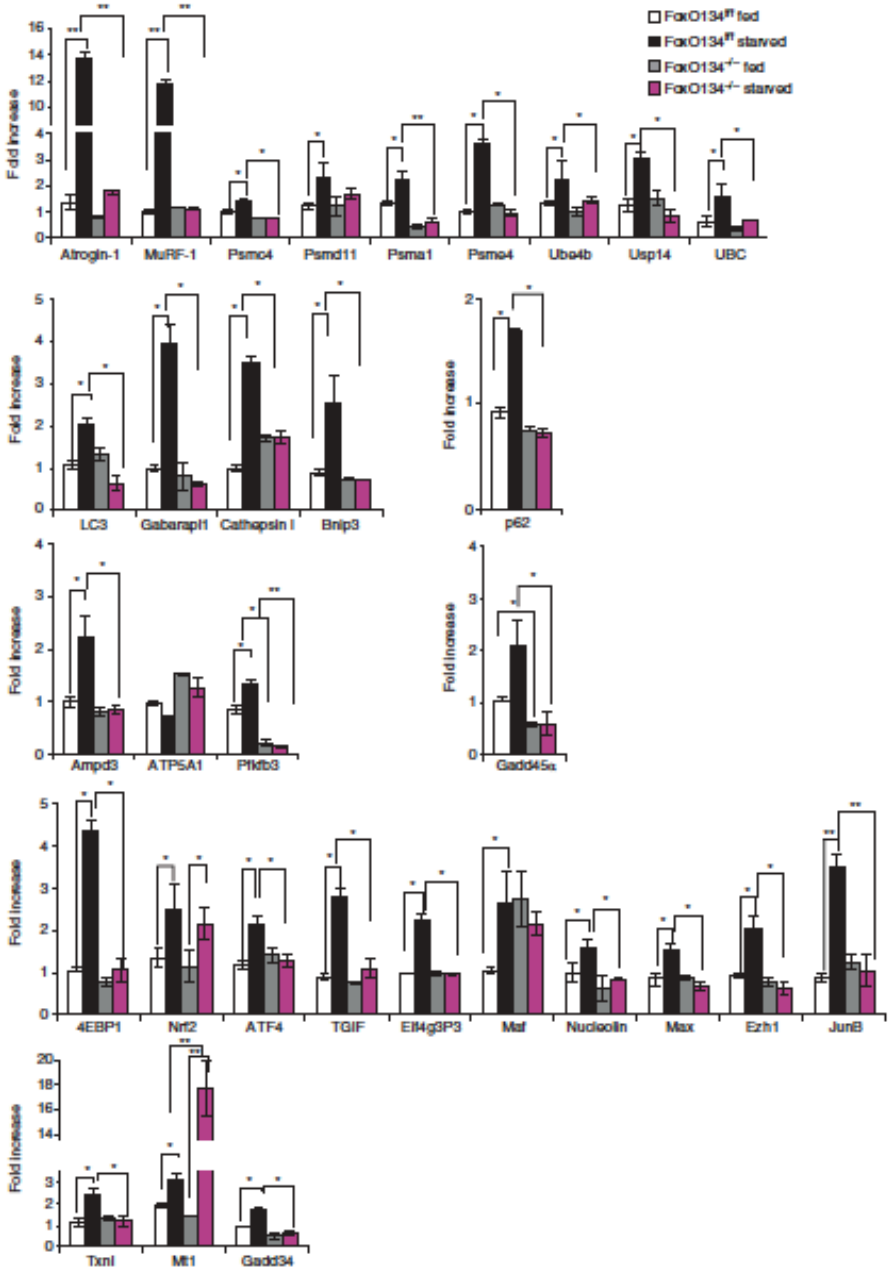

Fig.7: Absence of FoxOs prevent the induction of critical atrogenes. Quantitative RT–PCR of atrogenes from fed and 24-h starved tibialis anterior of control and FoxO1,3,4-/-mice. Data are normalized to GAPDH and expressed as fold increase of control-fed animals. N=4 muscles in each group Values are mean±s.e.m. *P<0.05,**P<0.01. (Student's t-test).

Consistent with morphology and force measurements, the induction of genes involved in protein breakdown was completely blocked in knockout mice. In fact, the ubiquitin system including the ubiquitin ligases (Atrogin1 and MuRF1), the ubiquitin gene (UBC), the de-ubiquitinating enzyme (USP14), the E3/E4 enzyme (Ube4b), several proteasome subunits (Psme4/PA200,

Psma1, Psmc4/Rpt3 and Psmd11/Rpn6) as well as the autophagy-related genes (LC3, Gabarapl, Bnip3, CathepsinL and p62/SQSTM1) were completely blocked in FoxO1,3,4-/- mice. Other pathways that are inhibited in knockout muscles are related to the unfolded protein response (ATF4 and GADD34), protein synthesis (4EBP1 and eIF4g), transcription regulators that negatively control Smad2/3 (TGIF) or positively affect Myc (MAX), DNA repair/ chromatin remodelling (GADD45a) and ribosome transcription/maturation/assembly (Nucleolin). Expression of genes that are related to oxidative stress were more variable. Nrf2/Nfe2l2 was not affected by FoxO deletion, while Thioredoxin was suppressed and Metallothionein1 was significantly induced in the absence of FoxO factors. Western blot analyses of some atrogenes involved in autophagy (p62, Gabarapl and Bnip3), chromatin remodelling/DNA repair (GADD45a), protein synthesis (4EBP1) and ubiquitin–proteasome confirmed their upregulation during fasting in control animals but not in FoxO1,3,4 knock-out.(fig.8 a,b,c,d).

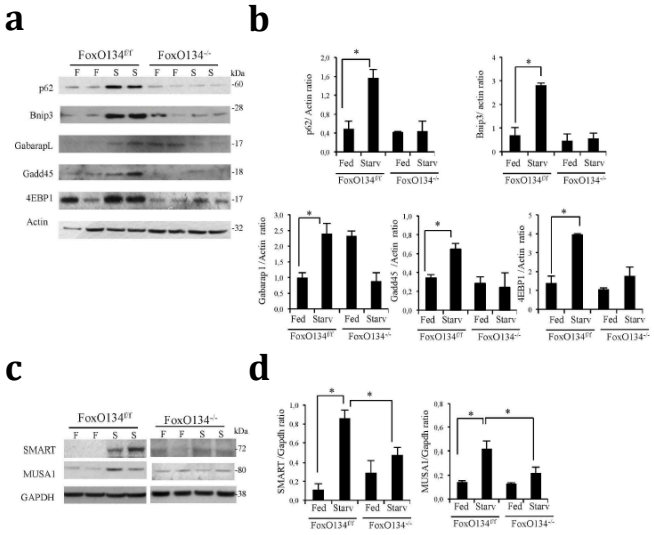

Fig.8: FoxOs are required for the expression of several atrogenes. (a) Representative Western blots of several atrophy-related genes. Protein extracts from fed and starved muscles of FoxO1,3,4f/f and FoxO1,3,4-/- mice were immunoblotted against p62, Bnip3, Gabarapl, Gadd45α and 4EBP1. Blots are representative of two groups of experiments. **(b)** The graphs show the densitometric quantification of the blots. At least 4 muscles for each group were used. **(c)** Representative Immunoblots of the novel atrophy-related ubiquitin ligase SMART and MUSA1. **(d)** Densitometric quantification was performed from 3 fed gastrocnemius from FoxO1,3,4f/f and from FoxO1,3,4-/- and 4 starved gastrocnemius from FoxO1,3,4f/f and from FoxO1,3,4-/-. Data are shown as mean ± s.e.m. Error bars indicate s.e.m. *p<0.05 (Student's t-test). F: fed, S: starved, Starv: starved

3.6 INDUCIBLE FoxOs LOSS PHENOCOPIES THE CONDITIONAL KNOCK-OUT

To support our findings, and to minimize the phenomenon of adaptation and compensations that occur with the constitutive deletion of the genes, we also explored the impact of somatic deletion of FoxO in the adult using tamoxifen treatment. In this case Cre recombinase is under the control of a muscle specific promoter, the human skeletal actin (HSA) and the deletion occurrs only after tamoxifen. We first set-up a an appropriate tamoxifen treatment protocol to obtain an efficient deletion of FoxO genes (Fig 9). Next, we assessed muscle mass during fasting by monitoring muscle mass and muscle force.

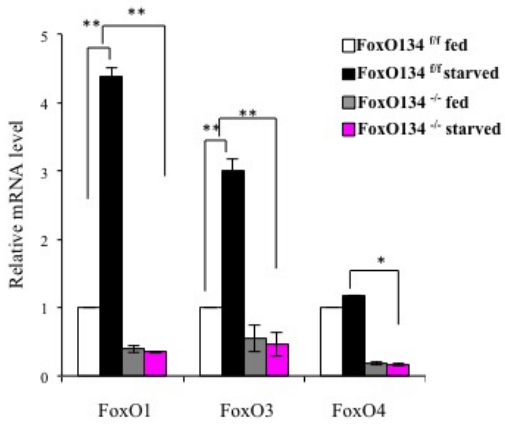

Fig.9: Tamoxifen-inducible muscle-specific FoxO1,3,4 knockout mice. FoxO1, FoxO3, FoxO4 mRNA expression were quantified by RT PCR in TA muscles of FoxO1,3,4-/- and control mice after tamoxifen treatment. Values are mean ± s.e.m. Error bars indicate s.e.m.*p<0.05, **p<0.01(Student's t-test)

Similar to the data obtained with the conditional FoxOs knockout model, we found that somatic deletion of FoxO1,3,4 prevented muscle loss (Fig. 10a) and muscle weakness during fasting (Fig. 10b). Consistent with the conditional knock-out, Akt activation and LC3 lipidation was reduced in FoxO knock-out when compared with controls (Fig. 10c). Autophagy flux measurements confirmed that FoxOs are required for autophagy induction

(Fig. 10d). The fact that two different FoxO1,3,4 knock-out mice resulted in comparable biological effects strongly supports the conclusion that the FoxO family is a master regulator of the atrophy programme under low nutrient conditions.

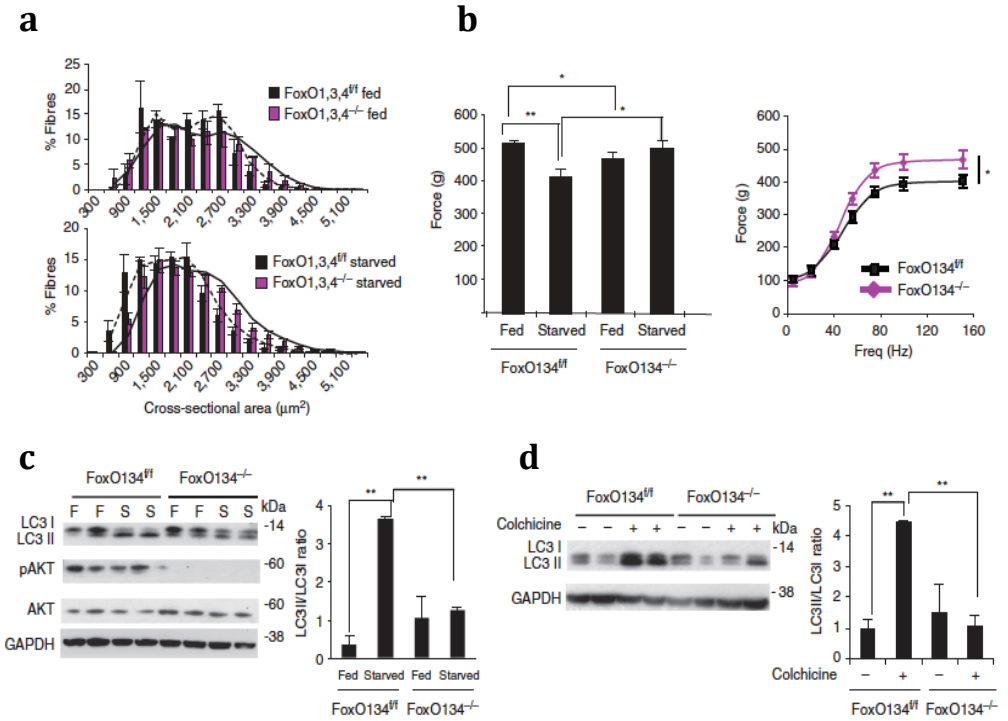

Fig.10: Acute inhibition of FoxOs phenocopies the conditional FoxO1,3,4 knockout. (a) Frequency histograms of gastrocnemius muscles showing the distribution of cross-sectional areas (mm2) of inducible muscle-specific FoxO1,3,4 mice after tamoxifen-dependent deletion of FoxO1,3,4 genes (FoxO1,3,4f/f: black bars and FoxO1,3,4-/- magenta bars) in fed (upper panel) and fasted (lower panel) conditions, n=3, each group. **(b)** Force measurements performed in vivo on gastrocnemius muscle showed that acute inhibition of FoxOs in adulthood prevents force drop during fasting. N=6 muscles in each group. Freq: Frequency. **(c)** Left, immunoblotting analyses of gastrocnemius homogenates after acute deletion of FoxO1,3,4-/- and controls. Right, quantification of LC3 lipidation. Data are representative of three independent experiments. **(d)** Autophagy flux is not increased in FoxO-deficient TA muscles. Inhibition of autophagy–lysosome fusion by colchicine treatment induces accumulation of LC3II band in starved control but not in starved FoxO1,3,4-/-muscles. Left, immunoblotting analyses of gastrocnemius homogenates. Right, quantification of LC3 lipidation.

3.7 FoxOs ARE REQUIRED FOR DENERVATION-DEPENDENT ATROPHY

To further determine whether the role of FoxO1,3,4 is critical in different catabolic conditions, we then used denervation as another model of muscle atrophy. Quantification of fibre size revealed that FoxO-deficient muscles

were partially protected from atrophy (Fig. 11a). When we monitored muscle force, we confirmed the histological data. Soleus muscle of FoxO1,3,4 knockout mice generated higher strength than controls in the basal condition (Fig. 11b) and FoxO deletion was able to partially prevent weakness and maintain the same force of innervated FoxO1,3,4f/f (Fig. 11 b,c). Analyses of signalling confirmed the downregulation of P-AKT in knockout muscles. Denervation induced an increase of total and phospho-4EBP1 protein in FoxO1,3,4 f/f but not in FoxO1,3,4-/- muscle (Fig. 11d). The changes in the phosphorylation of 4EBP1 were not ascribed to activation of the cellular energy sensor AMPK, revealed by checking its phosphorylation level or the downstream target ACC. In contrast to fasting, the autophagy system was mildly affected by the absence of FoxOs. Indeed, LC3 lipidation was slightly decreased in FoxO1,3,4-/- compared with controls after denervation (Fig. 11e). However, and consistent with fasting, the transcriptional upregulation of p62/SQSTM1 in denervated muscles was greatly attenuated (Figs 11e and 12).

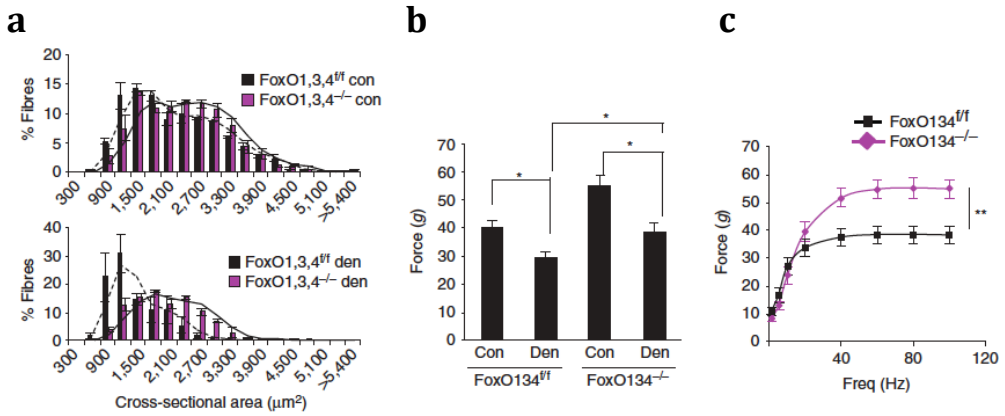

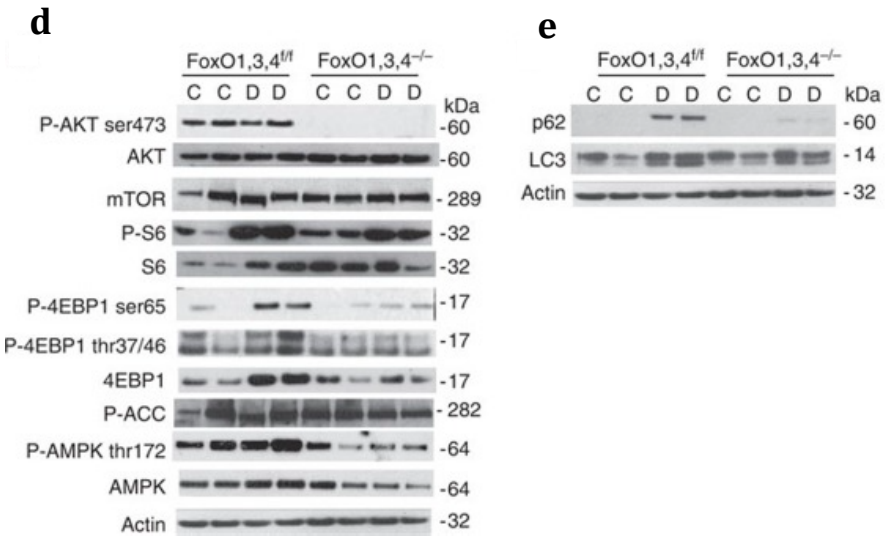

Fig. 11: Deletion of FoxOs in skeletal muscle partially prevents atrophy during denervation. (a) Frequency histograms of gastrocnemius muscles from FoxO1,3,4−/− and control mice showing the distribution of cross-sectional areas (μm2) of FoxO1,3,4f/f (black bars) and FoxO1,3,4−/− (magenta bars) in control (upper panel) or in denervation (lower panel). *n*=4 muscles each groups. **(b)** Force measurements preformed *ex vivo* on soleus muscles show that FoxO1,3,4−/− muscles are stronger than controls, both in basal condition and after 14 days from denervation. *n*=6 muscles in each group. **(c)** Force/frequency curves of denervated soleus highlight the higher strength generated by FoxO1,3,4−/− muscles when compared with controls. *n*=6 muscles in each group**.(d)** Immunoblots of gastrocnemius protein extracts reveal a decrease of AKT phosphorylation both in contralateral and in denervated muscles of FoxO1,3,4−/− mice. The increase of 4EBP1 protein is blunted in FoxOs knockout mice. **(e)** Immunoblots of autophagy-related proteins. FoxOs are required for p62 induction, while LC3 is less lipidated after 3 days of denervation. Data are representative of three independent experiments. Data are shown as mean±s.e.m. Error bars indicate s.e.m. **P*<0.05, ***P*<0.01 (Student's *t*-test). C, control; D, denervated.

When we tested the expression of the different atrophy-related genes, we found only a partial suppression of these genes (Fig. 12). Interestingly, the lists of FoxO-dependent genes during denervation and fasting do not completely overlap. For instance, the ROS detoxifying factor, Nrf2/Nfe2l2, was not affected by FoxO deletion in fasting, while it was less activated in denervated FoxO1,3,4 null muscles. Therefore, FoxO family members are necessary for muscle loss but their involvement in the atrophy programme depends on the catabolic condition.

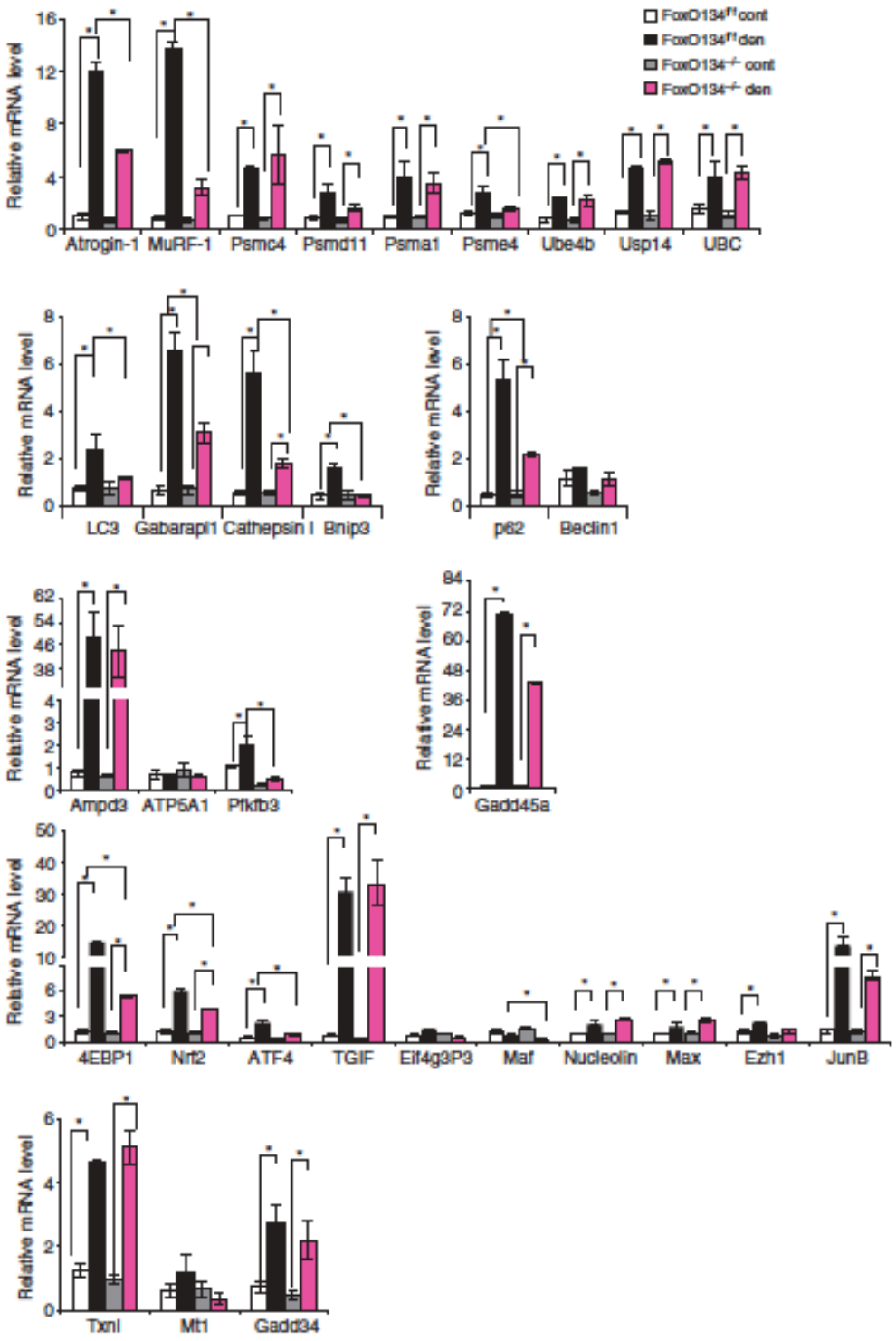

Fig.12: FoxOs are required for expression of several atrogenes after denervation. Quantitative RT–PCR of the indicated atrogenes after 3 days from denervation. Data are normalized to GAPDH and expressed as fold increase of control innervated muscles. Values are mean±s.e.m. *P<0,05, **P<0.01 (Student's t-test).; cont, control; den, denervated.

3.8 FoxOs REGULATE A NOVEL SET OF UBIQUITIN LIGASES

When we looked at the gene expression profiles in fasted muscles of FoxO1,3,4 knockout mice, we noticed a group of ubiquitin ligases that were upregulated in FoxO1,3,4f/f but not in FoxO1,3,4 -/- mice. This set of ubiquitin ligases includes MUSA1, a novel E3, that we have recently found to be critical in muscle atrophy (Sartori et al., 2013), Fbxo31, an E3 of SCF family involved in cyclinD degradation and tumour suppression (Santra et al., 2009), Itch, a HECT type ubiquitin ligase that regulates the half-life of transcription factors such as JunB, c-Jun and p63 (Melino et al., 2008) , and, finally, Fbxo21, a gene of unknown function but that contains an F-box motif and that we named SMART (Specific of Muscle Atrophy and Regulated by Transcription).

By quantitative RT–PCR, we confirmed that upregulation of MUSA1, SMART and FbxO31, but not Itch, is blunted or partially blocked in fasted or denervated muscles of FoxO1,3,4, knockout mice (Fig. 13 a,b).

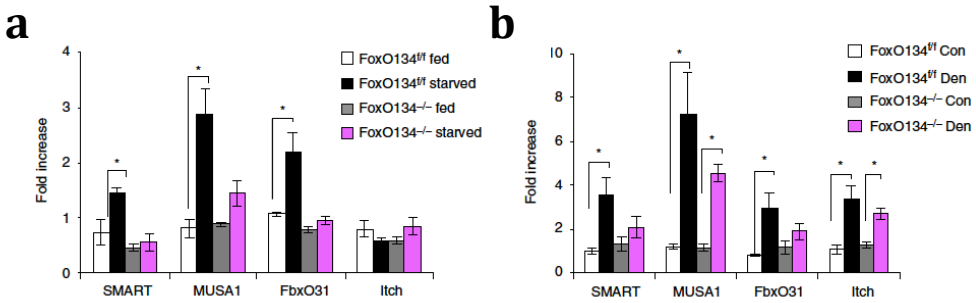

Fig.13: FoxO members control a new set of ubiquitin ligases. (a)qRT–PCR of the novel ubiquitin ligases MUSA1, Fbxo21/SMART, Fbxo31, Itch from 24 starved or denervated **(b)** FoxO1,3,4f/f and FoxO1,3,4-/- mice. Data are normalized to GAPDH and expressed as fold increase of fed control mice. n.4 muscles for each group.

To further prove that the FoxO family is sufficient for their expression, in collaboration with Goldberg's group we overexpressed FoxO3 in myotubes and we checked the expression of these E3s. Interestingly, FoxO3 was sufficient to induce the expression of MUSA1 but not the other ubiquitin ligases (Figure 14).

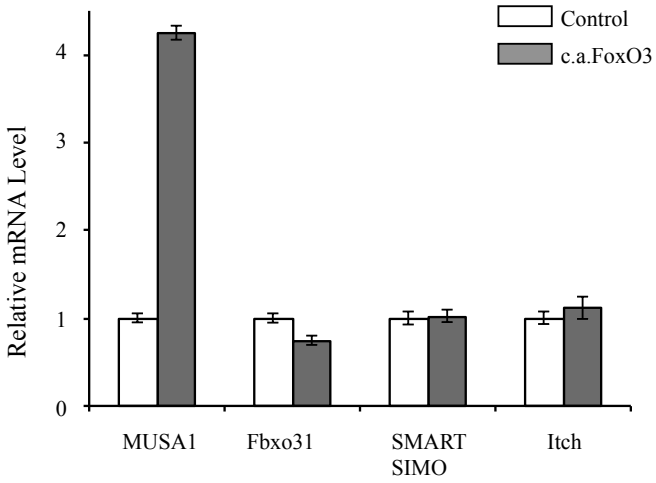

Fig.14: FoxO3 is sufficient to induce MUSA1, but not SMART, Itch or Fbox31. Quantitative RT-PCR of the different ubiquitin ligases in myotubes overexpressing c.a.FoxO3 and controls. Values are means ± s.e.m.Error bars indicate s.e.m**p<0.01(Student's t-test) c.a :constitutively active.

3.9 SMART IS A NOVEL E3 LIGASE REQUIRED FOR MUSCLE ATROPHY

To understand if Fbxo21 was an E3 ligase that belonged to the SCF group we performed an IP experiment. We immunoprecipitated Fbxo21 with a components of the complex SCF, Skp1, Cullin1 and Roc1, by western blot analysis confirmed that SMART forms an SCF complex with Skp1, Cullin1 and Roc1 (Fig. 15) and therefore belongs to the SCF family of E3 ligases.

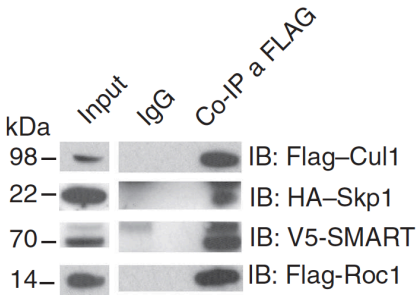

Fig.15: Smart is a novel ubiquitin ligase required for denervation-dependent atrophy. Co-immunoprecipitation experiment showing that SMART is a F-box protein that forms a SCF complex. C2C12 muscle cell lines were transfected with SMART, Skp1, Cul1 and Roc1 expression plasmids. After 24 h, cells were lysed and immunoprecipitation against FLAG-tag or control IgG was performed. Western blots for the different SCF components are shown.

Then, to confirm the role of SMART in promoting atrophy during denervation, we knocked down SMART in TA in vivo. Four different short hairpin RNAs (shRNAs) have been tested to specifically reduce SMART protein levels (Fig. 16a), three of which efficiently knocked down SMART. Next, we transfected oligo 4 into innervated and denervated muscles. These shRNAs did not affect the expression of the other atrophy-related ubiquitin ligases, MUSA, MuRF1 and atrogin1 both at protein and mRNA level (Fig. 16b, Fig. 17a).

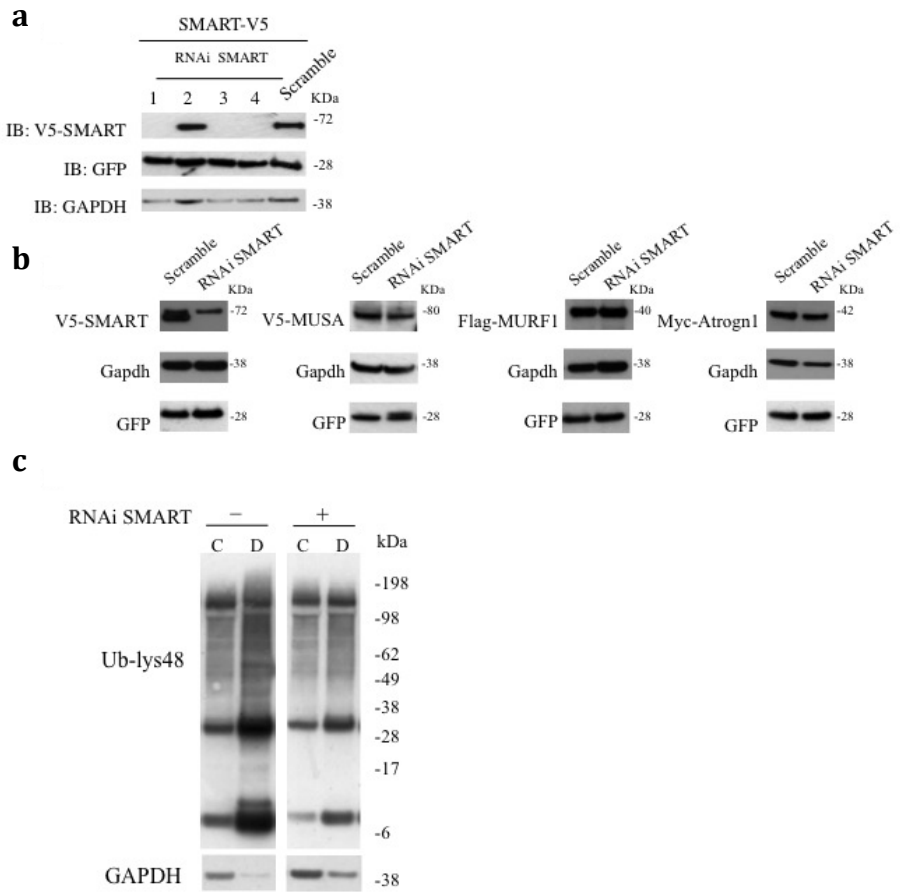

Fig.16: RNAi-mediated knockdown of SMART. **(a)** RNAi-mediated knockdown of SMART revealed by immunoblotting. Murine embryonic fibroblasts (MEFs) were transfected with vectors expressing different shRNAs against SMART together with vectors encoding murine V5-SMART. IB: immunoblotting **(b)** The shRNA against SMART does not interfere with MUSA, Atrogin1, and MuRF1 expression. C2C12 myoblast were co-transfected with vectors expressing shRNA against SMART (oligo 4) or scramble together with vectors encoding V5-SMART, V5- MUSA, Flag-MURF1 or Myc-Atrogin1. After 48 hours proteins were extracted and immunoblotted for V5, Flag or Myc tag. GADPH and GFP were detected as control of loading and transfection efficiency respectively. **(c)** Representative immunoblots against K48 polyUbiquitin chains of innervated or denervated TA muscles that were transfected with shRNAs against SMART or scramble. C: control, D: denervated.

Importantly, SMART inhibition significantly protected denervated muscles from atrophy (Fig. 17b). This sparing is due to the fact that by blocking SMART we greatly reduced protein ubiquitination in denervated muscles (Fig. 17c). Therefore, we have identified SMART as an additional critical gene whose upregulation is required for atrophy, yet must be carefully controlled to avoid excessive protein breakdown. In conclusion, our findings underline the concept that FoxO members are the master regulatory factor for protein homeostasis during catabolic conditions.

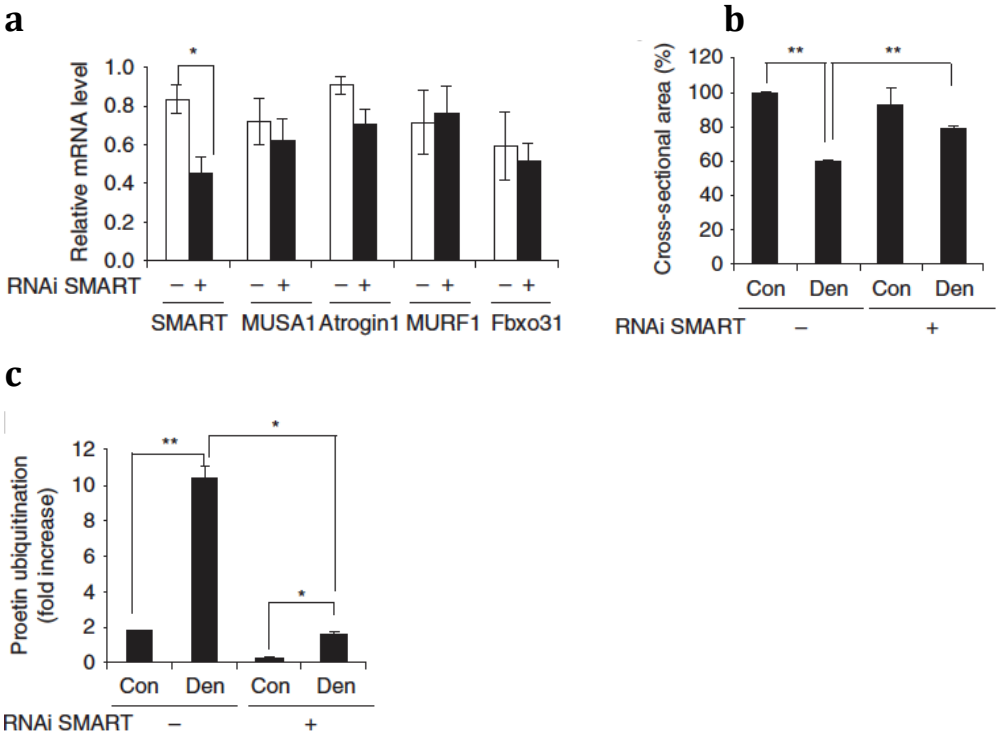

Fig.17: Smart is a novel ubiquitin ligase required for denervation-dependent atrophy. **(a)**RNAi-mediated knockdown of SMART revealed by quantitative RT–PCR (qRT–PCR). Adult TA muscles were transfected with bicistronic expressing vectors that encode either oligo 4 or scramble and GFP. Two weeks later TA muscles were collected, RNA extracted and endogenous SMART, MUSA1, Atrogin1, MuRF1 and Fbxo31 expression were analysed by qRT–PCR, n.4. **(b)** Inhibition of SMART prevents muscle atrophy in denervated muscles. Adult muscle fibres were co-transfected with bicistronic expressing vectors that encode shRNAs against SMART (oligo 4) or scramble and GFP and denervated. Two weeks later cross-sectional area of transfected fibres, identified by GFP fluorescence, was measured. n.6 muscles for each group. **(c)** Densitometric quantification of polyubiquitinated proteins in muscle extracts transfected with shRNAs against SMART or scramble. Values are normalized to GAPDH and expressed as fold increase of fed control mice. N=3 muscles for each group. Data are shown as mean±s.e.m. Error bars indicate s.e.m. *P<0.05, **P<0.01 (Student's t-test). con, control; den, denervated; IB, immunoblotting.

4. DISCUSSION

Muscle atrophy occurs in specific muscles with denervation or inactivity, but is also a systemic response to fasting and various diseases. The identification of the precise signaling cascades that regulate muscle wasting remains poorly understood. Forkhead box class O family member proteins (FoxOs) are highly conserved transcription factors with important roles in cellular homeostasis like apoptosis, ROS detoxification, glucose metabolism, DNA repair, cell cycle, stem cell maintenance and longevity. The role of FoxO transcription factors in the regulation of skeletal muscle protein degradation has been studied over the last years. FoxO has been shown to regulate the two major systems of protein breakdown in skeletal muscle, the ubiquitin–proteasome and the autophagy–lysosomal pathways. The ubiquitin-proteasome system is constitutively active in muscle but its activity increases significantly during muscle atrophy due to activation of two ubiquitin ligases: Atrogin-1/Mafbx and Murf1 (Gomes et al., 2001). The activation of these two genes is regulated by the transcription factor FoxO3. This factor is normally phosphorylated and inactivated by AKT/PKB kinase and this is due by the exclusion of FoxO3 from nucleus. Conversely, when this pathway is suppressed (es: during muscle atrophy), FoxO3 translocates into the nucleus where it can trascribe its target genes (Sandri et al., 2004; Stitt et al., 2004). Among the three FOXO family members, FoxO1 and FoxO3 have received the most attention as they are probably activated in all types of atrophy (Sandri et al., 2004), and they both induce components of the UPS and autophagy . The critical contribution in understanding muscle atrophy comes from the pioneering studies on gene expression profiling performed independently by groups of Goldberg and Glass. They used microarray studies to identify a set of 120 atrophy-related genes named atrogenes that were induced or repressed in various wasting conditions such as diabetes, chronic renal failure, cancer cachexia, fasting and denervation.

Moreover, the trascription factors that orchestrate this complex gene network are still largely unknown. For this reason, we have decide to

elucidate the specific function of FoxOs in skeletal muscle. Our findings highlight the FoxO family as one of the most important regulators of muscle loss. In fact, here we dissect the role of this family of trascription factors in the regulation of gene trascription and muscle adaptation during muscle atrophy by loss of function approaches.

The data that different genes involved in different pathways, including several ubiquitin ligases and proteasome subunits, are under FoxO regulation, is an important step towards the understanding of FoxO-dependent adaptation to stress such as nutritional deprivation. It is important to remember that one of the adaptive response to sustain muscle mass and cellular survival during catabolic condition is autophagy. Our data from different knockout mice highlight the concept that FoxOs are required to sustain autophagy induction under low nutrients and dominate mTOR signalling. It is worth to underline that FoxO deletion does not affect basal autophagy flux and indeed the knockout mice do not show any overt pathological phenotype that may resemble the features of muscle specific Atg7 knockout mice (Masiero et al., 2009). This is in contrast with the phenotype of the TSC1 knockout mice that display an hyperactivation of mTORC1 pathway leading to inhibition of basal autophagy flux and resulting in myopathic phenotype (Castets et al., 2013). FoxOs trascription factors are necessary to maintain autophagy flux under low nutrients, we founded that induction and maintenance of high autophagic flux for hours/days is entirely dependent on the FoxO family. The deletion of FoxO both in a muscle-specific manner and in an inducible muscle-specific manner resulted in suppression of autophagy during fasting represented by a block of LC3 lipidation and p62 accumulation. Importantly, in our work, we have characterize also the single FoxO1,3 and 4 knock-out mice and we shown that deletion of a single FoxO member is not sufficient to prevent muscle loss and autophagy activation supports the conclusion that there is significant redundancy among family members (Milan et al., 2015).

Interestingly, the sparing of muscle mass was observed only in FoxO3 knock-out mice after denervation, and was not only due to an effect on the classical

ubiquitin ligase atrogin1 and MuRF1 but also by action of FoxO3 on a different set of ubiquitin ligases. By microarray analysis, we have identified a group of novel ubiquitin ligases that are regulated by FoxO. Among the novel E3s we identified a gene that encodes an F-box protein (FbxO21) whose function was completely unknown and that we named SMART.

Gain- and loss-of-function experiments showed that FoxOs are required for SMART regulation and ChIP experiments revealed that both FoxO1 and FoxO3 are recruited on the promoter of these genes (Milan et al., 2015). We discovered SMART as a new E3 ligase that is part on a SCF complex, and future works are necessary to elucide its function in muscle atrophy and its substrates. However, deletion of FoxO3 and not of FoxO1 completely blunted SMART induction after denervation, suggesting that SMART is mainly under FoxO3 regulation. However, when we overexpressed FoxO3 only MUSA1 was induced, suggesting that FoxO3 is required for SMART induction but not sufficient and that other transcription factors are therefore involved in its regulation. MUSA1 is a novel ubiquitin ligase that we found to be critical for muscle atrophy during denervation and fasting. Expression of MUSA1 is regulated by Smad transcription factors in denervated muscles (Sartori et al., 2013). The possibility that Smads and FoxO cooperate for MUSA1 expression is consistent with the data that Smads recognize a very simple sequence that is extremely common in the genome and therefore, activated Smad proteins must associate with different DNA-binding cofactors for the recognition and regulation of specific target genes. Importantly, in keratinocytes, glioblastoma and neuroepithelial cells FoxOs are critical Smad partners for the expression of p21 and p15 genes (Seoane et al., 2004). Therefore, it is possible that Smads are the partners of FoxO and both are required for the optimal activation of the atrogenes during denervation. Nevertheless, during fasting most of the atrophy-related genes are completely dependent on FoxO. In addition to the FoxO dependent regulation of different ubiquitin ligases, it is important to emphasize that several proteasome subunits, ubiquitin C, the E4 enzyme and the de-ubiquitinating enzyme USP14 are also controlled by FoxOs. These genes are critical in several steps of ubiquitination and

proteasome-dependent degradation and might have an important role in control of protein degradation. For instance, it has recently been reported that expression of PSMD11 in human stem cells is sufficient to increase proteasome assembly and activity and, in C. elegans, a PSMD11 homologue induces resistance to oxidative stress and poly-glutamine aggregation and extends lifespan (Vilchez et al., 2012). Further work is needed to understand the interplay between the autophagy–lysosome and ubiquitin–proteasome systems in the context of different catabolic or even anabolic conditions, however, this work sets out the fundamentals for understanding the regulation of proteostasis in striated muscles.

nature COMMUNICATIONS

ARTICLE

Received 26 Sep 2014 | Accepted 18 Feb 2015 | Published 10 Apr 2015

DOI: 10.1038/ncomms7670 OPEN

Regulation of autophagy and the ubiquitin–proteasome system by the FoxO transcriptional network during muscle atrophy

Giulia Milan[1,*], Vanina Romanello[1,*], Francesca Pescatore[1,2,*], Andrea Armani[1], Ji-Hye Paik[3], Laura Frasson[1], Anke Seydel[1], Jinghui Zhao[4], Reimar Abraham[5], Alfred L. Goldberg[4], Bert Blaauw[2], Ronald A. DePinho[6] & Marco Sandri[1,2,7,8,9]

Stresses like low nutrients, systemic inflammation, cancer or infections provoke a catabolic state characterized by enhanced muscle proteolysis and amino acid release to sustain liver gluconeogenesis and tissue protein synthesis. These conditions activate the family of Forkhead Box (Fox) O transcription factors. Here we report that muscle-specific deletion of FoxO members protects from muscle loss as a result of the role of FoxOs in the induction of autophagy–lysosome and ubiquitin–proteasome systems. Notably, in the setting of low nutrient signalling, we demonstrate that FoxOs are required for Akt activity but not for mTOR signalling. FoxOs control several stress-response pathways such as the unfolded protein response, ROS detoxification, DNA repair and translation. Finally, we identify FoxO-dependent ubiquitin ligases including MUSA1 and a previously uncharacterised ligase termed SMART (Specific of Muscle Atrophy and Regulated by Transcription). Our findings underscore the central function of FoxOs in coordinating a variety of stress-response genes during catabolic conditions.

[1] Venetian Institute of Molecular Medicine, via Orus 2, 35129 Padova, Italy. [2] Department of Biomedical Sciences, University of Padova, 35131 Padova, Italy. [3] Department of Pathology and Laboratory Medicine, Weill Cornell Medical College, New York, New York 10065, USA. [4] Department of Cell Biology, Harvard Medical School, Boston, Massachusetts 02115, USA. [5] Department of Cancer Biology, U3 Pharma GmbH, Martinsried 82152, Germany. [6] Department of Cancer Biology, University of Texas MD Anderson Cancer Center, Houston, Texas 77030, USA. [7] Institute of Neuroscience, Consiglio Nazionale delle Ricerche, 35129 Padova, Italy. [8] Department of Medicine, McGill University, Montreal, Quebec H3AoG4, Canada. [9] Dulbecco Telethon Institute at Telethon Institute of Genetics and Medicine (TIGEM), 80131 Napoli, Italy. * These authors contributed equally to this work. Correspondence and requests for materials should be addressed to M.S. (email: marco.sandri@unipd.it).

Environmental transformations have selected for species that are able to quickly and efficiently regulate their physiology. Under stress conditions, mammalian cells activate compensatory mechanisms to adapt themselves to new situations. Depending on the stimuli, the adaptive response either require minor and fast metabolic changes or involves major and sustained adjustments that need transcription-dependent adaptations. Muscles are the largest protein reservoir in the body and serve as a source of amino acids that can be used for energy production by various vital organs (including heart, liver and brain) during catabolic periods, such as in cancer, sepsis, burn injury, heart failure and AIDS[1]. However, excessive and sustained protein degradation in skeletal muscle, and the resulting muscle loss (cachexia), is highly detrimental and can lead to death. Moreover, excessive loss of muscle mass is a poor prognostic index and impairs the efficacy of many different therapeutic treatments. Thus, cachexia ultimately aggravates diseases and increases morbidity and mortality.

In eukaryotic cells, most proteins are degraded via two proteolytic systems: the ubiquitin–proteasome and the autophagy–lysosome. In skeletal and cardiac muscles the two systems are coordinately regulated to remove proteins and organelles in atrophying cells[2,3]. Muscle atrophy requires a transcription-dependent programme to regulate a group of genes that are commonly up or downregulated in atrophying muscles during different catabolic conditions and that are named atrophy-related genes or atrogenes[1,4–8]. These genes encode enzymes that catalyse important steps in autophagy–lysosome, ubiquitin–proteasome, unfolded protein response, ROS detoxification, DNA repair, mitochondrial function and energy balance pathways. The transcription factors that orchestrate this complex gene network have been the focus of active investigation.

The two atrogenes with the greatest induction are two muscle-specific ubiquitin ligases, namely *atrogin1/MAFbx* and *MuRF1*[4,5]. Mice lacking these two enzymes are partially resistant to muscle atrophy induced by denervation[4]. However, the action of these two ubiquitin ligases cannot account for the degradation of all muscle proteins. A number of additional unknown ubiquitin ligases (E3s) are presumably activated during atrophy to promote the clearance of myofibrillar and soluble proteins and/or to limit anabolic processes. We have recently established that these atrophy-related ubiquitin ligases, as well as protein breakdown in general, are blocked by the growth-promoting IGF1/AKT pathway[8,9]. Members of the Forkhead Box (Fox) O family (FoxO1, 3 and 4), downstream targets of AKT, were identified as the main transcription factors regulating atrogin1 expression[8]. Importantly, we have also found that FoxO3 regulates autophagy coordinating the proteasomal-dependent removal of proteins with the autophagy-dependent clearance of organelles[2,10]. The use of FoxO1 knockout mice has established a role in muscle protein homeostasis showing partial protection from muscle loss during chronic kidney disease[11]. FoxO1 deficiency was associated with partial reduction in the expression of atrogin1, MuRF1 and the lysosomal enzyme, Cathepsin-L[11,12]. These studies linking FoxOs and muscle wasting prompted us to explore more fully the specific function of the entire FoxO family in skeletal muscle maintenance/loss and the potential for functional redundancy among the FoxO members and to illuminate the atrogene expression network focused on the identification of novel FoxO-dependent atrophy-related genes.

Here we show that specific deletion of FoxOs in skeletal muscles prevents muscle loss and force decline in response to fasting and denervation because the FoxO family is required for the induction of several atrophy-related genes. Moreover, we identify a novel ubiquitin ligase, named SMART (Specific of Muscle Atrophy and Regulated by Transcription), that plays a critical role in protein ubiquitination after denervation.

Results

Generation of a triple FoxO1,3,4 muscle-specific knockout. Since muscle wasting requires a transcriptional-dependent programme to induce the expression of a subset of genes and because FoxO family is sufficient to induce muscle atrophy, we generated mice with adult skeletal muscle-specific deletion of all three FoxO family members to unravel the role of this family in gene regulation and muscle adaptation during catabolic conditions. To that end, *FoxO1/3/4*-floxed mice (*FoxO1/3/4*$^{f/f}$) were crossed with a transgenic line expressing Cre recombinase under the control of muscle-specific MLC1f promoter (hereafter referred to as *FoxO1,3,4*$^{-/-}$). PCR analysis confirmed deletion of the floxed sequence from genomic DNA extracted from skeletal muscle (Fig. 1a). Quantitative reverse transcription–PCR (RT–PCR) and Western blot analyses showed a significant decrease or elimination of *FoxO1*, *FoxO3* and *FoxO4* transcripts and proteins, respectively (Fig. 1b,c). Since FoxO4 is mainly expressed in striated muscles[13], while FoxO1 and 3 are expressed in a variety of tissues, the traces of *FoxO1* and *3* messenger RNAs (mRNAs) come from endothelial, fibroblasts, macrophages and blood cells. Thus, we confirm a genetic model of muscle-specific inhibition of FoxO1,3,4 family.

Triple FoxO1,3,4 deletion in muscle does not affect fibre type. *FoxO1,3,4*$^{-/-}$ mice were indistinguishable in gross appearance from age-matched control *FoxO1,3,4*$^{f/f}$ mice and histological analysis of adult muscles revealed normal muscle architecture and absence of myopathic features such as centrally nucleated fibres (Fig. 1d). Succinate dehydrogenase staining showed no major changes in distribution of small β-oxidative mitochondrial rich versus large glycolytic mitochondrial poor fibres (Fig. 1e). Since FoxOs are important for glucose homeostasis in liver, we monitored glycogen levels in muscle. PAS staining revealed an almost identical distribution of glycogen stores (Fig. 1f). Analyses of myosin heavy chain expression (Fig. 1g) and distribution (Fig. 1h) did not reveal any significant difference between wild-type and FoxO1,3,4 knockout mice. These findings support the view that FoxO deficiency does not affect fibre type determination and basal glucose homeostasis and is permissive for normal muscle function. Quantification of cross-sectional area of fast muscles (Tibialis Anterior (TA) and Gastrocnemius) did not show any significant difference between knockout and controls (Fig. 1i, Supplementary Fig. 1).

FoxO inhibition prevents muscle loss and weakness. To further characterize the role of FoxO1,3,4 in skeletal muscles, we then analysed the phenotype of *FoxO1,3,4*$^{-/-}$ mice under conditions of muscle wasting. Initially, we used fasting as a model of muscle loss since it is an established condition that induces nuclear translocation of FoxO members and their binding to target promoters[2,8,14] (Supplementary Fig. 2) and we compared FoxO1,3,4 null muscles with controls. Importantly, FoxO1,3,4 knockout mice were completely spared from muscle loss after fasting (Fig. 2a, Supplementary Fig. 3). To understand whether sparing of muscle mass is also functionally relevant, we measured muscle force in living animals. While control fasted animals became significantly weaker than fed ones, *FoxO1,3,4*$^{-/-}$ gastrocnemius muscles did not loose strength after fasting (Fig. 2b). Importantly the comparison of force/frequency curve of fasted wild-type versus fasted FoxO1,3,4 null muscle underlined the important protection achieved by the absence of FoxO family when nutrients are low or absent (Fig. 2c). These findings confirm that the absence of FoxO members prevents atrophy and profound weakening. To explain this profound effect on sparing force and muscle mass, we monitored the level of the

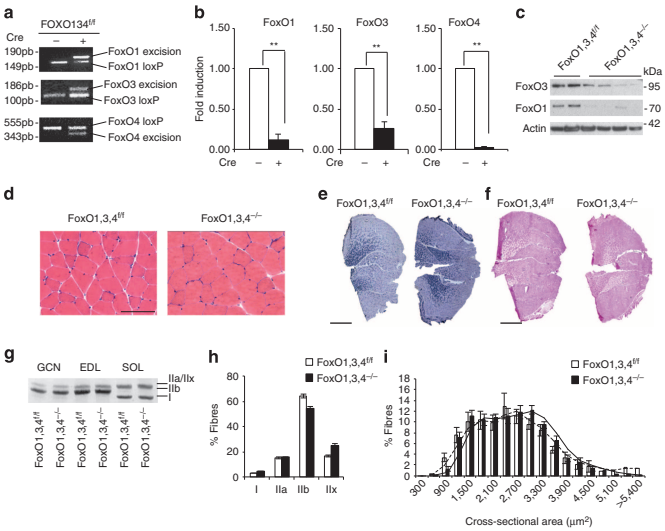

Figure 1 | Deletion of FoxOs is permissive for normal muscle function. (**a**) PCR analysis with genomic DNA from FoxO1,3,4$^{f/f}$ and FoxO1,3,4$^{-/-}$ gastrocnemius muscles. (**b**) *FoxO1*, *FoxO3* and *FoxO4* mRNA expression were quantified by RT-PCR in Tibialis Anterior (TA) muscle of *FoxO1,3,4*$^{-/-}$ and control mice. $n=4$ each group. (**c**) Immunoblot showing reduction of FoxO1 and FoxO3 proteins in homogenates of *FoxO1,3,4*$^{-/-}$ gastrocnemius muscles. Data are representative of three independent experiments. (**d**) Haematoxylin and eosin (Scale bar, 100 μm), (**e**) SDH (Scale bar, 1 mm) and (**f**) PAS staining (Scale bar, 1 mm) showing normal morphology, fibre type and glycogen of *FoxO1,3,4*$^{-/-}$ gastrocnemius muscle. (**g**) SDS-PAGE and (**h**) immunohistochemistry analysis of myosin heavy chain type I, IIA, IIB and IIX proteins in gastrocnemius muscles showing no differences between *FoxO1,3,4*$^{-/-}$ and *FoxO1,3,4*$^{f/f}$ mice. Data are representative of three independent experiments. (**i**) Frequency histograms showing the distribution of cross-sectional areas (μm^2) in TA of *FoxO1,3,4*$^{f/f}$ (white bars) and *FoxO1,3,4*$^{-/-}$ (black bars) fibres, $n=4$, each group. Data are shown as mean ± s.e.m. Error bars indicate s.e.m. $^{**}P<0.01$ (Student's *t*-test).

contractile protein, myosin, when nutrients are removed. As expected, fasting induced an important reduction of myosin content in controls, while FoxO1,3,4 knockout were completely protected (Supplementary Fig. 4a). The maintenance of myosins in knockout is consequent to inhibition of protein ubiquitination (Supplementary Fig. 4b-c).

FoxOs are critical for autophagy and protein ubiquitination. To explore the basis for sparing of muscle mass in absence of nutrients, we audited the signalling pathways linked to Insulin/IGF1 and energy. Interestingly, Akt, S6K and S6 phosphorylation, both in fed and fasted muscles, were reduced in knockout mice, while phosphorylation of 4EBP1, the other mTORC1 downstream target, was increased in FoxO-deficient TA muscle (Fig. 2d, Supplementary Fig. 5a). The energy–stress sensor AMPK and its downstream target ACC did not significantly differ from controls in fed and fasting conditions (Fig. 2d). Therefore, the changes in the pathways downstream energy and insulin/nutrients do not match with the important sparing of muscle mass in knockout mice when nutrients are absent.

Since the absence of nutrients is a potent stimulus for autophagy-dependent degradation and since FoxO is an inducer, while mTOR is a suppressor of autophagy–lysosome system, we checked the status of this system in *FoxO1,3,4*$^{-/-}$ mice. We monitored LC3 lipidation, LC3-positive vesicles and autophagy flux in *FoxO1,3,4*$^{f/f}$ and *FoxO1,3,4* $^{-/-}$ mice. Fasting induced LC3 lipidation (Fig. 2e, Supplementary Fig. 5b) and vesicles formation (Fig. 2f) in control but not in FoxO-deficient muscles. Autophagy flux was monitored by treating animals with colchicine, an established inhibitor of microtubule-mediated delivery of autophagosome to lysosome[15]. The inhibition of autophagosome fusion to lysosomes led to accumulation of lipidated LC3 in controls but not in FoxO1,3,4-deficient muscles (Fig. 2g). In conclusion, during fasting, despite mTOR signalling being partially inhibited, autophagy enhancement is completely blocked in *FoxO1,3,4*$^{-/-}$ muscle.

Absence of nutrients activates also the ubiquitin–proteasome system, leading to an increase of protein ubiquitination and, consequently, in proteasome-dependent degradation. Fasting resulted in an increase in both lysine-48 and lysine-63 poly-ubiquitinated proteins (Supplementary Fig. 4b,c), confirming an activation of the ubiquitination process in controls. Importantly, this increase was totally abolished in FoxO1,3,4 knockout mice.

Half of the atrophy-related genes are under FoxO regulation. Since muscle atrophy is characterized by transcription-dependent regulation of atrogenes (atrophy-related genes) and FoxO deficiency protects from muscle loss, we sought to identify genes under FoxO regulation. Gene expression profiles of fed and fasted control and *FoxO1,3,4*$^{-/-}$ muscles were compared with identify genes with blunted induction in the fasted *FoxO1,3,4*$^{-/-}$ mice relative to controls. Cross-referencing with the list of known

atrogenes[7], these analyses revealed that 29 of the 63 atrophy-related genes require FoxO for their normal induction during fasting (Fig. 2h, Supplementary Fig. 10). Quantitative RT–PCR confirmed that 26 of the atrophy-related genes were not induced in FoxO null muscles during fasting (Fig. 3). Consistent with morphology and force measurements, the induction of genes involved in protein breakdown was completely blocked in knockout mice. In fact both the ubiquitin system including the ubiquitin ligases (*Atrogin1* and *MuRF1*), the ubiquitin gene (*UBC*), the de-ubiquitinating enzyme (*USP14*), the E3/E4 enzyme

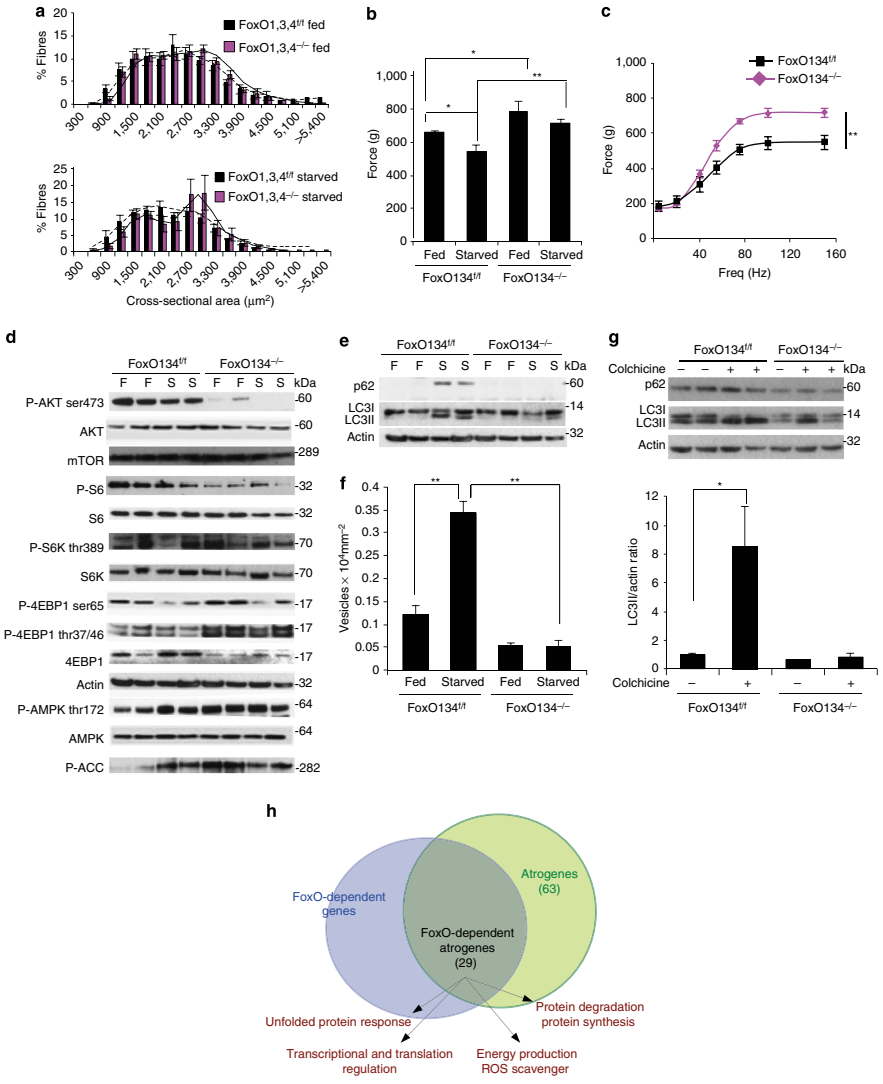

(*Ube4b*), several proteasome subunits (*Psme4/PA200, Psma1, Psmc4/Rpt3* and *Psmd11/Rpn6*) as well as the autophagy-related genes (*LC3, Gabarapl, Bnip3, Cathepsin L* and *p62/SQSTM1*) were completely blocked in *FoxO1,3,4*$^{-/-}$ mice. Other pathways that are inhibited in knockout muscles are related to the unfolded protein response (*ATF4* and *GADD34*), protein synthesis (*4EBP1* and *eIF4g*), transcription regulators that negatively control Smad2/3 (*TGIF*) or positively affect Myc (*MAX*), DNA repair/chromatin remodelling (*GADD45α*) and ribosome transcription/maturation/assembly (*Nucleolin*). Expression of genes that are related to oxidative stress were more variable; *Nrf2/Nfe2l2* was not affected by FoxO deletion, while *Thioredoxin* was suppressed and *Metallothionein1* was significantly induced in the absence of FoxO factors.

Western blot analyses of some atrogenes involved in autophagy (p62, Gabarapl and Bnip3), chromatin remodelling/DNA repair (GADD45α), protein synthesis (4EBP1) and ubiquitin–proteasome confirmed their upregulation during fasting in control animals but not in FoxO1,3,4 knockout (Supplementary Fig. 6).

Inducible FoxOs loss phenocopies the conditional knockout. To corroborate our findings, we also explored the impact of somatic deletion of FoxO in the adult via a tamoxifen-inducible muscle-specific FoxO knockout model. Following documentation of tamoxifen-induced deletion of FoxOs (Supplementary Fig. 7), we assessed muscle loss during fasting by monitoring muscle mass and muscle force. Similar to the above, we found that somatic deletion of FoxO1,3,4 prevented muscle loss (Fig. 4a) and muscle weakness during fasting (Fig. 4b). Consistent with the conditional knockout, Akt activation and LC3 lipidation was reduced in FoxO knockout when compared with controls (Fig. 4c). Autophagy flux measurements confirmed that FoxOs are required for autophagy induction (Fig. 4d). We then tested whether inhibition of FoxO members in adulthood blocked the activation of the atrogenes. Indeed, we confirmed most of the data obtained by the conditional FoxO1,3,4 knockout (Supplementary Fig. 8). The fact that two different FoxO1,3,4 knockout mice resulted in comparable biological effects strongly supports the conclusion that the FoxO family is a master regulator of the atrophy programme under low nutrient conditions.

FoxOs directly regulate atrophy-related genes. To determine whether the regulation of these atrogenes requires direct binding of FoxO transcription factors to their promoters and to identify the binding sites we performed chromatin immunoprecipitation (ChIP) experiments on fasted muscles of *FoxO1,3,4*$^{f/f}$. We also used *FoxO1,3,4*$^{-/-}$ as a negative control to validate the specificity of the immunoprecipitation. FoxO3 was recruited to almost all of the promoters so far analysed (Fig. 4e). We then asked whether the activation of these genes is strictly dependent on FoxO3 or whether other FoxO members can bind the same promoter region. We could immunoprecipitate FoxO1 but not FoxO4 because we did not find any ChIP grade antibody that was specific for FoxO4 without crossreacting with other FoxOs. Interestingly, FoxO1 was found to be significantly recruited to some promoters such as *MuRF1*, *p62*, *Cathepsin L* and *TGIF* (Fig. 4f). This finding suggests that regulation of some genes is shared by different FoxO members, while others preferentially recruit FoxO3.

FoxOs are required for denervation-dependent atrophy. To further determine whether the role of FoxO1,3,4 is critical in different catabolic conditions, we then used denervation as another model of muscle atrophy. Quantification of fibre size revealed that FoxO-deficient muscles were partially protected from atrophy (Fig. 5a, Supplementary Fig. 9). When we monitored muscle force, we confirmed the histological data. Soleus muscle of FoxO1,3,4 knockout mice generated higher strength than controls in the basal condition (Fig. 5b) and FoxO deletion was able to partially prevent weakness and maintain the same force of innervated *FoxO1,3,4*$^{f/f}$ (Fig. 5b,c). The decrease of force in denervated FoxO1,3,4-deficient soleus muscle is related to the presence of FoxO proteins in type I fibres that can promote protein breakdown in these myofibres. It is important to emphasize that the type I fibres express FoxOs because the promoter (MLC1f) driving the expression of Cre recombinase is active in type II fibres and not in type I fibres. However, comparison of the force/frequency curves of denervated wild-type versus denervated FoxO1,3,4 null soleus muscles underlines the important protection conferred by the absence of FoxO family when nerve is damaged (Fig. 5c). Analyses of signalling confirmed the downregulation of P-AKT in knockout muscles. Denervation induced an increase of total and phospho-4EBP1 protein in *FoxO1,3,4*$^{f/f}$ but not in *FoxO1,3,4*$^{-/-}$ muscle (Fig. 5d). The changes in the phosphorylation of 4EBP1 were not ascribed to activation of the cellular energy sensor AMPK, revealed by checking its phosphorylation level or the downstream target ACC. In contrast to fasting, the autophagy system was mildly affected by the absence of FoxOs. Indeed, LC3 lipidation was slightly decreased in *FoxO1,3,4*$^{-/-}$ compared with controls after denervation (Fig. 5e). However, and consistent with fasting, the transcriptional upregulation of *p62/SQSTM1* in denervated muscles was greatly attenuated (Figs 5e and 6). When we tested the expression of the different atrophy-related genes, we found only a partial suppression of these genes (Fig. 6). Interestingly, the lists of FoxO-dependent genes during denervation and fasting do not completely overlap (Supplementary Fig. 10). For instance, the

Figure 2 | Deletion of FoxOs prevents muscle loss and weakness during fasting. (**a**) Frequency histograms of cross-sectional areas (μm^2) of *FoxO1,3,4*$^{f/f}$ (black bars) and *FoxO1,3,4*$^{-/-}$ (magenta bars) fibres in fed (upper panel) and fasted (lower panel) conditions, $n=4$, each group. (**b**) Force measurements preformed *in vivo* on gastrocnemius showed that *FoxO1,3,4*$^{-/-}$ muscles preserve maximal tetanic force after fasting; $n=6$ muscles in each group. (**c**) Force/frequency curve of starved gastrocnemius muscle underlines the important protection achieved by the absence of FoxOs; $n=6$ muscles in each group. (**d**) Immunoblot of protein extracts from gastrocnemius muscles. Phosphorylation of AKT and S6 is reduced in fed and starved *FoxO1,3,4*$^{-/-}$ muscles when compared with controls. Data are representative of three independent experiments. (**e**) Immunoblot analysis of p62 and LC3 in homogenates of gastrocnemius muscles from fed and starved *FoxO1,3,4*$^{-/-}$ or controls. Fasting did not induce LC3 lipidation and p62 upregulation in FoxO-deficient muscles. Data are representative of three independent experiments. (**f**) Quantification of GFP-LC3-positive vesicles in *FoxO1,3,4*$^{f/f}$ and *FoxO1,3,4*$^{-/-}$ TA muscles; $n=4$ muscles in each group (**g**) Autophagy flux is not increased in FoxO-deficient TA muscles. Inhibition of autophagy–lysosome fusion by colchicine treatment induces accumulation of LC3II band in starved control but not in starved *FoxO1,3,4*$^{-/-}$ muscles. Upper panel: immunoblot analysis of gastrocnemius homogenates. Lower panel: quantification of LC3 lipidation. $n=4$ muscles in each group (**h**) The scheme shows the overlap between FoxO-dependent genes, identified by gene expression profiling of fed ($n=4$) and fasted ($n=4$) muscles from *FoxO1,3,4*$^{f/f}$ and *FoxO1,3,4*$^{-/-}$ and atrophy-related genes or atrogenes. The data in the graphs are shown as mean ± s.e.m. Error bars indicate s.e.m. *$P<0.05$, **$P<0.01$ (Student's t-test).

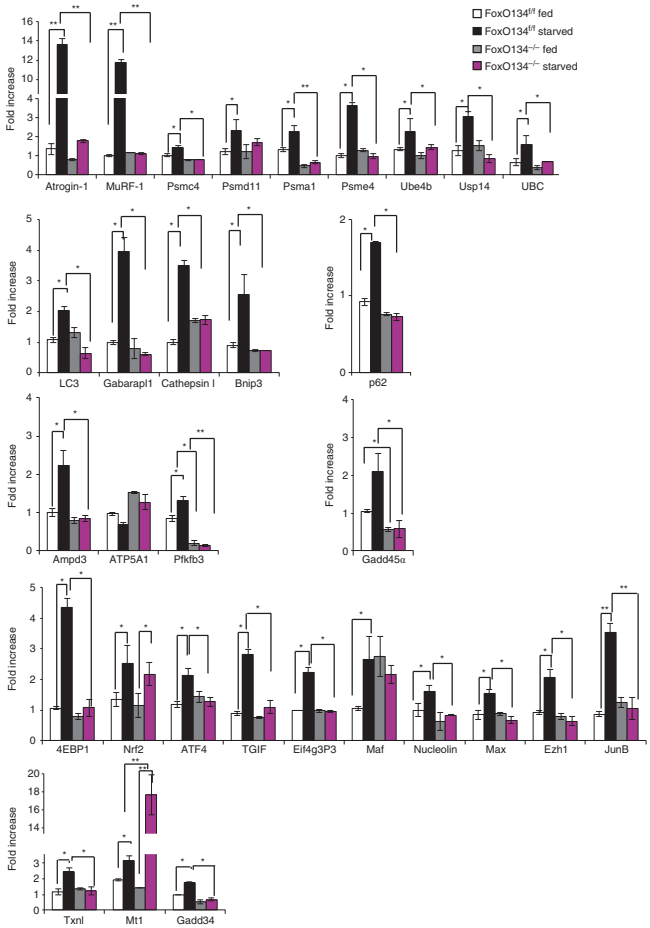

Figure 3 | Absence of FoxOs prevent the induction of critical atrogenes. Quantitative RT-PCR of atrogenes from fed and 24-h starved tibialis anterior of control and *FoxO1,3,4*$^{-/-}$ mice. Data are normalized to GAPDH and expressed as fold increase of control-fed animals. $n=4$ muscles in each group Values are mean ± s.e.m. $^{*}P<0.05$,$^{**}P<0.01$. (Student's *t*-test).

ROS detoxifying factor, *Nrf2/Nfe2l2*, was not affected by FoxO deletion in fasting, while it was less activated in denervated FoxO1,3,4 null muscles. Therefore, FoxO family members are necessary for muscle loss but their involvement in the atrophy programme depends on the catabolic condition.

FoxO members are redundant. Since all FoxO members are expressed in muscles and are under AKT regulation, we investigated whether they play synergistic roles or have specific functions. To address this point, we generated muscle-specific individual FoxO knockout animals. We used denervation as a model of muscle atrophy. Deletion of FoxO1 did not protect from muscle atrophy (Fig. 7a, Supplementary Fig. 11). However the presence of FoxO1 is required for the optimal induction of several atrophy-related genes including *MuRF1*, *Cathepsin L*, *Gabarap L*, *GADD45a* and *TGIF* (Supplementary Fig. 12).

Inhibition of FoxO3 led to a small but significant protection from denervation-induced muscle atrophy (Fig. 7b). The protection was mainly achieved in oxidative fibres

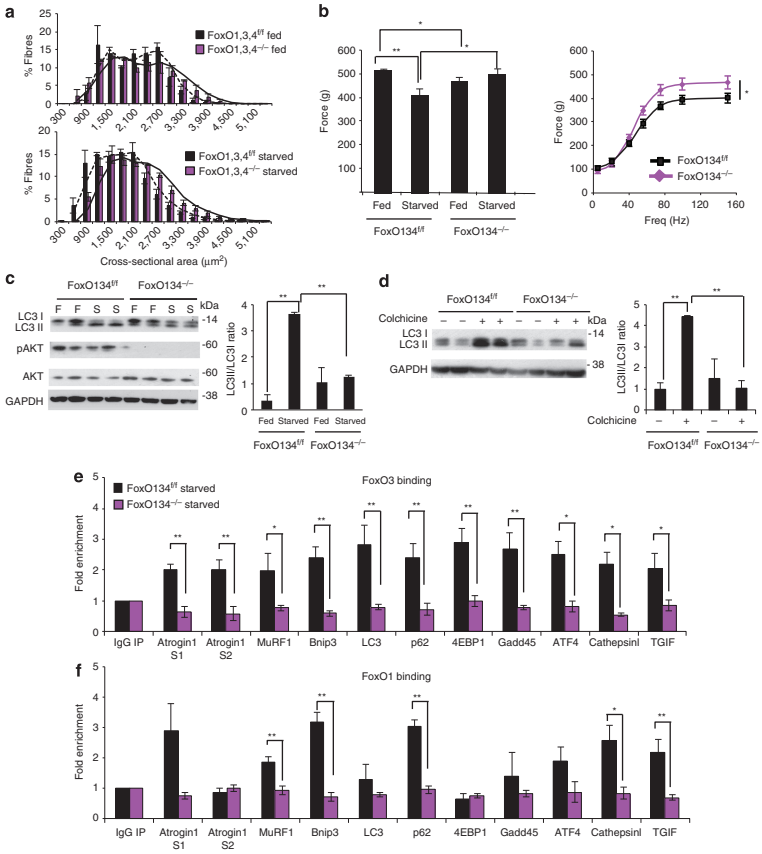

Figure 4 | Acute inhibition of FoxOs phenocopies the conditional FoxO1,3,4 knockout. (**a**) Frequency histograms of gastrocnemius muscles showing the distribution of cross-sectional areas (μm^2) of inducible muscle-specific FoxO1,3,4 mice after tamoxifen-dependent deletion of *FoxO1,3,4* genes (*FoxO1,3,4*$^{f/f}$: black bars and *FoxO1,3,4*$^{-/-}$: magenta bars) in fed (upper panel) and fasted (lower panel) conditions, $n=3$, each group. (**b**) Force measurements preformed *in vivo* on gastrocnemius muscle showed that acute inhibition of FoxOs in adulthood prevents force drop during fasting. $n=6$ muscles in each group. Freq: Frequency. (**c**) Left, immunoblotting analyses of gastrocnemius homogenates after acute deletion of FoxO1,3,4$^{-/-}$ and controls. Right, quantification of LC3 lipidation. Data are representative of three independent experiments. (**d**) Autophagy flux is not increased in FoxO-deficient TA muscles. Inhibition of autophagy–lysosome fusion by colchicine treatment induces accumulation of LC3II band in starved control but not in starved *FoxO1,3,4*$^{-/-}$ muscles. Left, immunoblotting analyses of gastrocnemius homogenates. Right, quantification of LC3 lipidation. (**e**,**f**) ChIP quantitative RT–PCR shows the recruitment of FoxO3 and FoxO1 on the promoters of selected atrophy-related genes. ChIP assays were performed in starved control and *FoxO1,3,4*$^{-/-}$ TA muscles. IgG was used as the reference. $n=3$ for each group. Data are shown as mean ± s.e.m. Error bars indicate s.e.m. $^{*}P<0.05$, $^{**}P<0.01$ (Student's *t*-test). S1: FoxO binding site 1; S2: FoxO binding site 2.

(Supplementary Fig. 13). Interestingly, when we checked the level of gene expression we found that *FoxO4* was strongly down-regulated in *FoxO3*$^{-/-}$ mice (Supplementary Fig. 14). Optimal expression of *Gabarapl, 4EBP1, Maf, Gadd45α, Pfkf3* and *Txn1* requires the presence of FoxO3 (Supplementary Fig. 14).

Ablation of FoxO4 did not significantly protect myofibres from atrophy after denervation (Fig. 7c and Supplementary Fig. 15) and did not reduce the expression of any atrogenes with the exception of a slight reduction of *GADD45α* and *Thioredoxin* (Supplementary Fig. 16).

FoxOs regulate a novel set of ubiquitin ligases. To explain why inhibition of FoxO3 slightly reduced muscle atrophy despite the

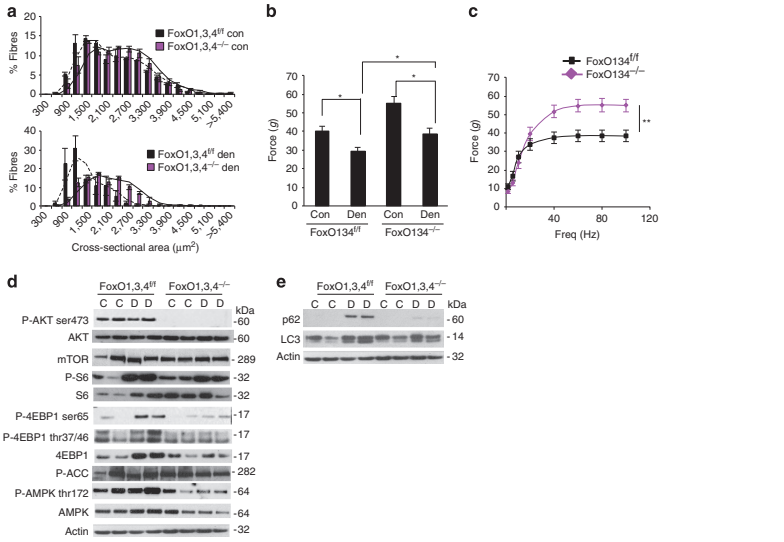

Figure 5 | Deletion of FoxOs in skeletal muscle partially prevents atrophy during denervation. (**a**) Frequency histograms of gastrocnemius muscles from *FoxO1,3,4*$^{-/-}$ and control mice showing the distribution of cross-sectional areas (μm^2) of *FoxO1,3,4*$^{f/f}$ (black bars) and *FoxO1,3,4*$^{-/-}$ (magenta bars) in control (upper panel) or in denervation (lower panel). $n=4$ muscles each groups. (**b**) Force measurements preformed *ex vivo* on soleus muscles show that *FoxO1,3,4*$^{-/-}$ muscles are stronger than controls, both in basal condition and after 14 days from denervation. $n=6$ muscles in each group. (**c**) Force/frequency curves of denervated soleus highlight the higher strength generated by *FoxO1,3,4*$^{-/-}$ muscles when compared with controls. $n=6$ muscles in each group. (**d**) Immunoblots of gastrocnemius protein extracts reveal a decrease of AKT phosphorylation both in contralateral and in denervated muscles of *FoxO1,3,4*$^{-/-}$ mice. The increase of 4EBP1 protein is blunted in FoxOs knockout mice. (**e**) Immunoblots of autophagy-related proteins. FoxOs are required for p62 induction, while LC3 is less lipidated after 3 days of denervation. Data are representative of three independent experiments. Data are shown as mean ± s.e.m. Error bars indicate s.e.m. *$P<0.05$, **$P<0.01$ (Student's *t*-test). C, control; D, denervated.

limited effects on induction of the atrophy-related genes, we looked for novel genes that might be involved in protein breakdown and that are selectively regulated by this FoxO member in denervated muscles. When we looked at the gene expression profiles in fasted muscles of FoxO1,3,4 knockout mice, we noticed a group of ubiquitin ligases that were upregulated in *FoxO1,3,4*$^{f/f}$ but not in *FoxO1,3,4*$^{-/-}$ mice. This set of ubiquitin ligases includes *MUSA1*, a novel E3, that we have recently found to be critical in muscle atrophy[16], *Fbxo31*, an E3 of SCF family involved in cyclinD degradation and tumour suppression[17], *Itch*, a HECT-type ubiquitin ligase that regulates the half-life of transcription factors such as JunB, c-Jun and p63[18], and, finally, *Fbxo21*, a gene of unknown function but that contains an F-box motif and that we re-named *SMART*.

By quantitative RT–PCR, we could validate that upregulation of *MUSA1, SMART* and *FbxO31*, but not *Itch*, is blunted or partially blocked in fasted or denervated muscles of FoxO1,3,4, knockout mice (Fig. 7d,e). To further prove that the FoxO family is sufficient for their expression, we overexpressed FoxO3 in myotubes and we checked the expression of these E3s. Interestingly, FoxO3 was sufficient to induce the expression of *MUSA1* but not the other ubiquitin ligases (Supplementary Fig. 17). We then analysed the promoter regions of these genes and checked whether endogenous FoxO1 and FoxO3 directly bind these regions. ChIP experiments on fasted muscle confirmed that both FoxO1 and FoxO3 bind to the promoters of *MUSA1* and *SMART* (Fig. 7f,g). However, we did not find any significant recruitment of FoxOs on *Itch* and *Fbxo31* promoters (Fig. 7f,g).

We checked whether expression of these ubiquitin ligases was suppressed in denervated muscles of the single FoxO knockout mice. Interestingly, FoxO3 deletion completely blunted the induction of *SMART* while ablation of the other FoxO members did not elicit any effect on the upregulation of these ubiquitin ligases (Fig. 7h–j). Therefore, FoxO3 is the main regulator of SMART in denervated muscles and inhibition of SMART may explain the partial protection of FoxO3 null muscles after denervation (Fig. 7b and Supplementary Fig. 13).

SMART is a novel E3 ligase required for muscle atrophy. IP experiments confirmed that SMART forms an SCF complex with Skp1, Cullin1 and Roc1 (Fig. 8a) and therefore belongs to the SCF family of E3 ligases. To confirm the role of SMART in promoting atrophy during denervation, we knocked down SMART in TA *in vivo*. Four different short hairpin RNAs (shRNAs) have been tested to specifically reduce SMART protein levels (Supplementary Fig. 18a), three of which efficiently knocked down SMART. Next, we transfected oligo 4 into innervated and

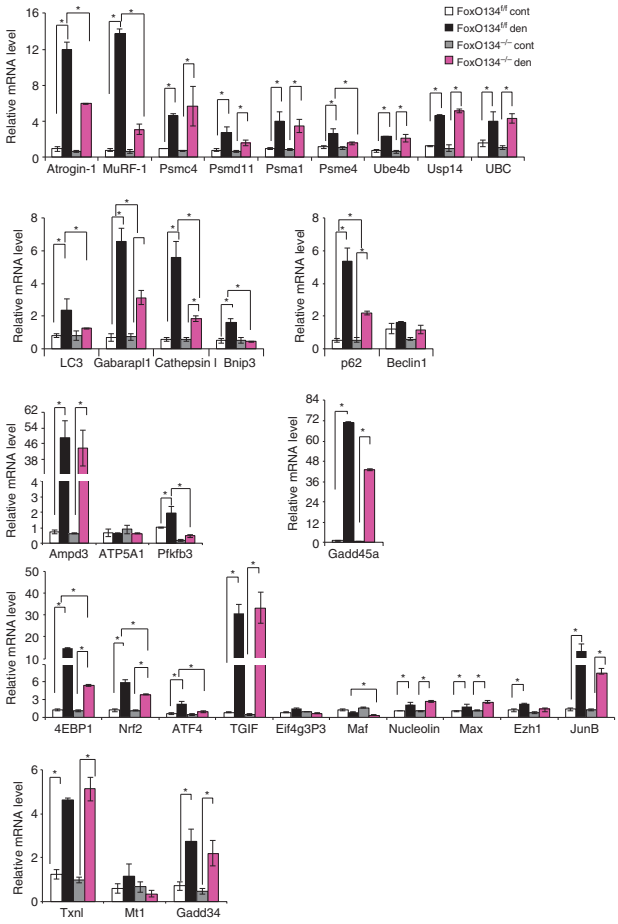

Figure 6 | FoxOs are required for expression of several atrogenes after denervation. Quantitative RT-PCR of the indicated atrogenes after 3 days from denervation. Data are normalized to GAPDH and expressed as fold increase of control innervated muscles. Values are mean ± s.e.m. *$P<0,05$, **$P<0.01$ (Student's *t*-test).; cont, control; den, denervated.

denervated muscles. These shRNAs did not affect the expression of the other atrophy-related ubiquitin ligases, MUSA, MuRF1 and atrogin1 both at protein and mRNA level (Supplementary Fig. 18b, Fig. 8b). Importantly, SMART inhibition significantly protected denervated muscles from atrophy (Fig. 8c). This sparing is due to the fact that by blocking SMART we greatly reduced protein ubiquitination in denervated muscles (Fig. 8d, Supplementary Fig. 18c). Therefore, we have identified *SMART* as an additional critical gene whose upregulation is required for atrophy, yet must be carefully controlled to avoid excessive protein breakdown. In conclusion, our findings underline the concept that FoxO members are the master regulatory factor for protein homeostasis during catabolic conditions.

Discussion

FoxOs are involved in a variety of biological process such as autophagy, apoptosis, ROS detoxification, glucose metabolism, DNA repair, cell cycle, stem cell maintenance and longevity[19,20]. Our work and that of others has shown that muscle atrophy is regulated by a transcription-dependent process that requires the expression of atrogenes. The transcription factors that orchestrate

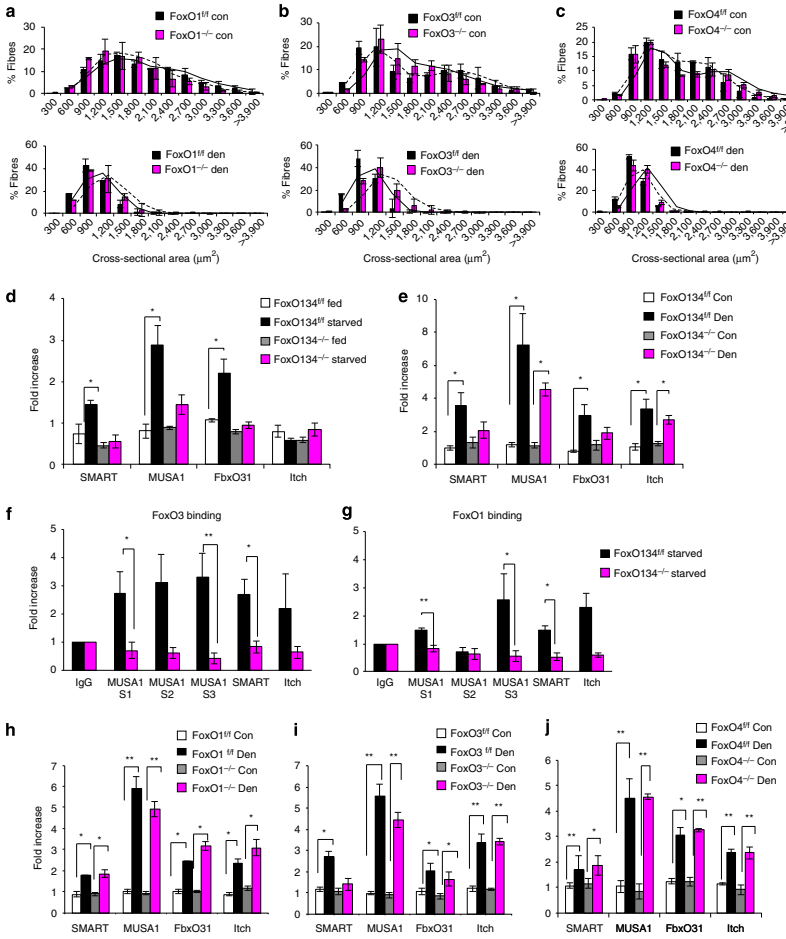

Figure 7 | FoxO members are redundant and control a new set of ubiquitin ligases. (**a**–**c**) Frequency histograms showing the distribution of cross-sectional areas (μm^2) of gastrocnemius muscles from muscle-specific (**a**) *FoxO1*$^{-/-}$, (**b**) *FoxO3*$^{-/-}$ and (**c**) *FoxO4*$^{-/-}$ mice. Data are shown as mean ± s.e.m. of four muscles each group. *$P<0.05$, **$P<0.01$. (**d**,**e**) qRT-PCR of the novel ubiquitin ligases *MUSA1, Fbxo21/SMART, Fbxo31, Itch* from 24 starved (**d**) or denervated (**e**) *FoxO1,3,4*$^{f/f}$ and *FoxO1,3,4*$^{-/-}$ mice. Data are normalized to GAPDH and expressed as fold increase of fed control mice. $n=4$ muscles for each group. (**f**) ChIP qPCR of FoxO3 and (**g**) FoxO1 on the promoters of *MUSA1, Fbxo21/SMART* and *Itch*. IgG was used as the reference. $n=3$. (**h**–**j**) qRT-PCR of *MUSA1, Fbxo21/SMART, Fbxo31, Itch* in (**h**) FoxO1, (**i**) FoxO3 and (**j**) FoxO4 knockout mice after 3 days of denervation. Values are normalized to GAPDH and expressed as fold increase of control mice. $n=4$ muscles for each group. Data are shown as mean ± s.e.m. Error bars indicate s.e.m. *$P<0.05$, **$P<0.01$ (Student's *t*-test). con control; den, denervated. MUSA1 S1, FoxO-binding site1; MUSA1 S2, FoxO-binding site2; MUSA1 S3, FoxO-binding site3.

this complex gene network are still largely unknown but our findings highlight the FoxO family as one of the most important regulators. The finding that different genes involved in different pathways, including several ubiquitin ligases and proteasome subunits, are under FoxO regulation, is an important step towards the understanding of FoxO-dependent adaptation to stress such as nutritional deprivation. For instance, one of the most important adaptive responses that is induced to maintain cellular survival under stress conditions is autophagy[21]. Our data from different knockout mice highlight the concept that

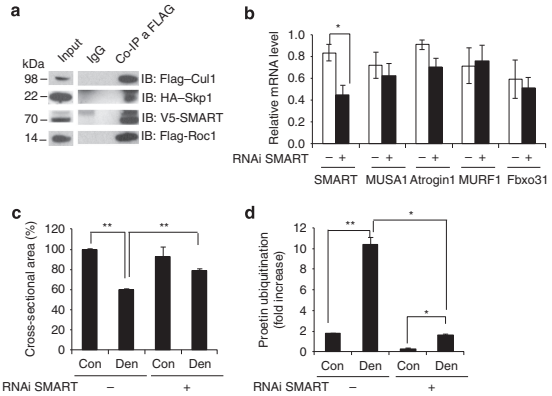

Figure 8 | Smart is a novel ubiquitin ligase required for denervation-dependent atrophy. (**a**) Co-immunoprecipitation experiment showing that SMART is a F-box protein that forms a SCF complex. C2C12 muscle cell lines were transfected with SMART, Skp1, Cul1 and Roc1 expression plasmids. After 24 h, cells were lysed and immunoprecipitation against FLAG-tag or control IgG was performed. Western blots for the different SCF components are shown. (**b**) RNAi-mediated knockdown of SMART revealed by quantitative RT–PCR (qRT–PCR). Adult TA muscles were transfected with bicistronic expressing vectors that encode either oligo 4 or scramble and GFP. Two weeks later TA muscles were collected, RNA extracted and endogenous *SMART, MUSA1, Atrogin1, MuRF1* and *Fbxo31* expression were analysed by qRT–PCR, $n=4$. (**c**) Inhibition of SMART prevents muscle atrophy in denervated muscles. Adult muscle fibres were co-transfected with bicistronic expressing vectors that encode shRNAs against *SMART* (oligo 4) or scramble and GFP and denervated. Two weeks later cross-sectional area of transfected fibres, identified by GFP fluorescence, was measured. $n=6$ muscles for each group. (**d**) Densitometric quantification of polyubiquitinated proteins in muscle extracts transfected with shRNAi against *SMART* or scramble. Values are normalized to GAPDH and expressed as fold increase of fed control mice. $n=3$ muscles for each group. Data are shown as mean ± s.e.m. Error bars indicate s.e.m. $^{*}P<0.05$, $^{**}P<0.01$ (Student's *t*-test). con, control; den, denervated; IB, immunoblotting.

FoxOs are required to sustain autophagic flux under low nutrients and dominate mTOR signalling on autophagy regulation. It is worth underlining that FoxO deletion does not affect basal autophagic flux and indeed the knockout mice do not show any overt pathological phenotype that may resemble the features of muscle-specific Atg7 knockout mice[22]. This is in contrast with the phenotype of TSC1 knockout mice, which display hyperactivation of the mTORC1 pathway leading to inhibition of basal autophagic flux and resulting in a myopathic phenotype[23]. Altogether these findings suggest that basal autophagy is controlled by mTOR and not by FoxOs, while induction and maintenance of high autophagic flux for hours/days is entirely dependent on the FoxO family. Indeed, deletion of FoxO both in a muscle-specific manner and in an inducible muscle-specific manner resulted in suppression of autophagy during fasting in face of mTOR inhibition. Importantly, the demonstration that deletion of a single FoxO member is not sufficient to prevent muscle loss and autophagy activation supports the conclusion that there is significant redundancy among family members.

Among the family members, FoxO3 deletion is less compensated by the other factors suggesting that FoxO3 is the most critical factor for the atrophy programme. Interestingly, the sparing of muscle mass in the single knockout is not only due to an effect on the classical ubiquitin ligase atrogin1 and MuRF1 but is due to FoxO action on a different set of ubiquitin ligases. Indeed we have identified a group of novel ubiquitin ligases that are regulated by FoxO. Among the novel E3s, we identified a gene that encodes an F-box protein (FbxO21) whose function was completely unknown and that we named SMART. Gain- and loss-of-function experiments showed that FoxOs are required for SMART regulation and ChIP experiments revealed that FoxO1 and FoxO3 are recruited on the promoter. However, deletion of FoxO3 and not of FoxO1 completely blunted *SMART* induction after denervation, suggesting that *SMART* is mainly under FoxO3 regulation. However, when we overexpressed FoxO3 only *MUSA1* was induced, suggesting that FoxO3 is required for *SMART* induction but not sufficient and that other transcription factors are therefore involved in its regulation.

MUSA1 is a novel ubiquitin ligase that we found to be critical for muscle atrophy during denervation and fasting. Indeed, RNAinterference (RNAi)-mediated inhibition of MUSA1 expression, *in vivo,* in denervated muscles, spares muscle mass. Conversely, excessive MUSA1 induction exacerbates muscle loss causing muscle cachexia[16]. Expression of MUSA1 is regulated by Smad transcription factors[16] in denervated muscles. The possibility that Smads and FoxO cooperate to promote MUSA1 expression is consistent with the finding that Smads require FoxO for the regulation of specific target genes. Therefore, it is possible that Smads are the partners of FoxO and both are required for the optimal activation of the atrogenes, at least during denervation. However, during fasting most of the atrophy-related genes are completely dependent on FoxO. In addition to the FoxO-dependent regulation of different ubiquitin ligases, it is important to emphasize that several proteasome subunits, ubiquitin C and the de-ubiquitinating enzyme USP14 are also controlled by FoxOs. These genes are critical in several steps of ubiquitination and proteasome-dependent degradation and might have an important role in control of protein degradation. For instance, it has recently been reported that expression of PSMD11 in human stem cells is sufficient to increase proteasome assembly

and activity and, in *C. elegans*, a PSMD11 homologue induces resistance to oxidative stress and poly-glutamine aggregation and extends lifespan[24].

Further work is needed to understand the interplay between the autophagy–lysosome and ubiquitin–proteasome systems in the context of different catabolic or even anabolic conditions, however, this work sets out the fundamentals for understanding the regulation of proteostasis in striated muscles.

Methods

Generation of muscle-specific FOXO1,3,4 knockout mice. Mice bearing *FoxO1,3,4*-floxed alleles (*FoxO1,3,4$^{f/f}$*) [25] were crossed with transgenic mice expressing Cre either under the control of a Myosin Light Chain 1 fast promoter (*MLC1f-Cre*)[2,26] or with transgenic expressing a *Cre-ER* driven by human skeletal actin promoter[27]. Genomic DNA isolated from *FoxO1,3,4$^{f/f}$* mice was subjected to PCR analysis. Cre-mediated recombination was confirmed by PCR with genomic DNA from gastrocnemius muscles using the primers Cre forward: 3′-CACCAGCC AGCTATCAACTCG-5′ and Cre reverse: 3′-TTACATTGGTCCAGCCACCAG-5′. Tamoxifen-inducible Cre was activated by special tamoxifen diet (*Tam400/Cre-ER Harlan*) or by i.p. Tamoxifen injection.

The genotyping analysis for each specific FoxO member was performed with the combination of the following primers: FoxO1 forward: 3′-GCT TAG AGC AGA GAT GTT CTC ACA TT-5′, FoxO1 reverse1: 3′-CCA GAG TCT TTG TAT CAG GCA AAT AA-5′, FoxO1 reverse2: 3′-CAA GTC CAT TAA TTC AGC ACA TTG A-5′, FoxO3 forward1: 3′-AGA TTT ATG TTC CCA CTT GCT TCC T-5′, FoxO3 forward2: 3′-TGC TTT GAT ACT ATT CCA CAA ACC C-5′, FoxO3 reverse: 3′-ATT CCT TTG GAA ATC AAC AAA ACT-5′, FoxO4 forward1: 3′- TGA GAA GCC ATT GAA GAT CAG A-5′, FoxO4 forward2: 3′-CTA CTT CAA GGA CAA GGG TGA CAG-5′, FoxO4 reverse: 3′-CTT CTC TGT GGG AAT AAA TGT TTG G-5′.

Animals and *in vivo* transfection experiments. Animals were handled by specialized personnel under the control of inspectors of the Veterinary Service of the Local Sanitary Service (ASL 16—Padova), the local officers of the Ministry of Health. Mice were housed in individual cages in an environmentally controlled room (23 °C, 12-h light–dark cycle) with *ad libitum* access to food and water. All procedures are specified in the projects approved by the Italian Ministero Salute, Ufficio VI (authorization numbers C65) and by the Ethics Committee of the University of Padova. All experiments were performed on 2- to 4-month-old male (28–32*g*) and female mice (25–28g); mice of the same sex and age were used for each individual experiment. *In vivo* transfection experiments were performed by i.m. injection of expression plasmids in TA muscle followed by electroporation[8]. For fasting experiments, control animals were fed *ad libitum*; food pellets were removed from the cages of the fasted animals. Denervation was performed by cutting the sciatic nerve of the left limb, while the right limb was used as control. Muscles were removed at various time periods after transfection and frozen in liquid nitrogen for subsequent analyses.

Gene expression analyses. Total RNA was prepared from TA muscles using Promega SV Total RNA Isolation kit. Complementary DNA (cDNA) generated with Invitrogen SuperScript III Reverse Transcriptase was analysed by quantitative real-time RT–PCR using Qiagen QuantiTect SYBR Green PCR Kit. All data were normalized to GAPDH and actin expression. The oligonucleotide primers used are shown in Supplementary Table 1.

Plasmids and antibodies for Western blot. *In vivo* transfection experiments used the yellow fluorescent protein (YFP)–LC3[2] and Fbxo21SMART-V5 plasmids. For the cloning of mouse *Fbxo21/SMART* gene, muscle cDNA was amplified by PCR using the primers forward: 3′-ACCATGGCGTCGGTAGCGGGGGACA-5′ and reverse: 3′-CTCGGCTGTGTCCTCCTTTGCACTG-5′.

The amplified sequence was cloned into pcDNA3.1/V5-His TOPO TA (Invitrogen) expression vector and sequenced. The list of the antibodies is described in Supplementary Table 2.

Uncropped blots are shown in Supplementary Fig. 19.

***In vivo* RNAi.** *In vivo* RNAi experiments were performed using at least three different sequences for each gene(Invitrogen BLOCK-iTTM Pol II miR RNAi Selected). The sequences are shown in Supplementary Table 3. For the validation of shRNA constructs, MEF cells were maintained in DMEM/10% FBS and transfected with shRNA constructs using Lipofectamine 2000 (Invitrogen). Cells were lysed 24 h or 48 h later and immunoblotting was performed.

Gene expression profiling. For each of the 4 conditions (*FoxO1,3,4$^{f/f}$* fed or starved and *FoxO1,3,4$^{-/-}$* fed or starved), we collected the gastrocnemius muscles of three mice thus yielding six muscles per condition.

RNA was prepared from these muscles using the TRIzol method (Life Technologies) followed by cleanup with the RNeasy kit (Qiagen). RNA concentration was determined by spectrophotometry and quality of the RNA was monitored using the Agilent 2100 Bioanalyzer (Agilent Technologies). RNA of the six muscles per condition was pooled equimolarly and used for further microarray analysis. cRNA was prepared, labelled and hybridized to Affymetrix Mouse Genome 430 2.0 Arrays using Affymetrix-supplied kits and according to standard Affymetrix protocols. Expression values were summarized using the Mas 5.0 algorithm. Genes that were up or downregulated on starvation compared with the fed condition were determined using Excel software. A threshold of 1.5 was used for the fold up or downregulation consistent with the fold change that can be reliably detected with these type of arrays.

***In vivo* ChIP assay.** We performed ChIP assay in adult skeletal muscles using the Magna ChIP A/G Chromatin Immunoprecipitation Kit (Millipore)[2,28]. Soluble chromatin was co-immunoprecipitated with rabbit polyclonal anti-FKHRL1 (FoxO3) sc-11351X (Santa Cruz Biotechnology), rabbit polyclonal anti-FKHR (FoxO1) sc-11350X (Santa Cruz Biotechnology) or an equal amount of normal rabbit IgG, sc-2027 (Santa Cruz Biotechnology). After decrosslinking of the DNA, samples were subjected to quantitative RT–PCR. The oligonucleotide primers used are shown in Supplementary Table 4. The regions of amplification contain the FOXO-binding sites for the promoter studied.

Immunoblotting and IP. Frozen gastrocnemius muscles were powdered by pestle and mortar and lysed in a buffer containing 50 mM Tris pH 7.5, 150 mM NaCl, 5 mM $MgCl_2$, 1 mM DTT, 10% glycerol, 2% SDS, 1% Triton X-100, Roche Complete Protease Inhibitor Cocktail, 1 mM PMSF, 1 mM $NaVO_3$, 5 mM NaF and 3 mM β-glycerophosphate. The lysis buffer used for MEF and C2C12 cells contained 50 mM Tris pH 7.5, 150 mM NaCl, 5 mM $MgCl_2$, 1 mM DTT, 10% glycerol, 1 mM EDTA, 0.5% Triton X-100 and the protease inhibitors listed above. Alternatively, lysis buffer contained 50 mM Tris HCl pH 7.2, 250 mM NaCl, 2% NP40, 0.1% SDS, 0.5% sodium deoxycholate 2.5 mM, EDTA pH8 with anti-phosphatase and anti-protease. The samples were immunoblotted and visualized with Super-Signal West Pico Chemiluminescent substrate (Pierce). Blots were stripped using Restore Western Blotting Stripping Buffer (Pierce) according to the manufacturer's instructions and reprobed if necessary. For Myosin analysis, gastrocnemius muscles were homogenized in myosin extraction buffer containing 1 M Tris pH 6.8, 10% SDS and 80% glycerol. SDS–PAGE was performed using polyacrylamide gel with a high glycerol concentration, which allows the separation of MYH isoforms. Myosins were identified with Coomassie blu staining.

For co-IP experiment C2C12 muscle cell lines were transfected with V5-SMART, HA-Skp1, FLAG-Cul1 and FLAG-Roc1 expression plasmids. After 24 h, cells were lysed in a buffer containing 50 mM Tris pH 7.5, 100 mM NaCl, 5 mM MgCl2, 1 mM DTT, 0.5% Triton X-100, protease and phosphatase inhibitors. About 1 mg of total protein was incubated at a ratio of 1:100 with the mouse monoclonal anti-FLAG antibody or non specific mouse IgG along with 30 µl of Protein A/G PLUS-Agarose sc-2003 (Santa Cruz Biotechnology) overnight at 4 °C. The beads were then washed three times with PBS plus Roche Complete Protease Inhibitor Cocktail 1X and were finally resuspended in 30 µl LDS Sample Buffer 1 × (NuPAGE Life Technolohy) and 50 mM DTT to be further analysed by Western blotting.

Histology and microscopy. Cryosections of transfected TA muscles were examined in a fluorescence microscope Leica DM5000B equipped with a Leica DFC300-FX digital charge-coupled device camera by using Leica DC Viewer software. Cryosections of TA were stained for haematoxilin and eosin and as well as for Succinate dehydrogenase and Periodic acid-Schiff. Cross-sectional area was measured using ImageJ software in at least 400 transfected fibres and compared with the area of age-matched control.. The fibre diameter was calculated as caliper width, perpendicular to the longest chord of each myofibre. The total myofibre number was calculated from entire muscle section based on assembled mosaic image (× 20 magnification). Fibre typing was determined by immunofluorescence using combinations of the following monoclonal antibodies: BA-D5 that recognizes type 1 MyHC isoform and SC-71 for type 2A MyHC isoform. Images were captured using a Leica DFC300-FX digital charge-coupled device camera by using Leica DC Viewer software, and morphometric analyses were made using the software ImageJ 1.47 version.

LC3-vesicle quantification. Cryosections of fed and 30-h fasted muscles from control and *FoxO1,3,4$^{-/-}$* mice that were transfected *in vivo* with YFP–LC3 were examined using an epifluorescence Leica DM5000B microscope equipped with a Leica DFC300-FX digital charge-coupled device camera by using Leica DC Viewer software. The fluorescent dots were counted and normalized for cross-sectional area.

Autophagic flux quantification. We monitored autophagic flux in 30 h of starvation using colchicine[15]. Briefly MLC *FoxO1,3,4$^{-/-}$* and *FoxO1,3,4$^{f/f}$* mice were

treated with 0,4 mg kg^{-1} colchicine or vehicle by i.p. injection and starved. The treatment was repeated at 15 h prior to muscle harvesting.

Adenovirus production and myotube transfection. *FOXO3* was cloned into a shuttle vector pAdTrack-CMV, which contains green fluorescent protein (GFP) under the control of a separate promoter. C2C12 mouse myoblasts were cultured in DMEM 10% FCS until the cells reached confluence. The medium was then replaced with DMEM 2% horse serum ('differentiation medium') and incubated for 4 days to induce myotube formation before proceeding with experiments. For infection, myotubes were incubated with adenovirus at a multiplicity-of-infection of 250 in differentiation medium for 18 h, and then the medium was replaced. The infection efficiency was typically >90%.

Muscle physiology. To determine force and contraction kinetics of gastrocnemius, mice were anesthetized by a mixture of Xylor and Zoletil, and a small incision was made from the knee to the hip, exposing the sciatic nerve. Before branching of the sciatic nerve, TeflonTM-coated 7 multistranded steel wires (AS 632; Cooner Sales, Chatsworth, CA, USA) were implanted with sutures on either sides of the sciatic nerve. To avoid recruitment of the ankle dorsal flexors the common peroneal nerve was cut. Torque production of the stimulated plantar flexors was measured using a muscle lever system (Model 305C; Aurora Scientific, Aurora, ON, Canada).

Ex vivo force measurements on soleus muscles were performed by dissecting it from tendon to tendon under a stereomicroscope and subsequently mounting between a force transducer (KG Scientific Instruments, Heidelberg, Germany) and a micromanipulator-controlled shaft in a small chamber, in which oxygenated Krebs solution was continuously circulated and temperature was maintained at 25 °C. The stimulation conditions were optimized, and the length of the muscle was increased until force development during tetanus was maximal.

Data were analysed using the PowerLab system (4SP, ADInstruments) and software (Chart 4, ADInstruments). The sciatic nerves were stimulated using supramaximal square wave pulses of 0.1-ms duration. Force generation capacity was evaluated by measuring the absolute maximal force that was generated during isometric contractions in response to electrical stimulation (frequency of 75–150 Hz, train of stimulation of 500 ms). Maximal isometric force was determined at L0 (length at which maximal tension was obtained during the tetanus). Force was normalized to the muscle mass as an estimate of specific force. Following force measurements, animals were killed by cervical dislocation and muscles were dissected, weighed and frozen in liquid nitrogen or in isopentane precooled in liquid nitrogen.

Statistical analysis and general experimental design. The sample size was calculated using size power analysis methods for *a priori* determination based on the s.d., and the effect size was previously obtained using the experimental methods employed in the study. For animal studies, we estimated sample size from expected number of knockout mice and littermate controls, which was based on mendelian ratios. We calculated the minimal sample size for each group by at least four organisms. Considering a likely drop-off effect of 10%, we set sample size of each group at five mice. To reduce the s.d., we minimized physiological variation by using homogenous animals with same sex and same age. The exclusion criteria for animals were pre-established. In case of death, cannibalism or sickness, the animal was excluded from analysis. Tissue samples were excluded in cases such as cryo-artefacts, histological artefacts or failed RNA extraction. We included animals from different breeding cages by random allocation to the different experimental groups. Animal experiments were not blinded, however, when applicable, the experimenters were blinded to the nature of samples by using number codes until final data analysis was performed. Statistical tests were used as described in the figure legends and were applied on verification of the test assumptions (for example, normality). Generally, data were analysed by two-tailed Student's *t*-test. For all graphs, data are represented as means ± s.e.m. For the measurement variables used to compare KO animals versus controls, or innervated animals versus denervated ones, the variance was similar between the groups.

References

1. Sandri, M. Signalling in muscle atrophy and hypertrophy. *Physiology (Bethesda)* **23,** 160–170 (2008).
2. Mammucari, C. *et al.* FoxO3 controls autophagy in skeletal muscle *in vivo*. *Cell Metab.* **6,** 458–471 (2007).
3. Sandri, M. Autophagy in skeletal muscle. *FEBS Lett.* **584,** 1411–1416 (2010).
4. Bodine, S. C. *et al.* Identification of ubiquitin ligases required for skeletal muscle atrophy. *Science* **294,** 1704–1708 (2001).
5. Gomes, M. D., Lecker, S. H., Jagoe, R. T., Navon, A. & Goldberg, A. L. Atrogin-1, a muscle-specific F-box protein highly expressed during muscle atrophy. *Proc. Natl Acad. Sci. USA* **98,** 14440–14445 (2001).
6. Lecker, S. H. *et al.* Multiple types of skeletal muscle atrophy involve a common program of changes in gene expression. *FASEB J.* **18,** 39–51 (2004).
7. Sacheck, J. M. *et al.* Rapid disuse and denervation atrophy involve transcriptional changes similar to those of muscle wasting during systemic diseases. *FASEB J.* **21,** 140–155 (2007).
8. Sandri, M. *et al.* Foxo transcription factors induce the atrophy-related ubiquitin ligase atrogin-1 and cause skeletal muscle atrophy. *Cell* **117,** 399–412 (2004).
9. Stitt, T. N. *et al.* The IGF-1/PI3K/Akt pathway prevents expression of muscle atrophy-induced ubiquitin ligases by inhibiting FOXO transcription factors. *Mol. Cell* **14,** 395–403 (2004).
10. Zhao, J. *et al.* FoxO3 coordinately activates protein degradation by the autophagic/lysosomal and proteasomal pathways in atrophying muscle cells. *Cell Metab.* **6,** 472–483 (2007).
11. Xu, J. *et al.* Transcription factor FoxO1, the dominant mediator of muscle wasting in chronic kidney disease, is inhibited by microRNA-486. *Kidney Int.* **82,** 401–411 (2012).
12. Yamazaki, Y. *et al.* The cathepsin L gene is a direct target of FOXO1 in skeletal muscle. *Biochem. J.* **427,** 171–178 (2010).
13. Furuyama, T., Nakazawa, T., Nakano, I. & Mori, N. Identification of the differential distribution patterns of mRNAs and consensus binding sequences for mouse DAF-16 homologues. *Biochem. J.* **349,** 629–634 (2000).
14. Sandri, M. *et al.* PGC-1alpha protects skeletal muscle from atrophy by suppressing FoxO3 action and atrophy-specific gene transcription. *Proc. Natl Acad. Sci. USA* **103,** 16260–16265 (2006).
15. Ju, J. S., Varadhachary, A. S., Miller, S. E. & Weihl, C. C. Quantitation of 'autophagic flux' in mature skeletal muscle. *Autophagy* **6,** 929–935 (2010).
16. Sartori, R. *et al.* BMP signalling controls muscle mass. *Nat. Genet.* **45,** 1309–1318 (2013).
17. Santra, M. K., Wajapeyee, N. & Green, M. R. F-box protein FBXO31 mediates cyclin D1 degradation to induce G1 arrest after DNA damage. *Nature* **459,** 722–725 (2009).
18. Melino, G. *et al.* Itch: a HECT-type E3 ligase regulating immunity, skin and cancer. *Cell Death Differ.* **15,** 1103–1112 (2008).
19. Eijkelenboom, A. & Burgering, B. M. FOXOs: signalling integrators for homeostasis maintenance. *Nat. Rev. Mol. Cell Biol.* **14,** 83–97 (2013).
20. Sandri, M. FOXOphagy path to inducing stress resistance and cell survival. *Nat. Cell Biol.* **14,** 786–788 (2012).
21. Mizushima, N. & Komatsu, M. Autophagy: renovation of cells and tissues. *Cell* **147,** 728–741 (2011).
22. Masiero, E. *et al.* Autophagy is required to maintain muscle mass. *Cell Metab.* **10,** 507–515 (2009).
23. Castets, P. *et al.* Sustained activation of mTORC1 in skeletal muscle inhibits constitutive and starvation-induced autophagy and causes a severe, late-onset myopathy. *Cell Metab.* **17,** 731–744 (2013).
24. Vilchez, D. *et al.* RPN-6 determines C. elegans longevity under proteotoxic stress conditions. *Nature* **489,** 263–268 (2012).
25. Paik, J. H. *et al.* FoxOs are lineage-restricted redundant tumor suppressors and regulate endothelial cell homeostasis. *Cell* **128,** 309–323 (2007).
26. Bothe, G. W., Haspel, J. A., Smith, C. L., Wiener, H. H. & Burden, S. J. Selective expression of Cre recombinase in skeletal muscle fibres. *Genesis* **26,** 165–166 (2000).
27. Schuler, M., Ali, F., Metzger, E., Chambon, P. & Metzger, D. Temporally controlled targeted somatic mutagenesis in skeletal muscles of the mouse. *Genesis* **41,** 165–170 (2005).
28. Raffaello, A. *et al.* JunB transcription factor maintains skeletal muscle mass and promotes hypertrophy. *J. Cell Biol.* **191,** 101–113 (2010).
29. Schmidt, E. K., Clavarino, G., Ceppi, M. & Pierre, P. SUnSET, a nonradioactive method to monitor protein synthesis. *Nat. Methods* **6,** 275–277 (2009).
30. Goodman, C. A. *et al.* Novel insights into the regulation of skeletal muscle protein synthesis as revealed by a new nonradioactive *in vivo* technique. *FASEB J.* **25,** 1028–1039 (2011).

Acknowledgements

This work was supported from Telethon-Italy (TCR09003, TCP04009), from the European Union (MYOAGE, contract: 223576 of FP7), ERC (282310-MyoPHAGY), the Italian Ministry of Education (MiUR) (PRIN 2010/2011), the Foundation Leducq and CARIPARO to M.S.

Author contributions

G.M. generated the triple FoxO1,3,4 muscle-specific knockout. G.M., V.R. and F.P. performed biochemical analyses, morphological, immunohistochemical and RNA analysis, muscle transfections and mouse treatments. G.M. and A.A. performed *in vivo* ChIP assay. A.A. performed immunohistochemical analysis. L.F. performed protein analysis and immunohistochemical analysis. A.S. performed immunohistochemical analysis and RNA analysis. J.Z. performed Adeno-mediated FoxO3 overexpression in C2C12 myotubes, RNA extraction and qRT–PCR. R.A. performed microarray analysis. B.B. analysed muscle mechanics. R.A.D. provided FoxO floxed mice. G.M., V.R., F.P., A.L.G. and M.S.

were involved in data analysis. G.M, V.R and M.S. designed the study, analysed the data and wrote the manuscript. All authors discussed the results and corrected the manuscript.

Additional information

Accession codes: The gene expression profiling data discussed in this publication have been deposited in the NCBI Gene Expression Omnibus and are accessible through GEO Series accession number GSE52667.

Supplementary Information accompanies this paper at http://www.nature.com/naturecommunications.

Competing financial interests: The authors declare no competing financial interests.

Reprints and permission information is available online at http://npg.nature.com/reprintsandpermissions.

How to cite this article: Milan, G. *et al.* Regulation of autophagy and the ubiquitin–proteasome system by the FoxO transcriptional network during muscle atrophy. *Nat. Commun.* 6:6670 doi: 10.1038/ncomms7670 (2015).

5. BIBLIOGRAPHY

Allen, D.L., and T.G. Unterman. 2007. Regulation of myostatin expression and myoblast differentiation by FoxO and SMAD transcription factors. *American journal of physiology. Cell physiology*. 292:C188-199.

Amirouche, A., A.C. Durieux, S. Banzet, N. Koulmann, R. Bonnefoy, C. Mouret, X. Bigard, A. Peinnequin, and D. Freyssenet. 2009. Down-regulation of Akt/mammalian target of rapamycin signaling pathway in response to myostatin overexpression in skeletal muscle. *Endocrinology*. 150:286-294.

Asada, S., H. Daitoku, H. Matsuzaki, T. Saito, T. Sudo, H. Mukai, S. Iwashita, K. Kako, T. Kishi, Y. Kasuya, and A. Fukamizu. 2007. Mitogen-activated protein kinases, Erk and p38, phosphorylate and regulate Foxo1. *Cellular signalling*. 19:519-527.

Bastie, C.C., Z. Nahle, T. McLoughlin, K. Esser, W. Zhang, T. Unterman, and N.A. Abumrad. 2005. FoxO1 stimulates fatty acid uptake and oxidation in muscle cells through CD36-dependent and -independent mechanisms. *The Journal of biological chemistry*. 280:14222-14229.

Bertaggia, E., L. Coletto, and M. Sandri. 2012. Posttranslational modifications control FoxO3 activity during denervation. *American journal of physiology. Cell physiology*. 302:C587-596.

Bodine, S.C., and L.M. Baehr. 2014. Skeletal muscle atrophy and the E3 ubiquitin ligases MuRF1 and MAFbx/atrogin-1. *American journal of physiology. Endocrinology and metabolism*. 307:E469-484.

Bodine, S.C., E. Latres, S. Baumhueter, V.K. Lai, L. Nunez, B.A. Clarke, W.T. Poueymirou, F.J. Panaro, E. Na, K. Dharmarajan, Z.Q. Pan, D.M. Valenzuela, T.M. DeChiara, T.N. Stitt, G.D. Yancopoulos, and D.J. Glass. 2001. Identification of ubiquitin ligases required for skeletal muscle atrophy. *Science*. 294:1704-1708.

Bonaldo, P., and M. Sandri. 2013. Cellular and molecular mechanisms of muscle atrophy. *Disease models & mechanisms*. 6:25-39.

Borden, K.L., and P.S. Freemont. 1996. The RING finger domain: a recent example of a sequence-structure family. *Current opinion in structural biology*. 6:395-401.

Bothe, G.W., J.A. Haspel, C.L. Smith, H.H. Wiener, and S.J. Burden. 2000. Selective expression of Cre recombinase in skeletal muscle fibers. *Genesis*. 26:165-166.

Brenkman, A.B., P.L. de Keizer, N.J. van den Broek, A.G. Jochemsen, and B.M. Burgering. 2008. Mdm2 induces mono-ubiquitination of FOXO4. *PloS one*. 3:e2819.

Brunet, A., A. Bonni, M.J. Zigmond, M.Z. Lin, P. Juo, L.S. Hu, M.J. Anderson, K.C. Arden, J. Blenis, and M.E. Greenberg. 1999. Akt promotes cell survival by phosphorylating and inhibiting a Forkhead transcription factor. *Cell*. 96:857-868.

Brunet, A., L.B. Sweeney, J.F. Sturgill, K.F. Chua, P.L. Greer, Y. Lin, H. Tran, S.E. Ross, R. Mostoslavsky, H.Y. Cohen, L.S. Hu, H.L. Cheng, M.P.

Jedrychowski, S.P. Gygi, D.A. Sinclair, F.W. Alt, and M.E. Greenberg. 2004. Stress-dependent regulation of FOXO transcription factors by the SIRT1 deacetylase. *Science*. 303:2011-2015.

Castets, P., S. Lin, N. Rion, S. Di Fulvio, K. Romanino, M. Guridi, S. Frank, L.A. Tintignac, M. Sinnreich, and M.A. Ruegg. 2013. Sustained activation of mTORC1 in skeletal muscle inhibits constitutive and starvation-induced autophagy and causes a severe, late-onset myopathy. *Cell metabolism*. 17:731-744.

Chung, S.Y., W.C. Huang, C.W. Su, K.W. Lee, H.C. Chi, C.T. Lin, S.T. Chen, K.M. Huang, M.S. Tsai, H.P. Yu, and S.L. Chen. 2013. FoxO6 and PGC-1alpha form a regulatory loop in myogenic cells. *Bioscience reports*. 33.

Cong, H., L. Sun, C. Liu, and P. Tien. 2011. Inhibition of atrogin-1/MAFbx expression by adenovirus-delivered small hairpin RNAs attenuates muscle atrophy in fasting mice. *Human gene therapy*. 22:313-324.

Daitoku, H., J. Sakamaki, and A. Fukamizu. 2011. Regulation of FoxO transcription factors by acetylation and protein-protein interactions. *Biochimica et biophysica acta*. 1813:1954-1960.

Eijkelenboom, A., and B.M. Burgering. 2013. FOXOs: signalling integrators for homeostasis maintenance. *Nature reviews. Molecular cell biology*. 14:83-97.

Essers, M.A., S. Weijzen, A.M. de Vries-Smits, I. Saarloos, N.D. de Ruiter, J.L. Bos, and B.M. Burgering. 2004. FOXO transcription factor activation by oxidative stress mediated by the small GTPase Ral and JNK. *The EMBO journal*. 23:4802-4812.

Fu, W., Q. Ma, L. Chen, P. Li, M. Zhang, S. Ramamoorthy, Z. Nawaz, T. Shimojima, H. Wang, Y. Yang, Z. Shen, Y. Zhang, X. Zhang, S.V. Nicosia, Y. Zhang, J.W. Pledger, J. Chen, and W. Bai. 2009. MDM2 acts downstream of p53 as an E3 ligase to promote FOXO ubiquitination and degradation. *The Journal of biological chemistry*. 284:13987-14000.

Furuyama, T., K. Kitayama, H. Yamashita, and N. Mori. 2003. Forkhead transcription factor FOXO1 (FKHR)-dependent induction of PDK4 gene expression in skeletal muscle during energy deprivation. *The Biochemical journal*. 375:365-371.

Glass, D.J. 2005. Skeletal muscle hypertrophy and atrophy signaling pathways. *The international journal of biochemistry & cell biology*. 37:1974-1984.

Goldberg, A.L. 1969. Protein turnover in skeletal muscle. II. Effects of denervation and cortisone on protein catabolism in skeletal muscle. *The Journal of biological chemistry*. 244:3223-3229.

Gomes, M.D., S.H. Lecker, R.T. Jagoe, A. Navon, and A.L. Goldberg. 2001. Atrogin-1, a muscle-specific F-box protein highly expressed during muscle atrophy. *Proceedings of the National Academy of Sciences of the United States of America*. 98:14440-14445.

Goodman, C.A., D.M. Mabrey, J.W. Frey, M.H. Miu, E.K. Schmidt, P. Pierre, and T.A. Hornberger. 2011. Novel insights into the regulation of skeletal muscle protein synthesis as revealed by a new nonradioactive in vivo

technique. *FASEB journal : official publication of the Federation of American Societies for Experimental Biology*. 25:1028-1039.
Greer, E.L., P.R. Oskoui, M.R. Banko, J.M. Maniar, M.P. Gygi, S.P. Gygi, and A. Brunet. 2007. The energy sensor AMP-activated protein kinase directly regulates the mammalian FOXO3 transcription factor. *The Journal of biological chemistry*. 282:30107-30119.
Grumati, P., L. Coletto, P. Sabatelli, M. Cescon, A. Angelin, E. Bertaggia, B. Blaauw, A. Urciuolo, T. Tiepolo, L. Merlini, N.M. Maraldi, P. Bernardi, M. Sandri, and P. Bonaldo. 2010. Autophagy is defective in collagen VI muscular dystrophies, and its reactivation rescues myofiber degeneration. *Nature medicine*. 16:1313-1320.
Huang, H., K.M. Regan, F. Wang, D. Wang, D.I. Smith, J.M. van Deursen, and D.J. Tindall. 2005. Skp2 inhibits FOXO1 in tumor suppression through ubiquitin-mediated degradation. *Proceedings of the National Academy of Sciences of the United States of America*. 102:1649-1654.
Jackson, P.K., and A.G. Eldridge. 2002. The SCF ubiquitin ligase: an extended look. *Molecular cell*. 9:923-925.
Jacobs, F.M., L.P. van der Heide, P.J. Wijchers, J.P. Burbach, M.F. Hoekman, and M.P. Smidt. 2003. FoxO6, a novel member of the FoxO class of transcription factors with distinct shuttling dynamics. *The Journal of biological chemistry*. 278:35959-35967.
Ju, J.S., A.S. Varadhachary, S.E. Miller, and C.C. Weihl. 2010. Quantitation of "autophagic flux" in mature skeletal muscle. *Autophagy*. 6:929-935.
Kaestner, K.H., W. Knochel, and D.E. Martinez. 2000. Unified nomenclature for the winged helix/forkhead transcription factors. *Genes & development*. 14:142-146.
Kamei, Y., S. Miura, M. Suzuki, Y. Kai, J. Mizukami, T. Taniguchi, K. Mochida, T. Hata, J. Matsuda, H. Aburatani, I. Nishino, and O. Ezaki. 2004. Skeletal muscle FOXO1 (FKHR) transgenic mice have less skeletal muscle mass, down-regulated Type I (slow twitch/red muscle) fiber genes, and impaired glycemic control. *The Journal of biological chemistry*. 279:41114-41123.
Lecker, S.H., A.L. Goldberg, and W.E. Mitch. 2006. Protein degradation by the ubiquitin-proteasome pathway in normal and disease states. *J Am Soc Nephrol*. 17:1807-1819.
Lecker, S.H., R.T. Jagoe, A. Gilbert, M. Gomes, V. Baracos, J. Bailey, S.R. Price, W.E. Mitch, and A.L. Goldberg. 2004. Multiple types of skeletal muscle atrophy involve a common program of changes in gene expression. *FASEB journal : official publication of the Federation of American Societies for Experimental Biology*. 18:39-51.
Lehtinen, M.K., Z. Yuan, P.R. Boag, Y. Yang, J. Villen, E.B. Becker, S. DiBacco, N. de la Iglesia, S. Gygi, T.K. Blackwell, and A. Bonni. 2006. A conserved MST-FOXO signaling pathway mediates oxidative-stress responses and extends life span. *Cell*. 125:987-1001.
Levine, B., and G. Kroemer. 2008. Autophagy in the pathogenesis of disease. *Cell*. 132:27-42.
Mammucari, C., G. Milan, V. Romanello, E. Masiero, R. Rudolf, P. Del Piccolo, S.J. Burden, R. Di Lisi, C. Sandri, J. Zhao, A.L. Goldberg, S. Schiaffino, and

M. Sandri. 2007. FoxO3 controls autophagy in skeletal muscle in vivo. *Cell metabolism*. 6:458-471.
Masiero, E., L. Agatea, C. Mammucari, B. Blaauw, E. Loro, M. Komatsu, D. Metzger, C. Reggiani, S. Schiaffino, and M. Sandri. 2009. Autophagy is required to maintain muscle mass. *Cell metabolism*. 10:507-515.
Melino, G., E. Gallagher, R.I. Aqeilan, R. Knight, A. Peschiaroli, M. Rossi, F. Scialpi, M. Malatesta, L. Zocchi, G. Browne, A. Ciechanover, and F. Bernassola. 2008. Itch: a HECT-type E3 ligase regulating immunity, skin and cancer. *Cell death and differentiation*. 15:1103-1112.
Milan, G., V. Romanello, F. Pescatore, A. Armani, J.H. Paik, L. Frasson, A. Seydel, J. Zhao, R. Abraham, A.L. Goldberg, B. Blaauw, R.A. DePinho, and M. Sandri. 2015. Regulation of autophagy and the ubiquitin-proteasome system by the FoxO transcriptional network during muscle atrophy. *Nature communications*. 6:6670.
Mizushima, N., and M. Komatsu. 2011. Autophagy: renovation of cells and tissues. *Cell*. 147:728-741.
Mizushima, N., A. Yamamoto, M. Matsui, T. Yoshimori, and Y. Ohsumi. 2004. In vivo analysis of autophagy in response to nutrient starvation using transgenic mice expressing a fluorescent autophagosome marker. *Molecular biology of the cell*. 15:1101-1111.
Mordier, S., C. Deval, D. Bechet, A. Tassa, and M. Ferrara. 2000. Leucine limitation induces autophagy and activation of lysosome-dependent proteolysis in C2C12 myotubes through a mammalian target of rapamycin-independent signaling pathway. *The Journal of biological chemistry*. 275:29900-29906.
Murgia, M., A.L. Serrano, E. Calabria, G. Pallafacchina, T. Lomo, and S. Schiaffino. 2000. Ras is involved in nerve-activity-dependent regulation of muscle genes. *Nature cell biology*. 2:142-147.
Nakae, J., Y. Cao, H. Daitoku, A. Fukamizu, W. Ogawa, Y. Yano, and Y. Hayashi. 2006. The LXXLL motif of murine forkhead transcription factor FoxO1 mediates Sirt1-dependent transcriptional activity. *The Journal of clinical investigation*. 116:2473-2483.
Obsil, T., and V. Obsilova. 2008. Structure/function relationships underlying regulation of FOXO transcription factors. *Oncogene*. 27:2263-2275.
Peserico, A., F. Chiacchiera, V. Grossi, A. Matrone, D. Latorre, M. Simonatto, A. Fusella, J.G. Ryall, L.W. Finley, M.C. Haigis, G. Villani, P.L. Puri, V. Sartorelli, and C. Simone. 2013. A novel AMPK-dependent FoxO3A-SIRT3 intramitochondrial complex sensing glucose levels. *Cellular and molecular life sciences : CMLS*. 70:2015-2029.
Petrovski, G., and D.K. Das. 2010. Does autophagy take a front seat in lifespan extension? *Journal of cellular and molecular medicine*. 14:2543-2551.
Raben, N., V. Hill, L. Shea, S. Takikita, R. Baum, N. Mizushima, E. Ralston, and P. Plotz. 2008. Suppression of autophagy in skeletal muscle uncovers the accumulation of ubiquitinated proteins and their potential role in muscle damage in Pompe disease. *Human molecular genetics*. 17:3897-3908.
Rommel, C., S.C. Bodine, B.A. Clarke, R. Rossman, L. Nunez, T.N. Stitt, G.D. Yancopoulos, and D.J. Glass. 2001. Mediation of IGF-1-induced skeletal

myotube hypertrophy by PI(3)K/Akt/mTOR and PI(3)K/Akt/GSK3 pathways. *Nature cell biology*. 3:1009-1013.

Sacheck, J.M., J.P. Hyatt, A. Raffaello, R.T. Jagoe, R.R. Roy, V.R. Edgerton, S.H. Lecker, and A.L. Goldberg. 2007. Rapid disuse and denervation atrophy involve transcriptional changes similar to those of muscle wasting during systemic diseases. *FASEB journal : official publication of the Federation of American Societies for Experimental Biology*. 21:140-155.

Salih, D.A., A.J. Rashid, D. Colas, L. de la Torre-Ubieta, R.P. Zhu, A.A. Morgan, E.E. Santo, D. Ucar, K. Devarajan, C.J. Cole, D.V. Madison, M. Shamloo, A.J. Butte, A. Bonni, S.A. Josselyn, and A. Brunet. 2012. FoxO6 regulates memory consolidation and synaptic function. *Genes & development*. 26:2780-2801.

Sanchez, A.M., R.B. Candau, and H. Bernardi. 2014. FoxO transcription factors: their roles in the maintenance of skeletal muscle homeostasis. *Cellular and molecular life sciences : CMLS*. 71:1657-1671.

Sandri, M. 2013. Protein breakdown in muscle wasting: role of autophagy-lysosome and ubiquitin-proteasome. *Int J Biochem Cell Biol*. 45:2121-2129.

Sandri, M., C. Sandri, A. Gilbert, C. Skurk, E. Calabria, A. Picard, K. Walsh, S. Schiaffino, S.H. Lecker, and A.L. Goldberg. 2004. Foxo transcription factors induce the atrophy-related ubiquitin ligase atrogin-1 and cause skeletal muscle atrophy. *Cell*. 117:399-412.

Santra, M.K., N. Wajapeyee, and M.R. Green. 2009. F-box protein FBXO31 mediates cyclin D1 degradation to induce G1 arrest after DNA damage. *Nature*. 459:722-725.

Sartori, R., G. Milan, M. Patron, C. Mammucari, B. Blaauw, R. Abraham, and M. Sandri. 2009. Smad2 and 3 transcription factors control muscle mass in adulthood. *American journal of physiology. Cell physiology*. 296:C1248-1257.

Sartori, R., E. Schirwis, B. Blaauw, S. Bortolanza, J. Zhao, E. Enzo, A. Stantzou, E. Mouisel, L. Toniolo, A. Ferry, S. Stricker, A.L. Goldberg, S. Dupont, S. Piccolo, H. Amthor, and M. Sandri. 2013. BMP signaling controls muscle mass. *Nature genetics*. 45:1309-1318.

Schiaffino, S., K.A. Dyar, S. Ciciliot, B. Blaauw, and M. Sandri. 2013. Mechanisms regulating skeletal muscle growth and atrophy. *The FEBS journal*. 280:4294-4314.

Schiaffino, S., and C. Reggiani. 2011. Fiber types in mammalian skeletal muscles. *Physiological reviews*. 91:1447-1531.

Schmidt, E.K., G. Clavarino, M. Ceppi, and P. Pierre. 2009. SUnSET, a nonradioactive method to monitor protein synthesis. *Nature methods*. 6:275-277.

Schuler, M., F. Ali, E. Metzger, P. Chambon, and D. Metzger. 2005. Temporally controlled targeted somatic mutagenesis in skeletal muscles of the mouse. *Genesis*. 41:165-170.

Senf, S.M., P.B. Sandesara, S.A. Reed, and A.R. Judge. 2011. p300 Acetyltransferase activity differentially regulates the localization and

activity of the FOXO homologues in skeletal muscle. *American journal of physiology. Cell physiology*. 300:C1490-1501.
Seoane, J., H.V. Le, L. Shen, S.A. Anderson, and J. Massague. 2004. Integration of Smad and forkhead pathways in the control of neuroepithelial and glioblastoma cell proliferation. *Cell*. 117:211-223.
Southgate, R.J., B. Neill, O. Prelovsek, A. El-Osta, Y. Kamei, S. Miura, O. Ezaki, T.J. McLoughlin, W. Zhang, T.G. Unterman, and M.A. Febbraio. 2007. FOXO1 regulates the expression of 4E-BP1 and inhibits mTOR signaling in mammalian skeletal muscle. *The Journal of biological chemistry*. 282:21176-21186.
Stitt, T.N., D. Drujan, B.A. Clarke, F. Panaro, Y. Timofeyva, W.O. Kline, M. Gonzalez, G.D. Yancopoulos, and D.J. Glass. 2004. The IGF-1/PI3K/Akt pathway prevents expression of muscle atrophy-induced ubiquitin ligases by inhibiting FOXO transcription factors. *Molecular cell*. 14:395-403.
Tsuchida, A., T. Yamauchi, Y. Ito, Y. Hada, T. Maki, S. Takekawa, J. Kamon, M. Kobayashi, R. Suzuki, K. Hara, N. Kubota, Y. Terauchi, P. Froguel, J. Nakae, M. Kasuga, D. Accili, K. Tobe, K. Ueki, R. Nagai, and T. Kadowaki. 2004. Insulin/Foxo1 pathway regulates expression levels of adiponectin receptors and adiponectin sensitivity. *The Journal of biological chemistry*. 279:30817-30822.
van der Horst, A., L.G. Tertoolen, L.M. de Vries-Smits, R.A. Frye, R.H. Medema, and B.M. Burgering. 2004. FOXO4 is acetylated upon peroxide stress and deacetylated by the longevity protein hSir2(SIRT1). *The Journal of biological chemistry*. 279:28873-28879.
van der Vos, K.E., P. Eliasson, T. Proikas-Cezanne, S.J. Vervoort, R. van Boxtel, M. Putker, I.J. van Zutphen, M. Mauthe, S. Zellmer, C. Pals, L.P. Verhagen, M.J. Groot Koerkamp, A.K. Braat, T.B. Dansen, F.C. Holstege, R. Gebhardt, B.M. Burgering, and P.J. Coffer. 2012. Modulation of glutamine metabolism by the PI(3)K-PKB-FOXO network regulates autophagy. *Nature cell biology*. 14:829-837.
Vilchez, D., I. Morantte, Z. Liu, P.M. Douglas, C. Merkwirth, A.P. Rodrigues, G. Manning, and A. Dillin. 2012. RPN-6 determines C. elegans longevity under proteotoxic stress conditions. *Nature*. 489:263-268.
Webb, A.E., and A. Brunet. 2014. FOXO transcription factors: key regulators of cellular quality control. *Trends in biochemical sciences*. 39:159-169.
Yamazaki, Y., Y. Kamei, S. Sugita, F. Akaike, S. Kanai, S. Miura, Y. Hirata, B.R. Troen, T. Kitamura, I. Nishino, T. Suganami, O. Ezaki, and Y. Ogawa. 2010. The cathepsin L gene is a direct target of FOXO1 in skeletal muscle. *The Biochemical journal*. 427:171-178.
Yu, L., C.K. McPhee, L. Zheng, G.A. Mardones, Y. Rong, J. Peng, N. Mi, Y. Zhao, Z. Liu, F. Wan, D.W. Hailey, V. Oorschot, J. Klumperman, E.H. Baehrecke, and M.J. Lenardo. 2010. Termination of autophagy and reformation of lysosomes regulated by mTOR. *Nature*. 465:942-946.
Zhao, J., J.J. Brault, A. Schild, P. Cao, M. Sandri, S. Schiaffino, S.H. Lecker, and A.L. Goldberg. 2007. FoxO3 coordinately activates protein degradation by the autophagic/lysosomal and proteasomal pathways in atrophying muscle cells. *Cell metabolism*. 6:472-483.